FUNCTIONAL IMAGING OF CENTRAL MECHANISMS UNDERLYING HUMAN PAIN PERCEPTION

Mary Elizabeth Nebel

A dissertation submitted to the faculty of the University of North Carolina at Chapel Hill in partial fulfillment of the requirements for the degree of Doctor of Philosophy in the Joint Department of Biomedical Engineering.

Chapel Hill
2010

Approved by:

Mark Tommerdahl, Ph.D.

Gregory Essick, D.D.S., Ph.D.

Oleg Favorov, Ph.D.

Stephen Folger, Ph.D.

Shawn Gomez, Ph.D.

ABSTRACT

Mary Elizabeth Nebel: Functional Imaging of Central Mechanisms Underlying Human Pain Perception

(Under the direction of Gregory Essick and Mark Tommerdahl)

Investigations of human somatosensory perception have demonstrated robust interactions between the submodalities of pain and touch, and there is increasing recognition that the systematic assessment of somatosensory perception in disorders characterized by persistent pain such as Temporomandibular Disorder (TMD) would greatly aid diagnosis and evaluation of treatment efficacy. To better understand the pathophysiological mechanisms underlying TMD, we investigated cortical processing interactions that occur between innocuous and noxious cutaneous input using functional magnetic resonance imaging (fMRI). Innocuous vibrotactile stimulation and noxious skin heating were delivered separately and concurrently to the hand of women with TMD and to pain-free, gender-matched controls (HC). Cortical responses evoked by innocuous vibrotactile stimulation alone differentiated TMDs from HCs, and the differences between the groups suggest cortical plasticity in TMD which primes areas to respond to innocuous vibrotactile input that normally would not, including parts of the pain matrix and auditory cortex. In contrast, pain ratings and cortical responses to noxious heat alone did not differ significantly between TMDs and HCs. However, additional group differences emerged in the cortical patterns characterizing interactions between somatosensory submodalities in subjects with and without TMD during concurrent stimulation that could not be

explained exclusively by group differences in the response to innocuous vibrotactile stimulation. Some of these differences in the interaction of innocuous and noxious somatosensory inputs were correlated with the severity of the TMD patients' clinical pain despite the fact that no significant correlations were observed between TMD pain and responses to vibrotactile or noxious heat stimulation alone. This suggests that cortical processing interactions between somatosensory submodalities more closely reflect individual experiences of persistent clinical pain than does the unimodal processing of innocuous vibrotactile or noxious heat input alone.

ACKNOWLEDGMENT

I would like to express my deepest gratitude to Dr. Essick and Dr. Tommerdahl for their guidance, patience, and invaluable knowledge. I would also like to thank Dr. Essick for providing the lab with goldfish crackers, which sustained me through many late nights.

DEDICATION

To my mom, who learned to pick up objects with her feet when she was unable to bend over to pick them up with her hands.

TABLE OF CONTENTS

LIST OF TABLES

LIST OF FIGURES

CHAPTER 1

A HISTORY OF PAIN

Acute pain is of paramount importance to human vitality, warning one of harm and promoting healing of damaged tissues. Despite its omnipotency, pain tends to seem remote to healthy individuals and often evokes skepticism rather than sympathy. The development of maladaptive persistent pain states in response to tissue injury is common, with one in six adults suffering from a chronic pain condition [1]; however, these people are often dismissed as malingerers and hypochondriacs. Even when pain is acknowledged and addressed, its remedy is generally insufficient because the mechanisms responsible for the initiation and persistence of pain are uncertain. Current therapies have limited efficacy, with up to 50% of treated subjects receiving inadequate pain relief [2].

Understanding what could cause pain to persist after an injury has healed requires knowledge of what causes pain at all. Pain has a legacy of being attributed to the activities of supernatural forces, including gods, gremlins, and more recently, extraterrestrial aliens, which all suggest that the experience of pain is itself mystical. The otherworldliness of pain has made it a longstanding preoccupation of philosophical, political, and religious musings. For instance, the transcendence of pain is a central theme of Judeo-Christian teachings: endurance of pain is the test of faith in the story of Job and is the path to redemption through the Crucifixion. In the utilitarian dialectic of the 18th and 19th centuries, pleasure was balanced against pain as a measure of the good of society [3].

Pain has also been the subject of several centuries worth of legitimate scientific inquiry, and the advancement of our understanding of pain etiology has paralleled a great expansion in our understanding of how the nervous system functions in general. René Descartes was one of the first philosophers to be influenced by the Scientific Revolution of the 17th century. Impressed by the experimental methods pioneered by Galileo, Kepler, and others to understand physics, Descartes argued that because the body was machine-like, its function could be investigated using similar techniques. In his work "*De homine,"* Descartes proposed one of the earliest concepts of modern physiology: a direct-line, static transmission system connecting injured tissues in the body to a pain center in the brain [4].

The mechanisms underlying Descartes' proposal were first seriously addressed in the 19th century, following a dramatic, cultural reconceptualization of pain. Increasingly, pain was viewed as a consequence, not of supernatural forces, but of determinable causes, and the fear of interfering with God's will by attempting to alleviate pain medically was replaced with a sense that determining a way to reduce pain for the greatest number of people was a positive good [3]. Investigations of spinal cord tracts revealed that distinct lesions resulted in separate and independent loss of tactile and pain-related perception. The fact that certain lesions could destroy a person's ability to detect touch while the ability to detect pain remained unchanged gave credence to the notion that a spinal pathway specifically designated for conducting painful input existed and led German physiologist Moritz Schiff to propose the specificity of pain, which claimed that pain was a sense independent of touch [5]. However, one objection to considering pain as an independent sense was that it could be elicited by different types of stimuli, which was not true of other accepted sensory modalities. German neurologist Wilhelm Erb proffered an alternative explanation of pain, the pattern theory, which reasoned that nerve impulse

patterns underlying pain were produced by vigorous stimulation of non-specific receptors and pathways that are normally concerned with other sensory experiences [5].

Sir Charles Scott Sherrington, an English neurophysiologist who later won the Nobel Prize in Medicine, suggested labeling stimuli capable of tissue damage as “noxious” regardless of physical character and postulated that the signaling of noxious events was the function of sense organs responsible for pain (nociceptors) [6]. This concept endowed pain with coherent and definable peripheral stimuli. Another critical conceptual step in understanding the mechanisms underlying pain perception was the recognition that the central nervous system is not a syncytium, but rather is composed of discrete cells that communicate with one another via functional connections, or synapses [7]. The discovery of functional connections between neurons allowed for the possibility that these connections could be altered and provided the basis of support for Sherrington’s preeminent theory that suppression of excitability in neural circuits is just as essential for integrative functioning as is excitability itself [8].

As technology improved and allowed for more sophisticated investigations of the anatomy and function of the nervous system, the debate between specificity and pattern theories of pain persisted with both sides continuing to accumulate supporting evidence. In 1965, Canadian psychologist Ronald Melzack and British physiologist Patrick Wall published a theory which accounted for some aspects of both the specificity and pattern theories. Their “gate control” theory of pain proposed a spinal cord mechanism that regulated the transmission of pain sensation between the periphery and the brain and a central control trigger, which could activate descending inhibitory fibers and influence afferent conduction [9]. The precise mechanisms of the gate control theory are still debated; however, according to Melzack, the most important contribution of the theory to biomedical science was not a specific mechanism

but the general idea that the central nervous system (CNS) is an essential component in pain processing and that the brain is “an active system that filters, selects, and modulates inputs”[10].

The gate control theory of pain is just one expression of the normal, competitive interactions that take place between different types of somatosensory information in the CNS. Complimentary to the gate control theory of pain is the gate control theory of touch, or the “touch gate,” which refers to the normal impairment of touch perception in response to activation of pain receptors within a spatially limited region on the body near the location of tactile stimulation [11, 12]. The convergence of pain and tactile processing in the CNS suggests that the experience of pain might not only be reflected in the processing of painful input, but might also be associated with modulation of somatosensory processing more generally. One plausible explanation for the pathological persistence of pain and the concomitant, diffuse sensory abnormalities that are observed, may be the dysfunction of mechanisms in the CNS that normally regulate the intensive, temporal, and spatial dimensions of somatosensory experience.

The overall aim of the work comprising this dissertation was to probe the operation of somatosensory regulatory mechanisms at the level of the cortex in healthy individuals and then to apply that knowledge to assess the functional status of these regulatory mechanisms in patients with persistent musculoskeletal pain. An enhanced theoretical understanding of the functional status of the somatosensory system in patients with chronic pain could lead to improved methods for assessing the cerebral cortical health of these individuals and the efficacy of therapeutic interventions.

CHAPTER 2

TEMPOROMANDIBULAR DISORDER MODIFIES CORTICAL RESPONSE TO TACTILE STIMULATION

A large portion of the work presented in this chapter was completed as a collaborative effort with the following researchers: Folger S, Tommerdahl M, Hollins M, McGlone F, and Essick G.

2.1. Abstract

Individuals with temporomandibular disorder (TMD) suffer from persistent facial pain and exhibit abnormal sensitivity to tactile stimulation. To better understand the pathophysiological mechanisms underlying TMD, we investigated cortical correlates of this abnormal sensitivity to touch. Using functional magnetic resonance imaging (fMRI), we recorded cortical responses evoked by low frequency vibration of the index finger in subjects with TMD and in healthy controls (HC). Distinct subregions of contralateral SI, SII, and insular cortex responded maximally for each group. Although the stimulus was inaudible, primary auditory cortex was activated in TMDs. TMDs also showed greater activation bilaterally in anterior cingulate cortex and contralaterally in the amygdala. Differences between TMDs and HCs in responses evoked by innocuous vibrotactile stimulation within SI, SII, and the insula paralleled previously reported differences in responses evoked by noxious and innocuous stimulation, respectively, in healthy individuals. This unexpected result may reflect a disruption of the normal balance between central resources dedicated to processing innocuous and noxious input, manifesting itself as increased readiness of the pain matrix for activation by even

innocuous input. Activation of the amygdala in our TMD group could reflect the establishment of aversive associations with tactile stimulation due to the persistence of pain.

Perspective: This article presents evidence that central processing of innocuous tactile stimulation is abnormal in TMD. Understanding the complexity of sensory disruption in chronic pain could lead to improved methods for assessing cerebral cortical function in these patients.

2.2. Introduction

A considerable body of evidence suggests that painful conditions are often accompanied by alterations in cutaneous sensory perception. Nathan reported that localized pain due to peripheral or central lesions can impair the perception of tactile stimuli within the painful region [13]; similarly, provoking pain in patients with pathological pain (e.g., tennis elbow) increases tactile detection thresholds in the area of pain referral [14]. In some clinical conditions, widespread impairment of tactile sensitivity has been documented. Patients with chronic cervicobrachialgia [15] and persistent patellofemoral pain[16] demonstrate systemic elevation of vibrotactile detection thresholds compared to healthy controls. Although the clinical presentations of these conditions differ, there is increasing recognition that systematic assessment of somatosensory perception in disorders characterized by persistent pain would greatly aid diagnosis and evaluation of treatment efficacy.

One condition in which local and widespread sensory disturbances have been examined is temporomandibular disorder (TMD), a non-specific diagnosis representing a constellation of conditions characterized by persistent facial pain and impaired oral function [17]. TMD, the most common chronic orofacial pain condition in the United States, impacts approximately 12% of the population [18]. Individuals with TMD frequently report pain in widespread body areas [19, 20], suggesting that central pathophysiological processes contribute to the persistence of

pain. In addition, TMD is associated with several co-morbid functional syndromes including fibromyalgia (18%) [21], vulvar vestibulitis [22], and irritable bowel syndrome (64%) [23].

Vibrotactile sensibility on the face of TMD patients is characterized by elevated detection threshold [24] and impaired frequency discrimination [25], a process shown to rely on intact somatosensory cortex [26]. Outside of the painful region, a marginal increase in vibrotactile detection threshold [25] is overshadowed by perceptual *amplification* of the intensity of suprathreshold tactile stimuli [27].

One interpretation of the association between persistent pain and abnormal tactile sensibility is that there is a disturbance in the normal balance between cortical noxious and non-noxious processing. Animal studies and neural network modeling indicate that regions of somatosensory cortex dominated by input from different spinal pathways interact disadvantageously when normal input is disrupted, for instance, by dorsal column transection [28]. Tissue injury and inflammation have also been shown to alter cortical responsivity to noxious and non-noxious stimulation in animal models of arthritis [29, 30]. In addition, neuroimaging studies of phantom limb pain reveal a correlation between cortical reorganization of somatic processing and the magnitude of pain experienced [31, 32]; however, pain coexists with extensive sensorimotor deafferentation which also contributes to cortical reorganization. Whether the vibrotactile perception impairments observed in individuals with TMD pain likewise reflect an abnormal topography of cortical somatosensory processing remains to be determined.

The purpose of the present study was to determine, using functional magnetic resonance imaging (fMRI), whether the decreased sensitivity to touch observed in TMD is associated with alterations in the magnitude and location of brain activity evoked by low frequency skin vibration.

2.3. Materials and Methods

Subjects

Twenty-five women consented to a protocol approved by the Institutional Review Board at UNC-Chapel Hill Medical Center. The sample population was restricted to women because the prevalence of TMD is significantly higher in women; 2 to 1 in the general population and 8 to 1 in the clinical setting [33]. Thirteen participants fulfilled Research Diagnostic Criteria (RDC) for TMD [17], average age (SD) was 28.7 (7.6) years; the other twelve participants were neurologically healthy controls whose average age was 28.8 (7.9) years. Immediately prior to the imaging session, each participant completed the Short-form McGill Pain Questionnaire (SF-MPQ) to assess her current level of pain [34].

Stimulation

While in the MRI scanner, low frequency vibration (tactile flutter) was applied to the distal pad of the right index finger using a purpose-designed piezoelectric tactile stimulator (PTS) [35]. Tactile stimuli were applied to the hand rather than to the temporomandibular region to identify the presence of global abnormalities in central somatosensory processing that could not be attributed to abnormalities in stimulus-evoked afferent activity from the site of the patients' pain complaints. A static surround limited the stimulation to a region under the 8-mm diameter Teflon contactor, which was attached to the bender element. Consistent with previous neuroimaging investigations of somatosensory cortex in primates, a 26 Hz sinusoidal stimulus with peak-to-peak amplitude of 400 μm was used. Flutter stimulation near this frequency generates robust and repeatable optical intrinsic signal (OIS) responses within the post-central gyrus in squirrel monkeys[36] . Flutter stimulus events were 4s in duration and repeated every 32s to allow adequate observation of the hemodynamic response to each event. Subjects were instructed to keep their eyes closed and to focus attention on the presence of the stimulus.

Twenty-three of the 25 subjects participated in two imaging sessions during which two functional imaging series of tactile flutter were completed. Each imaging series consisted of 14 flutter stimulus presentations for a total of 56 events. Two subjects (one TMD) completed a single imaging session for a total of 28 events. At the end of each imaging series, subjects were asked to rate the average intensity of the flutter stimulus using a labeled magnitude scale with the following anchor points: felt nothing (0), barely detectable (1.5), weak vibration (5), moderate vibration (16), strong vibration (33), very strong (50), and most intense vibration imaginable (100). Subjects were instructed to choose the most appropriate label range to describe the intensity of the stimulus and then convert that LABEL into a number. Subjects were familiarized with the scale and presented with two test stimuli to rate before entering the scanner room.

Imaging Parameters

Scanning was performed on a Siemens Magnetom Allegra, head-dedicated 3.0T scanner system Siemens AG, Erlangen, Germany) with 40 -mT/m gradients and a 30 cm radio frequency (RF) volume coil. Subject head motion was restricted using foam cushions, and earplugs and earphones were worn by subjects to reduce scanner noise. A total of 160 contiguous, high-resolution images covering the entire brain were acquired using a magnetization prepared rapid gradient echo (MPRAGE) T1-weighted sequence (TR: 1700ms, Echo Time (TE): 4.38 ms, Flip angle: 8, 1mm isotropic sampling). These structural images were aligned near-axially, parallel to the plane underlying the rostrum and splenium of the corpus callosum and were used for coregistration with the functional data. Whole brain functional images consisted of 50 slices collected using a gradient echo pulse sequence sensitive to blood oxygenation level dependent (BOLD) contrast with echo planar k-space sampling at a repetition rate (TR) of 3000ms (TE: 30ms, Flip angle: 90, Image matrix: 64 X 64, isotropic voxel size: $3mm^3$). The functional images

were aligned similarly to the structural images. A semi-automated, high-order shimming program ensured global field homogeneity. Imaging series began with two discarded RF excitations to allow the change in net magnetization of the sample following excitation to reach steady state equilibrium.

Image Data Analysis

Before any statistical analyses were performed, the following preprocessing steps were applied to the fMRI data to remove task-independent variability using FMRIB Software Library (FSL) version 4.1.2 [37, 38]: (i) brain extraction for non-brain removal [39], (ii) subject motion correction using MCFLIRT [40], (iii) temporal realignment to adjust for slice acquisition order using Fourier-space time-series phase shifting, (iv) spatial smoothing using a Gaussian filter with a FWHM 5mm kernel to boost the signal to noise ratio of the data, (v) grand-mean intensity scaling of the entire 4D dataset by a single factor, and (vi) high-pass temporal filtering to remove low frequency artifacts. Functional images of each subject were co-registered to structural images in native space, and structural images were warped into Montreal Neurological Institute (MNI) stereotaxic space to allow for intersubject comparison. The same transformation matrices used for structural-to-standard transformations were then applied to the co-registered functional images, and all registrations were performed using an intermodal registration tool (affine, 12 degrees of freedom). Voxel-wise temporal autocorrelation was estimated and corrected using FMRIB's Improved Linear Model [41].

Onset times of tactile flutter events were used to generate a regressor to model the hemodynamic response (HDR) to the stimulus. Model fitting generated whole brain images of parameter estimates and variances, representing average signal change from baseline. Group-wise activation images were calculated by a mixed effects higher level analysis using FMRIB Local Analysis of Mixed Effects (FLAME), with a cluster mean threshold of $z > 2.5$ and a cluster

corrected significance of $p < 0.05$ [42]. Following statistical thresholding, mixed effects group contrast images were restricted to voxels in which a significant, cluster corrected HDR was evoked by skin flutter in either group composing the contrast. The Jülich histologic atlas [43, 44] and the Harvard-Oxford cortical and subcortical structural atlases (Harvard Center for Morphometric Analysis, Charlestown, MA) were used to localize activation clusters. The final fMRI analysis step consisted of extracting average BOLD time courses from functional regions of interest (ROIs) identified to differentiate groups based on whole-brain analyses described above. Peak responses were compared between groups in these regions.

2.4. Results

Self-reported Present Pain

On average, TMD subjects reported their present pain intensity on the day of testing to be 2.4 on a 10 cm visual analog scale with end labels of no pain (0) and worst possible pain (10). Control subjects reported an average present pain intensity of 0.16 out of 10 on the day of testing.

Perceptual Ratings

On average, the TMD group rated the intensity of the flutter stimulation as 32.0 (SD = 15.4), corresponding to a level of "strong" on the labeled magnitude scale while the control group rated the intensity of the same stimuli as only 19.2, on average (SD = 12.5), corresponding to moderately intense. A t-test indicated that this difference in mean perceived intensity was significant ($p=0.03$).

Imaging Data

Individual Group Analysis

In a repeated measures analysis, no significant differences in the response to tactile flutter were observed between imaging sessions for either group; accordingly, for each subject

who completed two sessions, data from the two sessions were combined in subsequent analyses. For both groups, skin flutter evoked significant hemodynamic responses in established somatosensory processing areas, namely contralateral primary somatosensory cortex (SI), bilateral secondary somatosensory cortex (SII) and bilateral insular cortex. In addition, robust responses were evoked in both groups in sensory association areas, bilateral anterior cingulate cortex (ACC) and ipsilateral inferior parietal lobule, as well as in ipsilateral middle frontal gyrus, an area associated with attention to transient targets. Figure 1 illustrates the pattern of activation for each group in these regions, and Table 1 indicates the MNI coordinates of all significant activation clusters in the control group while Table 2 lists the coordinates of all significant activation clusters in the TMD group. Up to four local maxima within each activation cluster are listed since several clusters span more than one cortical region.

Between-group analyses

Different patterns of activation in response to skin flutter were observed for the TMD and control groups. Direct comparison of (control – TMD) and (TMD – control) flutter contrasts revealed areas within the above mentioned clusters in which one group demonstrated significantly greater activation than the other; Table 3 lists MNI coordinates of all active regions demonstrating a significant group effect.

SI

Both the control group and the TMD group displayed significant responses in contralateral SI and SII; however, Figure 2 illustrates the distinct patterns of activation within these regions for the two groups. SI activation for the control group ("A" in Figure 2) was posterior and lateral to SI activation for the TMD group ("B" in Figure 2) according to the MNI coordinates listed in Table 3. Figure 2 also indicates average hemodynamic time courses for both groups derived from contralateral SI voxels identified by the whole brain analysis to

differentiate between groups. In the posterior region of area 1, the response of the control group was significantly greater than that of the TMD group 3-9 seconds after the onset of skin flutter stimulation ($p < 0.01$ for all three time points); see "A" in Figure 2. In the more anterior portion of SI, the peak of the TMD HDR at 3 seconds was significantly greater than that of the controls ($p < 0.04$); see "B" in Figure 2.

SII and primary auditory cortex (A1)

Separation between groups also occurred in contralateral SII, with the mass of the control HDR ("C" in Figure 2) residing in parietal operculum subregions OP1 and OP4 [45, 46] and with the TMD group's SII activation extending from OP1 ("D" in Figure 2) across the Sylvian fissure and into neighboring primary auditory cortex ("E" in Figure 2). Local maxima were identified on either side of the Sylvian fissure in both TMD activation maps (Table 2) and TMD – control contrast maps (Table 3). Using the Jülich histologic atlas, it was determined that 20% of the contralateral SII cluster listed in Table 3 resided in primary auditory cortex (A1) [47]. No statistical difference was observed between the time to or magnitude of peak TMD HDR in SII and A1. On the ipsilateral side, no region of SII demonstrated greater activation to skin flutter in the control group than in the TMD group. The TMD group showed greater activation than the control group in OP1 and again this activation extended into primary auditory cortex (Figure 3); approximately 24% of the cluster labeled ipsilateral SII in Table 3 was located in ipsilateral A1.

SII and A1 are located adjacently on opposite banks of the Sylvian fissure, and previous research has suggested that extensive overlap may occur in fMRI responses evoked by tactile and auditory stimulation when data is combined across subjects due to their close anatomical proximity [48]. To verify that activation of primary auditory cortex was not caused by a mis-registration of individual subject data onto the standard atlas, we inspected subject responses on their individual high-resolution anatomical images. Activation of contralateral A1 was found

in all 13 TMD subjects and activation of ipsilateral A1 was found in 9 of 13 TMD subjects. Figure 4 contains fMRI activations evoked by tactile stimulation from two exemplary TMD subjects and one healthy control; activation clearly extends into A1 for both TMD subjects but remains in SII for the control subject.

Insula, ACC & amygdala

Figure 5 depicts brain areas outside of those regions traditionally associated with tactile processing in which the TMD group showed greater activation than controls. Although both groups displayed bilateral ACC activation, the control group's ACC HDR was surpassed in magnitude and spatial extent by the HDR of the TMD group; see "A" in Figure 5. The between-group flutter contrast also revealed a dissociation of the HDR in contralateral insular cortex. The control group demonstrated greater evoked activity in an anterior region of the insula while conversely, the TMD group showed greater evoked activity in a more posterior region ("B" in Figure 5). Unexpectedly, activation evoked by skin flutter was also greater for the TMD group in the contralateral amygdala; refer to "C" in Figure 5.

2.5. Discussion

To the best of our knowledge, the present report is the only examination of brain activity evoked by innocuous vibrotactile digit stimulation in TMD patients. The gross morphology of cortical activation elicited by skin flutter in our controls was similar to patterns previously reported [35, 49-51], including contiguous activation of SI and SII [52]. The results are also consistent with the hypothesis that, in TMD, differences exist in the location and magnitude of cortical processing of vibrotactile stimulation, adding more evidence to our understanding of the disruption of the somatosensory system in a chronic pain condition.

The finding that, on average, TMD subjects perceived flutter stimulation as more intense than controls is consistent with published reports of TMD patients experiencing perceptual

amplification of innocuous levels of pressure stimulation, rating weak pressures as more intense compared to controls [27]. These ratings should be interpreted with caution since we did not perform a rigorous calibration of the scale with each participant to minimize intersubject differences in its use.

SI

Group comparisons revealed differences between controls and TMDs in evoked activity within the hand region of SI. The SI hand region is composed of a number of cytoarchitectonically defined subdivisions (areas 3a, 3b, 1, and 2) and the Jülich histologic atlas indicated that the SI cluster in which the control group demonstrated greater activation than the TMD group belonged to area 1, while the SI cluster in which the TMD group showed greater activation than controls was more anterior and medial (Table 3), and spanned areas 1 and 3b [53, 54]. Attempting to assign cytoarchitectonic labels to fMRI activation foci is prone to error due to substantial image processing and inter-subject variability [54]; however, areas 3b and 1 are traditionally regarded as the SI core for processing input from cutaneous receptors. The stability of the location and spatial extent of SI activity evoked by flutter of increasing intensity has been demonstrated by OIS[36] and fMRI monkey studies[55], suggesting that this group difference in the location of maximal response is not simply reflective of greater tactile intensity experienced by TMDs. Painful and innocuous stimuli appear to drive different neuronal populations within somatosensory cortex, and the general orientation of the shift in maximal BOLD response between controls and TMDs is similar to the pattern of response observed when comparing activity evoked by innocuous and noxious stimulation of the hand in both healthy humans [56-58] and in squirrel monkeys [59-61]; the fringe of SI that responds to painful stimulation of the hand is anterior and medial to the core SI hand tactile locus.

Changes in SI tactile responsivity have been studied in patients with other persistently painful conditions with mixed results. Using fMRI to study complex regional pain syndrome (CRPS), Pleger et al observed a reduction in SI activity evoked by tactile stimulation in CRPS compared to healthy controls [62] while the CRPS subjects in the magnetoencephalography (MEG) study of Vartiainen et al demonstrated enhanced SI responsivity to tactile stimulation compared to controls [63]. Accounting for methodological differences, we consider both of these results consistent with our findings. The SI subregion in which our chronic pain group showed decreased activity compared to controls was located near the crown of the postcentral gyrus, making it difficult to detect using MEG which is intrinsically insensitive to radially oriented flow. A weaker magnet in the Pleger study necessitated the use of larger voxels and increased spatial smoothing; partial volume effects could have caused blurring of activity within the two distinct SI subregions we identified to show opposing group effects, with the net effect being decreased evoked activity in the chronic pain state.

SII & A1

The group differences we observed in the SII response to flutter appear to be consistent with comparisons of SII responsiveness to innocuous versus noxious stimulation in healthy subjects. The contralateral SII locus of activation for the control group was anterior to the SII locus of activation for the TMD group. One of the earliest monkey electrophysiological studies suggested that anterior SII consisted of neurons responsive to tactile input while posterior SII included polysensory and nociceptive neurons [64]. In a more recent meta-analysis of reported SII activations from human functional imaging studies of hand stimulation, Eickhoff et al found that SII voxels associated with non-painful stimulation, situated at the border between cytoarchitectonically defined OP1 and OP4, were anterior to SII voxels in OP1 associated with pain-related activity [45]. Additionally, Ferretti et al demonstrated two distinct SII subregions of

activation in the anterior-posterior direction, with only the posterior subregion of activation exhibiting modulation due to pain intensity [65]. The activation of the posterior subregion of SII by innocuous stimulation in our TMD group further suggests that this stimulation engaged circuits normally reserved for processing noxious stimulation.

Both groups exhibited a BOLD response in ipsilateral SII. However, the response of the TMD group was greater in magnitude and spatial extent. Pain-related activity has been shown to be more widely dispersed on both sides of the cortex than activity evoked by innocuous vibrotactile stimulation in pain-free subjects,[66, 67] and rat models of neuropathic pain have demonstrated bilateral increases in somatosensory cortex responsivity[68]. Thus, the recruitment of additional SII processing resources on the ipsilateral side in TMD further implicates an influence of TMD pain on the processing of the vibrotactile stimuli.

Given that many activities that produce tactile sensations also produce sound, it is not surprising that a growing body of evidence suggests that tactile stimulation can activate auditory cortex [69-73] and that horizontal connections between auditory cortex and somatosensory cortex exist [73-75]. This close anatomical and physiological relationship between cortical regions nominally belonging to separate modalities may help to explain behavioral interactions between hearing and touch [76-78]. What is surprising is that our TMD group, using conservative spatial smoothing [70], showed greater activation in primary auditory cortex than our control group. The results suggest that the posterior subregion of SII (activated in our TMD group) has readier access to A1, by reason of anatomical proximity, than does the anterior subregion of SII (activated in our HC group), raising the intriguing possibility that behavioral interactions between somatosensation and hearing might be more substantial in TMD patients than in controls and that auditory responses to some stimuli occur even when they are inaudible to the ear. Indeed, somatosensory input can modulate the intensity and character of tinnitus

[79], the symptoms of which are more common in individuals with TMD than in the general population [80]. Further investigation of the connectivity between somatosensory and auditory cortex in the human brain is needed before any definite conclusions can be drawn.

Insula, ACC & amygdala

Also surprising was that flutter stimulation evoked activity in the contralateral amygdala of our TMD group. To our knowledge, no neuroimaging investigation of innocuous tactile stimulation in humans has demonstrated a significant response in the amygdala; however, animal studies have provided evidence of amygdala sensitization following the induction of an inflammatory chronic pain state [81] and have emphasized the role of the amygdala [81, 82] as well as the insula [83] and ACC [84] in the modulation of pain behavior, all three of which showed greater activation in our TMD group than in our control group. The amygdala plays a critical role in learning the association between aversive and neutral stimuli in classical conditioning [85], and amygdala activation in response to what should be an affectively neutral stimulus could be consistent with the hypothesis proposed by Apkarian that chronic pain is a state of continuous learning in which aversive associations are continuously made with incidental events, like innocuous tactile stimulation, due to the persistent presence of pain [86]. Drawing conclusions about the emotional implications of amygdala activation is beyond the scope of this study, and given the association between TMD and hypervigilance[87], we must also recognize the possible influence of attentional differences on processing in the insula[88] and ACC[89]. However, the expectation of pain has been shown to increase the BOLD response evoked by nonpainful stimulation in the insula and ACC [90], and similar to the dissociation of group activations we observed within SI and SII, the subregion of the insula in which our TMD group showed maximal activity reportedly responds to noxious but not to innocuous stimuli [57].

A limiting factor of the present study is our sample size; although the number of subjects included in this study is comparable to many functional neuroimaging investigations, it may be small considering the heterogeneity in the clinical presentation of TMD. Despite this heterogeneity, we detected a disruption in the cortical processing of innocuous vibrotactile digit stimulation in TMD, and considered together, these subtle, yet significant differences suggest cortical plasticity in TMD which primes areas to respond to innocuous vibrotactile input that normally would not, including parts of the pain matrix and auditory cortex. Further investigation of how these processing differences are influenced by concurrent acute pain could help to explain their functional significance. Improving our understanding of the complexity of sensory disruption in chronic pain could allow for the development of more accurate chronic pain models needed to test and improve the efficacy of therapeutic interventions.

2.6. Acknowledgments

The authors would like to thank Steven Smith and MRI technologists Kathy Wilber, Amber Abernethy, James Barnwell, and Emilie Kearns for assistance with data acquisition as well as Ollie Monbureau and Mike Young for technical assistance. This work was supported by NIH grant P01 NS045685.

Table 1. Regions activated by skin flutter in controls. Only clusters with a mean threshold of z > 2.5 and a cluster corrected significance of p < 0.05 are listed. Up to four local maxima in each cluster are listed. C = side contralateral to the site of skin stimulation, I = side ipsilateral to the site of skin stimulation.

Controls :			Montreal Neurologic Institute Coordinates (mm)			
Side	Region	Cluster size (voxels)	X	Y	Z	Z_{max}
C	SII OP1	3275	-50	-28	20	6.83
	SII OP4		-46	-6	8	6.68
	Insula		-40	-2	12	6.59
	SI		-54	-24	56	6.08
I	Anterior Insula	106	40	6	4	3.82
I	Anterior Insula	45	38	22	4	3.82
I	Inferior Parietal Lobule	880	56	-40	56	5.75
	SII OP1		64	-28	28	5.32
I,C	Anterior Cingulate	177	2	26	38	4.49
I	Middle Frontal Gyrus	340	38	46	22	4.66
C	Superior Frontal Gyrus	145	-34	54	12	4.26

Table 2. Regions activated by skin flutter in TMDs. Only clusters with a mean threshold of z > 2.5 and a cluster corrected significance of p < 0.05 are listed. Up to four local maxima in each cluster are listed. C = side contralateral to the site of skin stimulation, I = side ipsilateral to the site of skin stimulation.

TMDs:			Montreal Neurologic Institute Coordinates (mm)			
Side	Region	Cluster size (voxels)	X	Y	Z	Z_{max}
C	SI	351	-52	-36	56	4.60
	SI		-54	-18	54	4.57
C	SII OP1	623	-52	-20	14	5.73
	A1		-48	-22	12	4.88
I	SII	204	50	-20	16	4.16
	A1		46	-20	10	3.23
C	Anterior Insula	331	-34	14	4	5.28
	Anterior Insula		-40	12	-10	4.16
C	Posterior Insula	286	-40	-10	-6	5.28
	Amygdala		-24	-10	-12	4.46
I	Anterior Insula	201	36	18	2	4.53
	Anterior Insula		32	26	2	4.28
C	Pallidium	147	-12	4	-4	4.72
I	Midbrain	558	6	-18	-16	4.61
I	Thalamus		4	-18	0	4.37
C	Thalamus		-16	-22	2	3.36
I	Planum Temporale	52	56	-32	18	4.10
C	Inferior Parietal Lobule	51	-40	-54	44	4.03
I	Inferior Parietal Lobule	186	58	-46	50	4.49
C	Paracingulate Gyrus	1154	-4	14	44	5.32
I	Paracingulate Gyrus		8	16	46	5.07
I	Anterior Cingulate		4	38	14	4.79
C	Anterior Cingulate		-6	32	18	4.24
I	Frontal Pole	37	38	46	2	3.83
I	Middle Frontal Gyrus	164	48	34	26	4.43

Table 3. Flutter responsive regions demonstrating a significant group effect. Only clusters with a mean threshold of z > 2.5 and a cluster corrected significance of p < 0.05 are listed. Up to four local maxima in each cluster are listed. C = side contralateral to the site of skin stimulation, I = side ipsilateral to the site of skin stimulation.

Controls > TMDs:			Montreal Neurologic Institute Coordinates (mm)			
Side	Region	Cluster size (voxels)	X	Y	Z	Z_{max}
C	Insula	145	-44	-2	12	5.22
	SII OP4		-48	-4	8	4.75
C	SII OP1	222	-60	-22	24	4.41
C	SI	54	-60	-26	46	3.82
	SI area 1		-52	-30	56	3.63
TMDs > Controls:						
C	Thalamus	501	-8	-28	-2	4.91
I	Thalamus		12	-24	8	4.37
C	SI area 1	102	-54	-22	52	4.17
	SI area 3b		-46	-18	52	3.91
C	Planum Temporale	289	-54	-30	14	4.09
	SII OP1		-50	-22	14	3.96
	SII OP1		-44	-34	20	3.93
	A1		-44	-24	8	3.44
I	A1	189	44	-22	6	4.57
	SII OP1		48	-24	18	4.31
C	Insula	46	-48	-10	-8	3.86
C	Anterior Cingulate	731	-6	2	40	5.10
I	Anterior Cingulate		4	8	40	4.9
C	Amygdala	22	-24	-10	-12	3.94

Figure 1. Flutter Responsive Regions. Masks of the main effect response to skin flutter for the control group only in yellow, the TMD group only in blue, and for both groups in green. A cluster mean threshold of $z > 2.5$ and a cluster corrected significance of $p < 0.05$ were used. Activation masks are overlayed on average anatomical images for all 25 subjects.

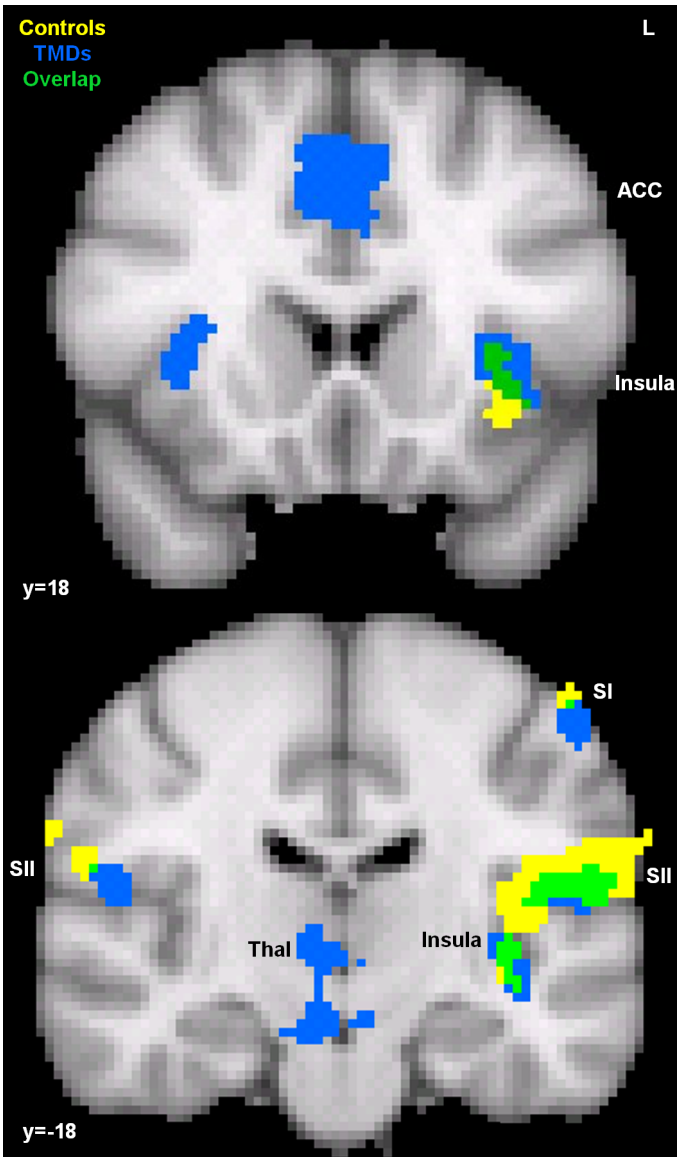

Figure 2. Comparison of mean percent signal change for controls and TMDs in subregions of somatosensory cortices contralateral to the stimulation site. (A) The subregion of SI in which controls showed greater activation than the TMD group was posterior to **(B)** the subregion of SI in which the peak of activation was greater for TMDs than controls. **(C)** & **(D)** Similar dissociations in activation were found between the groups in SII with the greater evoked response in the TMD group extending to primary auditory cortex **(E).** * indicates a statistically significant difference in the average percent signal change between groups at a particular time. Outlined regions are according to the Julich histological atlas.

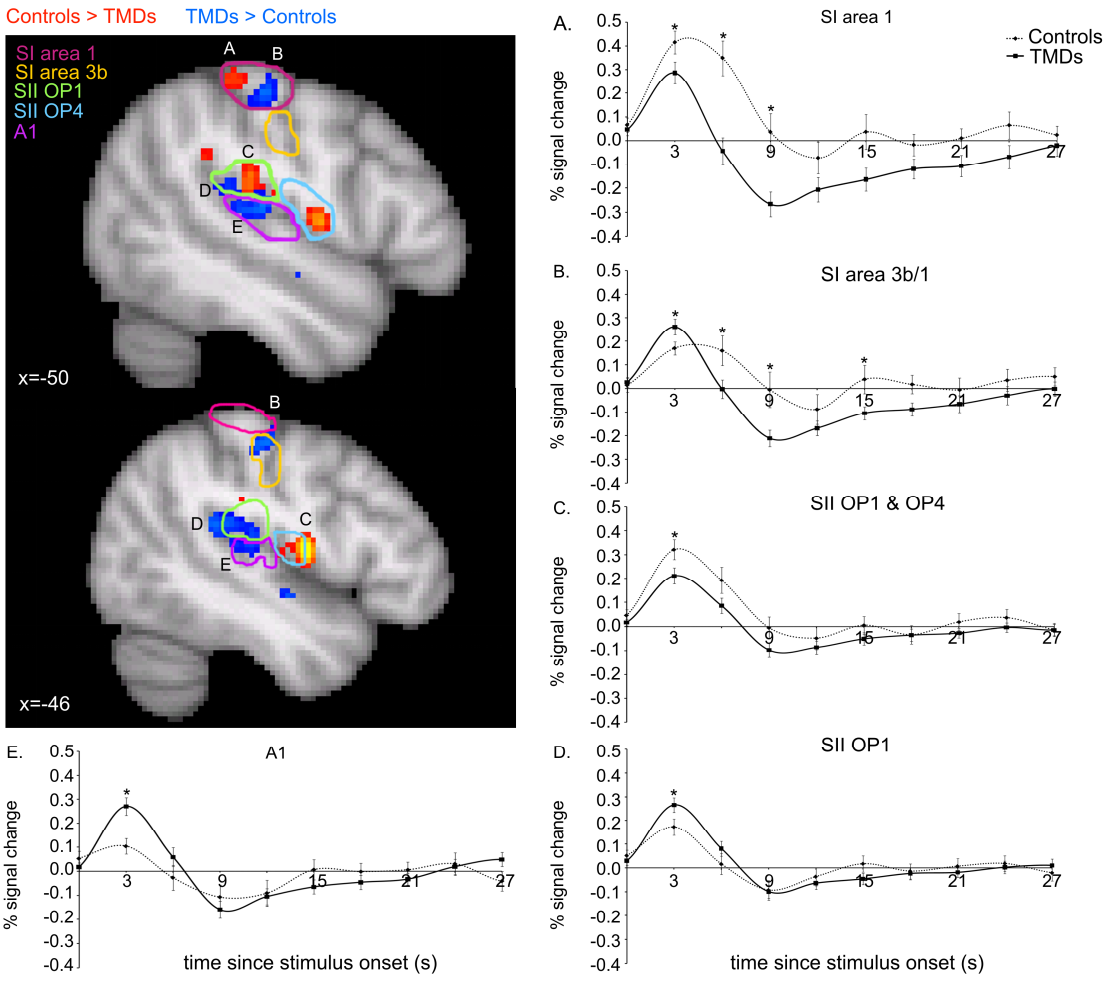

Figure 3. **Comparison of mean percent signal change in SII and primary auditory cortex ipsilateral to the site of skin stimulation.** The TMD group demonstrated greater activation in both **(A)** ipsilateral SII and **(B)** ipsilateral A1. Unlike on the contralateral side, there was no subregion of ipsilateral SII in which controls exhibited greater activation than TMDs in response to skin flutter. * indicates a statistically significant difference in the average percent signal change between groups at a particular time. Outlined regions are according to the Julich histological atlas.

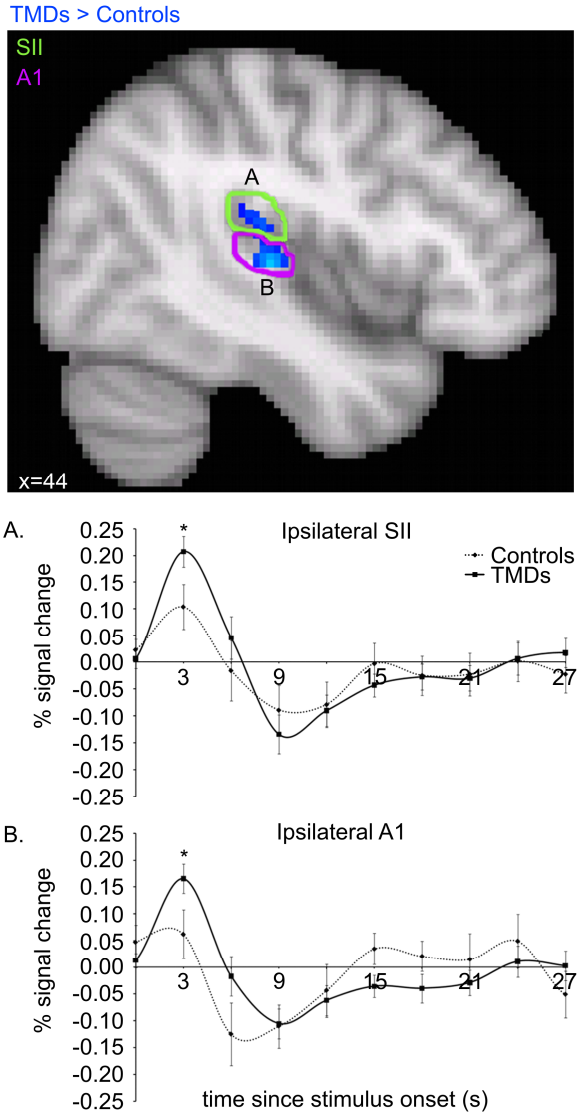

Figure 4. **Representative fMRI of SII and A1 activations during finger stimulation in individual subjects.** The Sylvian fissure is denoted by a black line overlaying individual activation maps. The parietal operculum (SII) is located above the Sylvian fissure while the transverse temporal gyrus (A1) is located below the Sylvian fissure. Only clusters with a mean threshold of $z > 2.5$ and a cluster corrected significance of $p < 0.05$ are shown. Skin flutter elicited BOLD activations on both sides of the Sylvian fissure in TMD subjects **(A)** and **(B)** but only in SII in controls **(C)**. HC = Healthy Control.

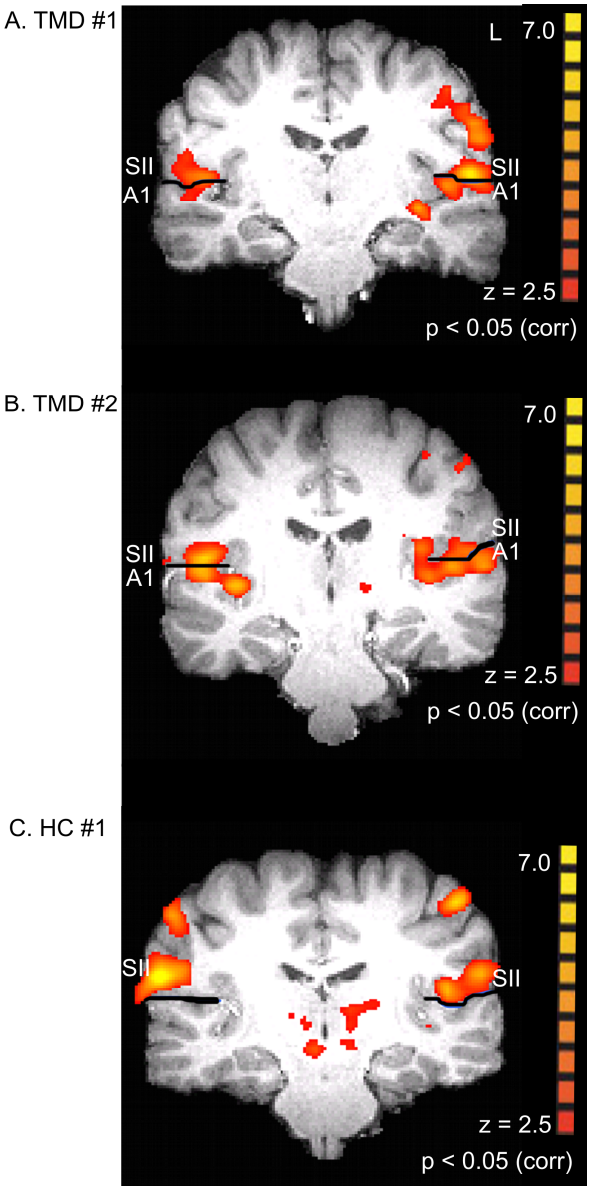

Figure 5. Comparison of mean percent signal change for controls and TMDS in (A & B) affective and (C) emotional processing areas. * indicates a statistically significant difference in the average percent signal change between groups at a particular time.

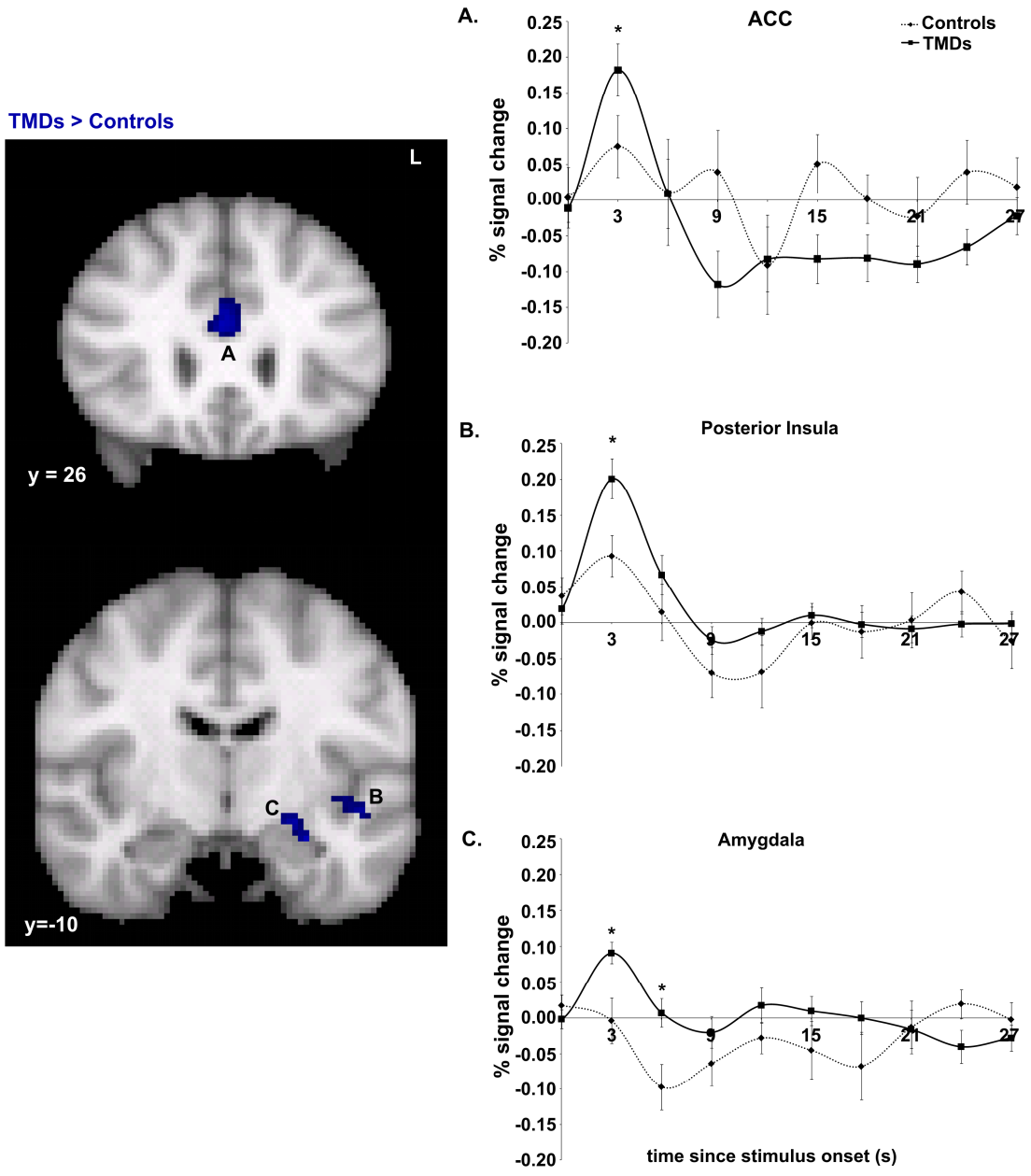

CHAPTER 3

TOUCH-PAIN INTERACTIONS IN TMD: THE EFFECT OF NOXIOUS HEAT ON RESPONSES IN SOMATOSENSORY CORTEX TO INNOCUOUS FLUTTER

A large portion of the work presented in this chapter was completed as a collaborative effort with the following researchers: Folger S, Tommerdahl M, Pelphrey K, Kahn K, and Essick G.

3.1. Abstract

To better understand the pathophysiological mechanisms underlying temporomandibular disorders (TMD), a form of persistent musculoskeletal pain in the orofacial region, we investigated the impact of noxious heat on the cortical response to vibrotactile stimulation using functional magnetic resonance imaging (fMRI). Innocuous vibrotactile stimulation and noxious skin heating were delivered separately and concurrently to the hand of subjects with TMD and to healthy controls (HC). SI was identified as an area of convergence of these two somatosensory submodalities in both groups of subjects; however, the convergence differed between HCs and TMDs. In HCs, SI responses evoked by concurrent stimulation of both submodalities were smaller than predicted by the sum of the unimodal SI responses as has been demonstrated in previous studies reported in the literature. However, in TMDs, SI responses evoked by concurrent stimulation were larger than predicted by the sum of the SI responses to unimodal stimulation. Furthermore, these superadditive SI responses in TMD subjects were correlated with the patients' McGill present pain intensity scores. Significant correlations between peak SI responses evoked by either innocuous vibrotactile stimulation or noxious skin

heating alone with present pain intensity scores in TMD subjects were not observed, suggesting that interactions in the processing of innocuous vibrotactile and noxious heat input more closely reflect individual experiences of persistent clinical pain than the unimodal processing of innocuous vibrotactile or noxious heat input alone.

Perspective: This article presents evidence that cortical mechanisms underlying the modulation of vibrotactile processing by noxious heat input are abnormal in TMD. A potential neuromechanistic explanation for this abnormal processing may involve activity dependent interneurons connecting subregions of SI that are affected by persistent clinical pain.

3.2. Introduction

Investigations of human somatosensory perception have demonstrated robust interactions between the submodalities of pain and touch. Apkarian et al reported the existence of a "touch gate," a submodality interaction in which thermally induced pain elevates vibrotactile detection thresholds and increases the perceived intensity of suprathreshold vibrotactile stimuli in healthy individuals [11, 91]. Different types of experimentally evoked pain including that from capsaicin injection [92] and electrical stimulation [58] have also been shown to impair tactile perception in pain-free subjects.

Information from nociceptors and mechanoreceptors is transmitted through the spinal cord and brain stem via distinct pathways; however, convergence between pain and touch pathways appears to occur at a relatively early stage of the somatosensory projection. Neurophysiological observations from non-human primates suggest that the responses evoked in primary somatosensory cortex (SI) by innocuous tactile stimulation and noxious skin heating are consistent with the published demonstrations of the effect of pain on touch in humans [59, 60, 93]. Evidence from human neuroimaging also indicates that the neural correlate of the

perceptual decline of touch sensitivity induced by nociception may lie in somatosensory cortices [58, 94, 95].

The convergence of pain and tactile processing in the cortex suggests that the experience of pain might not only be reflected in the processing of painful input, but might also be associated with modulation of somatosensory processing more generally. Transection of the spinothalamic tract at a cervical level of the spinal cord in patients with chronic pain has been shown to be followed not only by pain relief but also by a rapid increase in SI responsivity to innocuous electrical stimulation without producing any detectable changes in spinal or brainstem responses [96]. In addition, tactile sensory impairments have been observed in association with several clinical pain states, including temporomandibular disorders (TMD) [24, 97], a musculoskeletal condition characterized by persistent pain in the muscles of mastication, pain in the temporomandibular joint, and limited jaw function [17]. Individuals with TMD have exhibited degradation not only of the ability to detect vibrotactile stimuli compared to pain-free controls but also of the ability to discriminate between suprathreshold vibrotactile stimuli that differ only in frequency [25]. However, perceptual amplification of localized mechanical stimulation has also been observed in the presence of TMD pain [98], and the determination of a clear relationship between levels of either spontaneous or palpation-evoked pain in TMD patients and perceptual abnormalities remains elusive [25].

Observations disclosed in other human studies have demonstrated that the effect of pain on vibrotactile perception and the central nervous system processing of vibrotactile input are not explicable solely in terms of nociception-induced central inhibition even in pain-free subjects. Depending on the parameters of the noxious stimulus, perceptual gain ("hyperalgesia") as well as perceptual decline ("hypoesthesia") of somatosensory stimuli can be evoked in healthy subjects following both intracutaneous capsaicin injection [92] and

conditioning electrical stimulation of C-nociceptors [58]. Whether fMRI activity in contralateral SI increases or decreases when noxious heat is applied to the hand has been shown to depend on the spatial properties of the stimulus even when stimulus temperatures were adjusted to evoke equivalent pain intensity ratings, suggesting that cortical fMRI activity patterns for seemingly constant perceptions are not necessarily constant [99].

In order to further our understanding of the complexity of somatosensory dysfunction associated with the persistence of TMD pain, we recently investigated how cortical processing of innocuous tactile stimulation applied to the hand is altered in TMD. Responses in distinct subregions of contralateral SI, secondary somatosensory cortex (SII) and insular cortex differentiated TMD from healthy control (HC) subjects [100], and the differences between the groups in the responses evoked within SI, SII, and the insula paralleled previously reported differences in responses evoked in healthy individuals by noxious and innocuous stimulation, respectively. We suggested that these subtle, yet significant, differences may reflect cortical plasticity in TMD, manifesting itself as increased readiness for even non-orofacial cortical areas to respond to innocuous vibrotactile input that normally would not. Given this difference in cortical responsivity, the purpose of the present study was to characterize the endogenous modulation of tactile processing by experimentally induced noxious stimulation.

3.3. Materials and Methods

3.3.1. Subjects

Twenty-six women consented to a protocol approved by the Institutional Review Board at the UNC Chapel Hill. Thirteen participants fulfilled the Research Diagnostic Criteria (RDC) for TMD [17]; average age (SD) was 30.0 (9.8) years. The remaining 13 participants were neurologically healthy, pain-free controls whose average age (SD) was 28.2 (8.1) years. Twenty-

four of these subjects (12 TMD) provided data for the investigation of psychophysical and BOLD responses to innocuous flutter stimulation, which were reported in a recent publication [100].

3.3.2. Stimulation

To characterize the effect of noxious skin heating on the brain's response to innocuous tactile input, three types of stimuli were presented: 1) innocuous, low frequency vibration of the skin referred to as flutter (F), 2) noxious skin heating (H), and 3) concurrent flutter and noxious heat (FH). All stimuli were applied to the same dermatome of the hand. A piezoelectric tactile stimulator (PTS) generated a 26Hz (400µ peak-to-peak amplitude) sinusoidal stimulus which was applied to the distal pad of the right index finger during flutter events; a static surround limited the stimulation to a region under the 8-mm diameter Teflon contactor. Flutter events were 4 seconds in duration and occurred every 32 seconds; 14 events comprised a single imaging series. Skin heating stimuli were delivered to the right thenar eminence using an MR-compatible peltier device with a contact area of 2.6cm^2 (TSA-II, Medoc Advanced Medical Systems, Ramat Yishai, Israel). A Velcro strap was used to secure the thermal probe to the hand throughout the imaging session. During skin heating events, the thermal probe ramped from a baseline level approximating skin temperature (32˚C) to a moderately noxious level (49˚C) at a rate of 6˚C/s. The probe remained at this temperature for 4s before ramping down to the baseline level at a rate of -6˚C/s. Noxious skin heating events occurred every 62s to allow adequate observation of the hemodynamic response to each event, and seven events comprised an imaging series. The timing of FH events was similar to that of noxious skin heating with flutter being presented while the thermal probe was at 49˚C.

3.3.3. Experimental Protocol

All 26 subjects completed 12 fMRI scans divided over two imaging sessions to minimize subject fatigue. Session A consisted of two scans of flutter stimulation and four scans of noxious

skin heating; session B consisted of two scans of flutter and four scans of concurrent flutter and heat. Flutter scans were collected during both imaging sessions to evaluate intra-subject variability, and these data have been previously reported [100]. The order of imaging sessions for each subject and the order of scan types within each session were randomized. Subjects were instructed to keep their eyes closed and to concentrate on the presence of the stimulus.

Immediately prior to imaging, each participant completed the Short-form McGill Pain Questionnaire (SF-MPQ) to assess her current level of pain [34]. At the end of both F and FH scans, subjects were asked to rate the average intensity of skin flutter experienced using a labeled magnitude scale with the following anchor points: felt nothing (0), barely detectable (1.5), weak vibration (5), moderate vibration (16), strong vibration (33), very strong (50), and most intense vibration imaginable (100). At the end of H scans, subjects rated the average intensity of heat pain experienced using a similar scale. Subjects were instructed to choose the most appropriate label range to describe the intensity of the stimulus and then to convert that label range into a number. Subjects were familiarized with the scale and presented with two test stimuli to rate before entering the scanner room.

3.3.4. Imaging Parameters

Scanning was performed on a Siemens Magnetom Allegra, head-dedicated 3.0T scanner system with 40 -mT/m gradients and a 30 cm radio frequency (RF) volume coil. Foam cushions were used to restrict subject head motion, and earplugs and earphones were worn by subjects to reduce scanner noise. A total of 160 contiguous, high-resolution images covering the entire brain were acquired using a magnetization prepared rapid gradient echo (MPRAGE) T1-weighted sequence (TR: 1700ms, Echo Time (TE): 4.38 ms, Flip angle: 8, 1mm isotropic sampling). These structural images were aligned near-axially, parallel to the plane underlying the rostrum and splenium of the corpus callosum and were used for coregistration with the functional data.

Whole brain functional images consisted of 50 slices collected using a gradient echo pulse sequence sensitive to blood oxygenation level dependent (BOLD) contrast with echo planar k-space sampling at a repetition rate (TR) of 3000ms (TE: 30ms, Flip angle: 90, Image matrix: 64 X 64, isotropic voxel size: $3mm^3$). The functional images were aligned similarly to the structural images. A semi-automated, high-order shimming program ensured global field homogeneity. Imaging series began with two discarded RF excitations to allow the change in net magnetization of the sample following excitation to reach steady state equilibrium.

3.3.5. Image Data Analysis

The image analysis package FMRIB Software Library (FSL) version 4.1.2 [37, 38] was used for image processing and statistical analysis. Functional data were temporally realigned to adjust for interleaved slice acquisition order, corrected for subject motion using MCFLIRT [40], and spatially smoothed using a Gaussian filter with a FWHM 5mm kernel. A high-pass temporal filter with a cutoff period of 100 seconds was applied to remove low frequency artifacts from functional data, and each 4D dataset was scaled by its mean global intensity. Functional and structural images were stripped of non-brain matter [39] to improve registration. Functional images of each subject were then co-registered to structural images in native space, and structural images were warped into Montreal Neurological Institute (MNI) stereotaxic space and resampled to 2 X 2 X 2 mm^3 voxels to allow for intersession and intersubject comparison. The same transformation matrices used for structural-to-standard transformations were then applied to the co-registered functional images, and all registrations were carried out using an intermodal registration tool (affine, 12 degrees of freedom). Voxel-wise temporal autocorrelation was estimated and corrected using FMRIB's Improved Linear Model [41].

Input functions representing the timing of each event type (F, H, FH) were convolved with a double γ function to construct the regressors for a voxel-by-voxel analysis within the

framework of the general linear model. In a previously reported repeated measures analysis, no significant differences in the response to tactile flutter were observed between imaging sessions for either group [100]; accordingly, data for each participant were pooled over sessions using fixed-effects general linear modeling. To ensure equal numbers of trials among the three event types, we randomly selected two of the four F scans to include in the subject-level, fixed-effects model. Within each subject, contrast images were created for each event type versus rest and for differences between the FH response observed (OFH) and the FH response predicted by the sum of the responses evoked by F and H alone (PFH), either superadditive (OFH > PFH) or subadditive (PFH > OFH) to identify areas of information convergence.

Conventional voxel-by-voxel mixed-effects analyses were used to assess each of the contrasts across individuals and groups. Group-wise z statistic images were thresholded using clusters determined by $z > 2.3$ and a cluster corrected significance of $p < 0.05$ [42]. Following statistical thresholding, mixed-effects group contrast images of integration effects were restricted to voxels in which a significant, cluster corrected response was evoked by any one of the three event types in either group. The Harvard-Oxford cortical and subcortical structural atlases (Harvard Center for Morphometric Analysis, Charlestown, MA) and the Jülich histologic atlas were used to localize activation clusters [43, 44]. Average BOLD time courses were extracted from functional regions of interest (ROIs) identified to differentiate groups based on whole-brain analyses described above to help visualize the interaction between innocuous and noxious responses in these areas. Peak parameter estimates were then extracted from these regions and converted to percent change values using the featquery utility within FSL. Finally, to investigate individual differences regarding the influence of clinical and experimental pain on the brain's response to flutter input, multiple regression analyses between fMRI data and reported pain intensity ratings were performed within these ROIs.

3.4. Results

Analyses of psychophysical and cortical BOLD responses to the innocuous flutter stimulation were described in the previous publication of this series of reports [100]. In this paper, we focus on group responses to noxious heat and differences in the interaction in the concurrent processing of the flutter stimuli and noxious heat.

3.4.1. Self-reported Present Pain

On average, TMD subjects reported their present pain intensity on the day of imaging session A to be 2.3 on a 10 cm visual analog scale with end labels of no pain (0) and worst possible pain (10). TMD subjects reported an average present pain intensity of 2.8 out of 10 on the day of imaging session B. Control subjects reported an average present pain intensity of 0.14 out of 10 on the day of session A and 0.18 out of 10 on the day of session B. A paired t-test indicated that the difference in present pain intensity between the two sessions was not significant for either group (Figure 6). When we combined pain reports for both sessions, the TMD group reported significantly more pain on the day of testing than the HC group ($p < 0.001$).

3.4.2. Response to noxious skin heating

3.4.2.1. Perceptual Ratings

The subjective experience of pain intensity evoked by the 49˚C stimulus applied to the hand differed markedly across individuals in both the control and TMD groups (Figure 7A). On average, the TMD group rated the intensity of pain as 37.0 (SD = 18.0), corresponding to a level between "strong" and "very strong" on the labeled magnitude scale while the control group rated the intensity of the same stimuli as 34.0, on average (SD = 14.0), corresponding to a level of "strong." This small difference in mean perceived intensity was not statistically significant ($p < 0.18$). Average heat pain ratings were not significantly correlated with the present pain

intensity ratings of the TMD subjects (Figure 7B), indicating that subjects' clinical pain did not affect their ratings of the noxious heat.

3.4.2.2. Imaging Data

Individual Group Analysis

Analysis of fMRI data revealed a common network of evoked pain related activity in controls and TMDs. For both groups, noxious heat evoked statistically significant, positive hemodynamic responses throughout the lateral pain system including bilateral SII [44, 46], anterior insular cortex, and the pallidum. Both groups also demonstrated evoked activity in components of the medial pain system including bilateral anterior insula, anterior cingulate cortex (ACC), and posterior mid-cingulate cortex (pmCC). Contralateral middle frontal gyrus (MFG) and bilateral inferior parietal lobule (IPL) were also engaged by noxious heat in HCs and TMDs. Table 4 indicates the MNI coordinates of all significant activation clusters by group, and Figure 8A illustrates the pattern of activation for each group in these regions.

Between Group Analyses

Evaluation of (control – TMD) and (TMD – control) heat pain contrasts revealed no areas in which the two groups demonstrated a statistically significant difference in their response to noxious heat.

3.4.2.3. Relationship between perceptual and cortical responses to noxious heat

We found a statistically significant, positive correlation between heat pain ratings and peak percent change parameter estimates for H responses in SII in both groups (Figure 9).

3.4.3. Effect of noxious skin heating on innocuous flutter stimulation

3.4.3.1. Perceptual Ratings

Healthy controls rated the intensity of flutter stimulation in the presence of heat producing pain as 16.2, on average (SD=11.5), which corresponded to "moderately intense."

Compared to perceived flutter intensity ratings reported by HCs in the absence of heat producing pain [100], these ratings were 17.7% lower, on average (SD=5.4%). TMD subjects rated the intensity of flutter in the presence of heat producing pain as 31.8 (17.5), on average, a rating that corresponded to a level between "moderately intense" and "strong." Although five of 13 TMD subjects perceived a decrease in flutter stimulation intensity with the addition of concurrent noxious heat, the TMD group on average reported a 10.7% (SD=37.2%) increase in perceived flutter intensity in the presence of heat producing pain (Figure 10). The difference between groups in the heat pain-evoked change in flutter ratings was statistically significant ($p<0.01$).

3.4.3.2. Imaging Data

Individual Group Analysis

For both groups, concurrent flutter and noxious heat stimulation of the hand elicited statistically significant BOLD responses in somatosensory processing areas, namely SI, SII, and insular cortex. In addition, HCs and TMDs demonstrated robust responses bilaterally in ACC, pmCC, and the inferior parietal lobule, which are sensory association areas. Table 5 lists the coordinates of all significant FH activations for HCs; Table 6 lists significant FH clusters in TMDs, and Figure 8B illustrates the pattern of activation for each group in these regions.

A number of these regions also exhibited statistically significant differences between the FH response observed and the FH response predicted by the sum of the responses evoked by F and H alone within each group, suggesting that flutter and noxious heat input to these areas interacted. For the control group, subadditive responses (PFH > OFH) were identified in contralateral SI, bilateral SII, and bilateral insula. No statistically significant superadditive responses (OFH > PFH) were identified. For the TMD group, superadditive responses were found bilaterally in SI and pmCC. No statistically significant subadditive responses were

observed. Table 7 lists the coordinates of all clusters showing significant differences between predicted and observed BOLD responses evoked by concurrent flutter and noxious heat stimulation.

Between Group Analyses

Evaluation of (HC – TMD) and (TMD – HC) contrasts revealed several regions in which one group demonstrated a greater difference between the predicted and observed response evoked by concurrent stimulation. Consistent with the individual group analyses, HCs exhibited greater subadditive responses than TMDs in contralateral SI and IPL (Figure 11A) while TMDs showed greater superadditive responses than HCs in contralateral SI and bilateral pmCC (Figure 6B). The subadditive classification is relatively nonspecific since a voxel in SI that shows the same percent signal change in response to each condition, e.g., (F, H, FH) = (.3%, .3%, .3%), would be classified as subadditive because FH < (F + H) even though the voxel responded equally well to the uni- and bi-modal stimulation. Extracting HDRs from SI voxels labeled subadditive that did not show a significant response to FH in HCs, we observed that the addition of noxious heat almost entirely suppressed any positive BOLD response (Figure 11C). This is in contrast with the remaining SI subadditive voxels, which responded similarly for all three stimulation conditions (Figure 11D), suggesting that flutter and noxious heat input converged in these voxels without interacting. The classification of superadditive is more specific, indicating a level of response enhancement beyond that which can be explained by two non-interactive information streams. In the TMD group, the peak of the SI response to FH was greater than the sum of the peaks for flutter and noxious heat alone (Figure 11E). Flutter and noxious heat evoked reciprocal responses in these superadditive SI voxels, but when combined, the SI response was augmented.

3.4.3.3. Relationship between changes in flutter perception and cortical processing

A strong, negative correlation was observed in HCs between peak percent change values for subadditive responses in SI and changes in the perceived intensity of flutter stimulation in the presence of noxious heat ($R^2 = 0.79$, $p < 0.0004$, Figure 12, solid line). In other words, upon application of noxious heat, the perceived intensity of flutter stimulation decreased as the difference between the predicted and observed SI FH response increased among HCs but not among TMDs (Figure 12, dashed line).

SI superadditive responses were found to be positively correlated with McGill present pain intensity scores for TMD subjects (R^2=0.72, $p < 0.0003$); TMDs who experienced greater levels of clinical pain on the day of imaging demonstrated greater augmentation of observed SI FH responses with respect to predicted SI FH responses (Figure 13A, dashed line). No such significant correlation between peak percent change responses for either F or H in SI and present pain intensity scores (Figure 13B), suggesting that processing interactions between F and H input are more closely related to individual experiences of ongoing clinical pain than the processing of F or H input alone.

3.5. Discussion

To the best of our knowledge, the present report is the first examination of brain activity associated with the interaction between flutter and noxious skin heating input in individuals with persistent musculoskeletal pain. The results highlight several main findings: (1) Within the processing network common to unimodal and bimodal stimulation, differences emerged in the cortical patterns characterizing interactions between somatosensory submodalities in subjects with and without TMD. (2) These differences in the interaction of innocuous and noxious input are related to the severity of the TMD patients' clinical pain and

emerge despite the fact that pain ratings and cortical responses to noxious heat alone did not differ significantly between TMD patients and control subjects.

Common cortical network

Concurrent flutter and noxious heat engaged a network that included all areas responsive to noxious heat alone plus areas reported to be responsive to flutter stimulation alone in these same subjects [100]. The cortical network of activation elicited by noxious heat in both groups was similar to patterns previously reported by various investigators. First, SII is commonly activated bilaterally in heat pain studies [67, 101-104]. Second, anterior cingulate [57, 105], mid-cingulate [106, 107], and insular cortices [57, 104, 105] are all components of the limbic system, are all routinely activated during PET and fMRI studies involving heat-evoked pain, and have all been implicated in processing the affective dimension of pain. Third, prefrontal cortical areas have also been shown to be activated by heat pain and may be related to cognitive variables such as memory, stimulus evaluation, or pain catastrophizing [67, 108, 109].

Interactions between innocuous and noxious input

SI was identified as an area of submodality convergence in both groups. In HCs, flutter alone evoked a positive BOLD response in SI voxels exhibiting convergence while noxious heat alone evoked no response or a small, negative BOLD response in these voxels. In TMDs, flutter alone similarly evoked a positive BOLD response in SI voxels identified as integrative while noxious heat evoked a negative BOLD response. When flutter and noxious heat were delivered concurrently, the two groups of subjects differed in the effect of submodality convergence both on tactile perception and on SI responsiveness.

Consistent with published psychophysical evidence of a touch-gate in healthy individuals [11, 12, 91], all 13 HCs perceived a reduction in the intensity of flutter stimulation in the

presence of heat producing pain. Since SI is critical for tactile sensation and the magnitude of response evoked in SI has been shown to depend on the intensity of tactile stimulation [36, 55, 110], it would be reasonable to expect that the diminished perception of flutter reported by HCs would reflect a suppression of the SI response evoked by flutter with the addition of concurrent noxious heat. In fact, we observed a close correlation between the magnitude of noxious heat induced changes in the perception of flutter intensity and noxious heat induced changes in SI responsivity. In HCs, SI was identified as a region in which the interaction of innocuous and noxious processing produced a response that was smaller than predicted by the sum of the responses to unimodal stimulation. Since the response to concurrent FH stimulation more closely resembled the response to H alone, this difference appeared to be due to a suppression of the flutter response by noxious heat, a finding that corroborates evidence from previous human neuroimaging studies indicating that experimentally evoked pain can inhibit SI [58, 59, 94, 95] and that the magnitudes of SI inhibition and sensory perceptual decline are correlated [58]. In addition, optical intrinsic signal (OIS) imaging data from squirrel monkeys suggest that inhibitory interneurons connecting subregions of SI may be responsible for this modulation of SI responsivity to tactile stimulation by noxious heat [59, 60]; noxious heat evokes reciprocal optical intrinsic signal changes in subregions 3b/1 and 3a of SI, and correlation analysis of the time courses of these changes indicates that activity evoked by noxious heat in the fringe of SI (3a/2) suppress activity in the core (3b/1). It has also been demonstrated that stimulus evoked decreases of the BOLD signal represent, at least in part, a reduction of neuronal activity itself [111], further suggesting that neuronal inhibition contributed to the decreases in SI BOLD signals observed during concurrent FH stimulation.

In contrast to HCs, SI information convergence in TMDs produced BOLD responses to FH stimulation that were larger than would be predicted by the sum of the responses to unimodal

stimulation. This enhancement of SI responsiveness was consistent with the perceived increase in flutter intensity reported on average in the TMD group in the presence of heat producing pain. Evidence from intracellular microelectrode recordings in squirrel monkeys points to a possible neuromechanistic explanation for the opposing effects of noxious heat on tactile perception and processing that we observed between TMDs and HCs. The action of corticocortical connections between subregions of SI that respond to innocuous and noxious input may depend on the level of rapidly adapting (RA) neuron activity; when SI RA neuron activity is weak, nociceptor afferent drive makes it weaker, decreasing mean firing rate (MFR) and the degree to which RA neurons entrain to flutter stimulation, but when SI RA neuron activity is strong, nociceptor afferent drive either has no effect or enhances SI activity, increasing MFR and entrainment [93]. We reported in a previous publication that BOLD responses evoked by innocuous flutter stimulation alone in these TMD subjects were enhanced in a subregion of SI compared to controls [100]. As an indirect measure of neuronal activity, enhanced BOLD responses indicate that the stimulus-evoked RA neuron activity in SI is stronger than normal, and consistent with the stimulus-dependent polarity theory, stronger RA neuron activity was made stronger still when delivered in the presence of noxious heat.

The activity dependence of the effect of nociceptor afferent drive on SI responsivity may also explain the variable effect we observed within the TMD group of noxious heat on flutter intensity ratings. On average, flutter intensity ratings increased in the presence of noxious heat in the TMD group; however, for 5 of the 13 TMD subjects, flutter intensity ratings decreased in the presence of noxious heat. A post hoc analysis comparing SI BOLD responses to flutter alone in TMD subjects reporting a reduction in flutter intensity to those reporting an increase in flutter intensity in the presence of noxious heat revealed that, on average, TMD subjects whose flutter

intensity ratings decreased, demonstrated a weaker peak percent signal change response in SI than did TMD subjects whose flutter intensity ratings increased (Figure 14).

Also in contrast to HCs, no significant correlation was found in the TMD group between the amplitude of noxious heat induced changes in the perception of flutter intensity and noxious heat induced changes in SI responsivity despite the fact that flutter intensity ratings increased on average and superadditive responses were evoked within SI. Even when we subdivided the TMD group by the effect of noxious heat on the flutter intensity ratings, we still did not detect a correlation between noxious heat induced changes in flutter intensity ratings and changes in SI responsivity. It is possible that the emergence of superadditive responses in SI during concurrent FH stimulation reflected changes in the perception of the noxious heat. Electrophysiological data from squirrel monkeys have demonstrated that the magnitude of spike firing in SI nociresponsive neurons associated with a short-duration noxious heat stimulus increases linearly with the temperature of the stimulus [61]. Observations from human studies also suggest that BOLD responses in SI reflect the perceived intensity of evoked pain both in healthy controls [112] and chronic pain patients [113, 114]. Since we did not also collect data during concurrent stimulation with the subjects' attention directed towards the noxious heat stimulus, we cannot know with certainty if the emergence of superadditive responses reflected changes in TMD subjects' perception of the noxious heat. It is also possible that both sensory inputs may have influenced the subjects' ratings of flutter during concurrent FH scans even though subjects were instructed to direct their attention exclusively towards the flutter stimulus.

Relation to ongoing clinical pain

Although noxious heat induced superadditive responses in SI were not correlated with noxious heat induced changes in flutter intensity ratings in the TMD group, noxious heat

induced superadditive responses in SI were correlated with the subjects' McGill present pain intensity scores. This contrasts to the lack of a significant correlation between peak BOLD responses evoked by either F or H alone in SI and the present pain intensity scores in TMD subjects, suggesting that processing interactions between F and H input more closely reflect individual experiences of clinical pain than the processing of F or H input alone. A relationship between persistent pain and SI responsiveness has been observed in other chronic pain populations. As examples, cortical reorganization in SI has been shown to increase with the intensity of phantom limb pain [31] and can be reversed when phantom pain is eliminated [32]. In chronic regional pain syndrome patients, pain relief associated with a combination of morphine and an NMDA-receptor antagonist therapy was related to suppression of SI during movement [115]. Whether the superadditive SI responses observed in the present study would be reduced with the reduction of clinical pain is a question that remains for future investigation.

Lack of significant group differences in the perception of noxious heat

We observed the differences described above in the effect of noxious heat stimulation on tactile perception and on cortical patterns of somatosensory submodality integration in HCs and TMDs despite not detecting significantly different perceptual or cortical responses to noxious heat alone between groups, further suggesting that only the interaction between innocuous and noxious input differs for the two group of subjects. We predicted that TMD subjects would perceive the heat pain stimulus as more intense than controls; rather, we observed only that the subjective experience of pain intensity evoked by a 49˚C stimulus to vary widely across individuals in both the HC and TMD groups. Thus, the small group difference that was observed in subjective pain perception was not statistically significant. TMD represents a heterogeneous constellation of painful conditions, and patients experience TMD pain both with and without concurrent altered sensitivity to painful modalities such as heat. Some

psychophysical studies have provided evidence for generalized hyperalgesia in TMD, reporting lowered ischemic and heat pain thresholds in TMD patients within the clinically painful region as well as outside of it [116-119]; however, other investigations have reported normal pain perception in TMD subjects [120, 121]. Because pain is a complex, personal experience influenced by multiple interactive biopsychosocial processes, identical noxious stimuli can produce different experiences of pain across individuals. Possible group differences between control and TMD subjects' sensitivity to thermal pain could have been confounded by the high within-group variability in thermal pain perception and by intersubject differences in the use of the rating scale since we did not perform a rigorous calibration of the scale with each participant.

Lack of significant group differences in the cortical response to noxious heat

That we observed no significant group difference in the patterns of activation evoked by H alone is consistent with the fact that we observed no significant group difference in subjective pain perception. Neuroimaging investigations of other chronic pain conditions such as fibromyalgia (FM) and chronic low back pain have demonstrated that group differences in central pain processing emerge when subjective pain perception is unequal in control and chronic pain groups; when subjective pain perception is equated, painful stimuli evoke activation throughout a similar network of brain regions in subjects with and without chronic pain [113, 114, 122]. In addition, Coghill et al demonstrated that varying perceptual responses to heat pain in healthy individuals are accompanied by differential central processing of noxious input and are not simply the result of response bias or measurement error [123]. In fact, we found a positive correlation between heat pain ratings and peak percent signal change responses in SII in both groups, which is consistent with reports indicating a role for SII in the sensory-discriminative aspect of pain perception [67, 102, 103].

The fact that we failed to detect a significant SI response to noxious heat in either group is also not unprecedented; meta-analyses of neuroimaging studies using various imaging modalities and types of painful stimuli also reported inconsistent activation of SI [107, 124]. It is unlikely that the absence of a significant SI response was due to the relatively short duration of our noxious heat stimuli since it has been shown that the magnitude of BOLD percent signal changes evoked by short (3-4s) and long duration heat pain stimuli is similar [125]; however, several neurophysiological and anatomical considerations could account for this inconsistency. The size of an uninterpolated functional volume element (voxel) in this study was 3 X 3 X 3 mm^3 and the use of much larger voxels is common; thus, the signal obtained from each voxel was influenced by hundreds of thousands of neurons. Although nociresponsive neurons are known to exist in SI, their numbers are far fewer than the number of SI neurons identified to encode tactile input [126, 127]. As has been mentioned, evidence from animal studies indicates the presence of corticocortical inhibitory interactions between subdivisions of SI [59, 60]; the precise somatotopic organization of SI and the probable mixture of excitatory and inhibitory effects of nociceptive input to SI may lead to focal activations which are degraded by anatomic variability when averaging across subjects. In single-unit physiology, multisensory integrative response amplification is greater with weaker stimuli [128] and it is possible that our inability to detect responses to noxious heat stimulation alone on the group level helped strengthen the group differences we observed in submodality integrative responses within SI.

A limiting factor of the present study is our sample size; although the number of subjects included in this study is comparable to many functional neuroimaging investigations, it may be small considering the heterogeneity in the clinical presentation of TMD. Despite this heterogeneity, we detected a disruption in the cortical convergence of innocuous and noxious input in TMD which manifested itself as a reversal in the effect of noxious heat input on SI

responsivity to innocuous flutter compared to controls. The cortical dynamics evoked by concurrent innocuous and noxious skin stimulation appear to be more closely coupled with individual pain experience than the responses evoked by innocuous or noxious skin stimulation alone. Further investigation of how these differences in submodality convergence affect the endogenous modulation of pain by touch would continue to improve our understanding of the complexity of sensory disruption in chronic pain.

3.6. Acknowledgments

The authors would like to thank Steven Smith and MRI technologists Kathy Wilber, Amber Abernethy, James Barnwell, and Emilie Kearns for assistance with data acquisition as well as Ollie Monbureau and Mike Young for technical assistance. This work was supported by NIH grant P01 NS045685.

Table 4. Regions activated by noxious skin heating in control and TMD groups. Only significant clusters of activation corrected for multiple comparisons ($p<0.05$) are listed. Up to three significant peak activations in each cluster are listed. C = side contralateral to the site of skin stimulation, I = side ipsilateral to the site of skin stimulation.

Region	Side	Cluster Size	Peak Voxel Z	MNI Coordinates x,y,z (mm)
Controls				
Insula, Pallidum, SII	I	5986	6.07	40, 10, -4
			5.63	40, 0, 4
			5.17	14, 6, -6
			4.87	46, 0, 0
Insula, Pallidum, SII OP1	C	4409	6.13	-38, 14, -8
			4.61	-10, 2, -6
			4.60	-40, -20, 12
Posterior mid-cingulate, ACC	I,C	3099	6.77	4, -24, 26
			6.13	4, 26, 30
			5.82	-6, -22, 28
			4.93	0, 30, 34
Frontal pole, Middle frontal gyrus	C	1073	4.67	-36, 46, 8
			3.76	-40, 34, 20
Inferior parietal lobule PFm	C	734	4.34	-52, -46, 46
Inferior parietal lobule PFm	I	382	4.33	58, -42, 52
TMDs				
Insula, Middle frontal gyrus, Pallidum, Precentral gyrus BA44	I	6456	6.64	38, 20, -2
			6.53	42, 38, 20
			5.94	14, 2, -6
			5.76	54, 6, 16
Pallidum, Insula, Middle frontal gyrus, Insula Id1	C	4143	6.91	-12, 8, -4
			5.8	-34, 18, -10
			5.69	-42, 34, 18
			4.85	-38, -16, -2
Paracingulate gyrus, ACC	I, C	1997	6.94	6, 18, 48
			5.59	6, 14, 38
			4.81	-10, 24, 32
Inferior parietal lobule PF	I	1073	6.3	52, -38, 48
Cerebellum	C	977	5.70	-34, -62, -38
Inferior parietal lobule PF/PFm	C	759	4.91	-54, -44, 44
Posterior mid-cingulate	C, I	725	5.97	-4, -22, 26
			5.88	6, -26, 26
SII	C	532	4.70	-60, -18, 18
Thalamus	I	470	4.80	12, -16, 6

Table 5. Regions activated by concurrent flutter and noxious skin heating in HCs. Only significant clusters of activation corrected for multiple comparisons ($p<0.05$) are listed. Up to three significant peak activations in each cluster are listed. C = side contralateral to the site of skin stimulation, I = side ipsilateral to the site of skin stimulation.

Region	Side	Cluster Size	Peak Voxel Z	MNI Coordinates x,y,z (mm)
Insula, frontal pole, Inferior frontal gyrus	I	4870	6.86	38, 20, 4
			6.21	44, 18, -4
			5.63	42, 48, 4
			5.44	58, 10, 12
Inferior parietal lobule PF, SII OP1	I	2951	5.81	54, -36, 44
			5.62	68, -28, 26
			5.24	60, -26, 28
Cerebellum	I	1075	5.86	22, -68, -50
Pallidum, Thalamus	I	1044	4.75	20, 2, 0
			4.60	16, -10, 14
Insula, Posterior insula, Putamen	C	4214	6.91	-40, 14, -4
			6.49	-38, 0, 8
			5.83	-40, -16, 10
			5.18	-26, 0, -8
Inferior parietal lobule PFm/Pga, SI	C	2284	5.83	-54, -52, 48
			5.81	-68, -28, 28
			4.51	-56, -32, 54
Paracingulate gyrus, ACC	C, I	1391	5.13	-6, 30, 34
			4.89	4, 26, 32
			4.49	-2, 28, 26
SII OP1, A1	C	1144	6.37	-48, -20, 16
			5.72	-44, -18, 8
Cerebellum	C	1049	4.93	-32, -58, -36
Posterior mid-cingulate	C, I	782	5.74	-2, -28, 30
			5.47	6, -26, 28
Frontal pole	C	778	5.47	-36, 48, 10

Table 6. Regions activated by concurrent flutter and noxious skin heating in TMDs. Only significant clusters of activation corrected for multiple comparisons ($p<0.05$) are listed. Up to three significant peak activations in each cluster are listed. C = side contralateral to the site of skin stimulation, I = side ipsilateral to the site of skin stimulation.

Region	Side	Cluster Size	Peak Voxel Z	MNI Coordinates x,y,z (mm)
Insula, Insula Id2, Thalamus, Putamen	C	3817	7.87	-34, 16, 2
			6.29	-40, -14, -2
			5.89	-16, -14, 8
			5.47	-26, 2, -6
Cerebellum	C	2479	5.95	-36, -52, -38
Inferior parietal lobule PF, SI, Angular gyrus	C	2136	5.68	-58, -46, 48
			4.94	-54, -32, 52
			4.79	-48, -58, 40
ACC	C, I	2004	6.08	-10, 26, 26
			5.70	6, 26, 34
Frontal pole	C	974	5.32	-36, 52, 16
Posterior mid-cingulate	C, I	885	5.5	-4, -30, 24
SII OP1	C	414	5.46	-54, -30, 22
			5.0	-48, -22, 18
Insula, Frontal pole, Putamen, Middle frontal gyrus	I	6754	7.49	44, 12, -4
			6.91	46, 38, 22
			5.85	16, 12, -2
			5.7	42, 26, 34
Inferior parietal lobule PF/PFm, Anterior intra-parietal sulcus hIP1, SII OP1	I	2964	5.47	58, -40, 52
			4.9	38, -56, 36
			4.52	60, -18, 16
Cerebellum	I	993	5.32	18, -66, -52
Superior parietal lobule 7M	I	313	5.79	10, -72, 38

Table 7. Regions of innocuous flutter and noxious heat convergence in HCs and TMDs. Only significant clusters of activation corrected for multiple comparisons ($p<0.05$) are listed. Up to three significant peak activations in each cluster are listed. C = side contralateral to the site of skin stimulation, I = side ipsilateral to the site of skin stimulation.

Region	Side	Cluster Size	Peak Voxel Z	MNI Coordinates x,y,z (mm)
HC PFH > OFH				
SII OP4, OP1, Insula	C	1395	4.59	-46, -4, 8
			4.11	-60, -24, 18
			3.66	-42, -4, -4
Insula, Putamen, SII OP4	I	1063	4.26	42, 2, -2
			3.69	18, 10, -2
			3.31	50, 0 , 10
SI	C	489	3.93	-56, -28, 50
TMD OFH < PFH				
SI	C	1413	4.05	-32, -36, 54
			4.00	-34, -40, 54
Posterior mid-cingulate	I,C	1590	3.56	8, -2, 40

Figure 6. Average pain on the day of testing. Clinical pain experienced on the day of testing did not differ significantly between session A and B within groups but did differ significantly between the healthy control (HC) group and the TMD group.

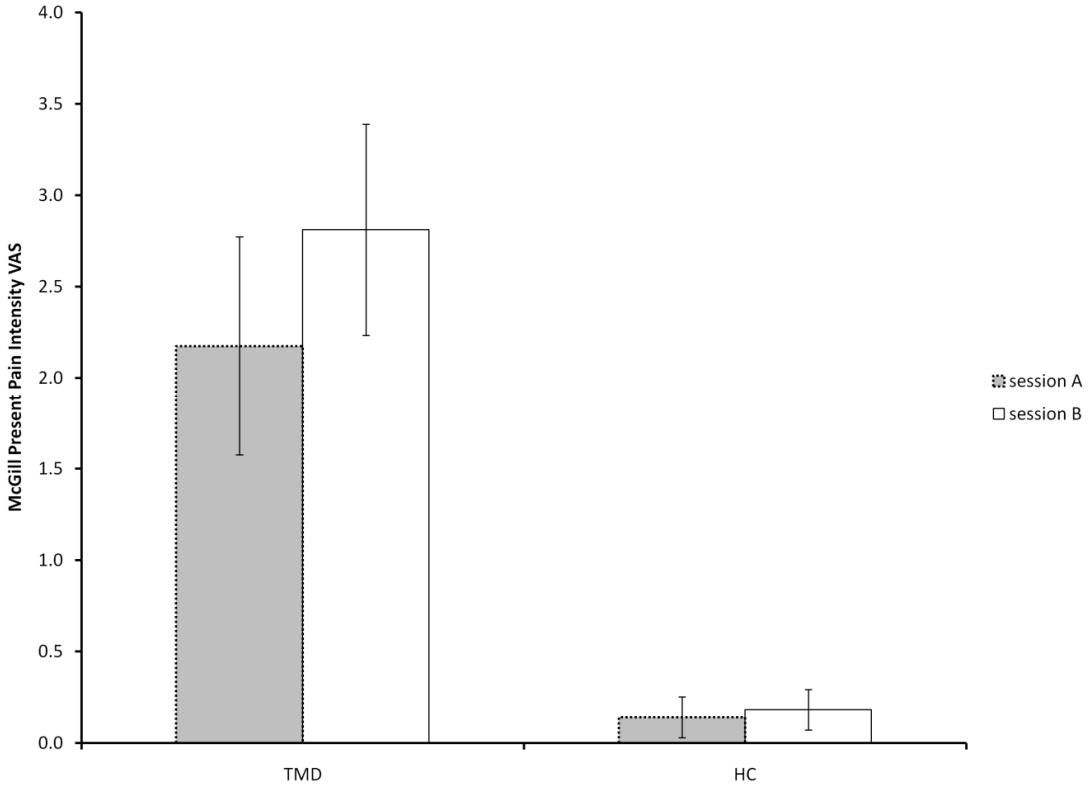

Figure 7. Experimentally-evoked and present clinical pain. (A) The distribution of average heat pain intensity ratings demonstrates that the subjective experience of pain intensity evoked by a 49˚C stimulus differed across individuals in both control and TMD groups. The solid horizontal line indicates the mean for all 26 subjects. **(B)** Heat pain intensity ratings in TMD subjects were not correlated with reports of their present clinical pain levels.

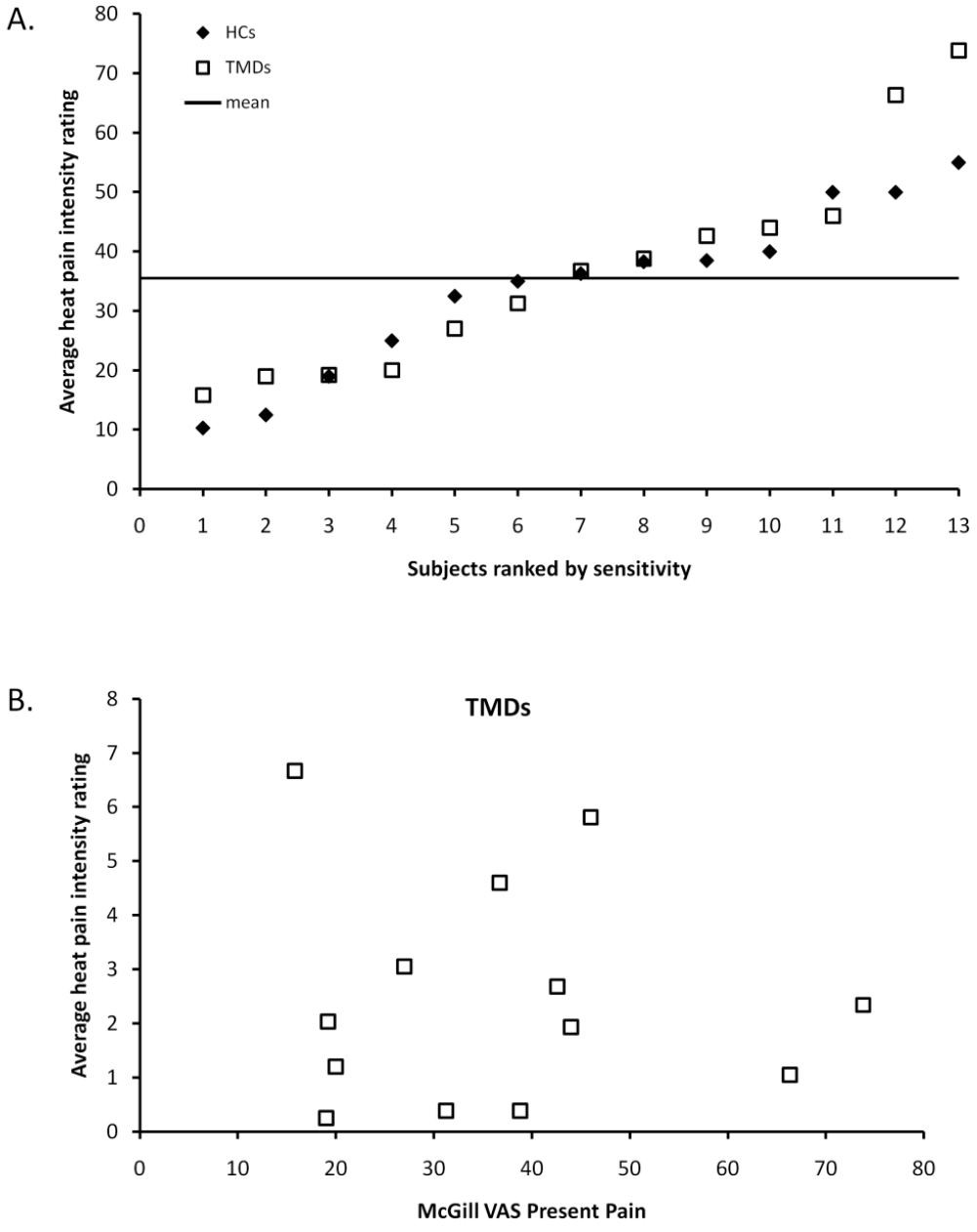

Figure 8. Activity evoked by noxious heat alone and by concurrent flutter and noxious heat. Masks of significant clusters of activation evoked by **(A)** noxious heat and **(B)** concurrent flutter and heat for the control group only in yellow, the TMD group only in blue, and for both groups in green. A cluster mean threshold of $z > 2.5$ and a cluster corrected significance of $p < 0.05$ were used. Activation masks are overlayed on average anatomical images for all 26 subjects. Insula activation is circled. ACC = Anterior Cingulate Cortex, Ins = Insula, MFG = Middle Frontal Gyrus, PC = posterior Mid-Cingulate Cortex, Pd = Pallidum, PF = Inferior parietal lobule PF, SII = Secondary Somatosensory Cortex, Thal = Thalamus

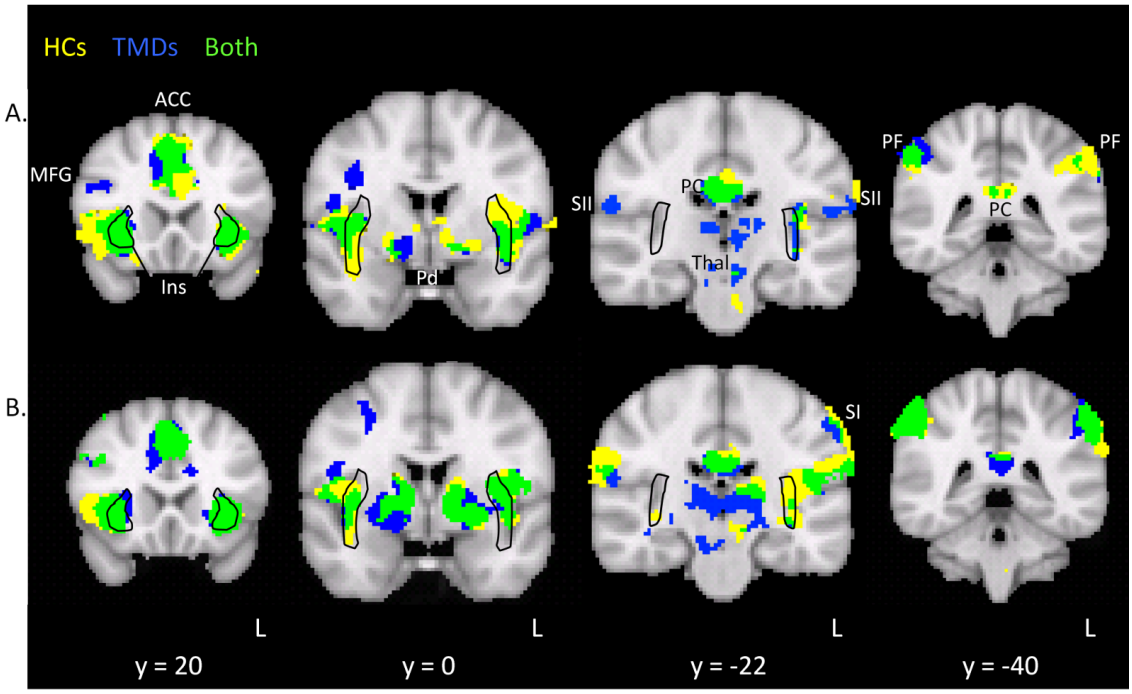

Figure 9. Relationship between reported heat pain intensity and brain response in SII. There was a positive correlation between peak responses evoked in SII by noxious heat and average heat pain intensities reported among HCs and TMDs.

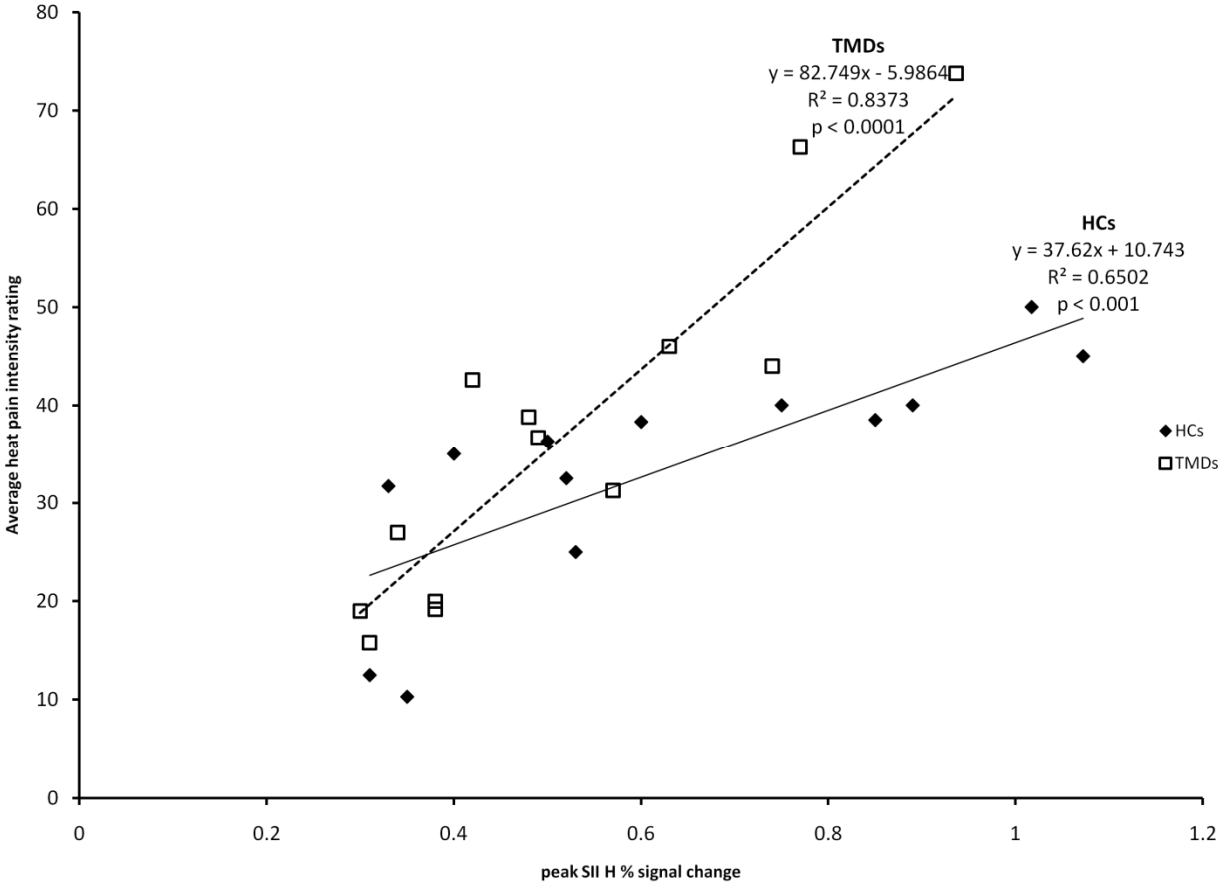

Figure 10. Effect of noxious heat on perceived flutter intensity. On average, the healthy control group (HC) perceived flutter to be 17.7% less intense in the presence of heat producing pain. Although five of 13 TMD subjects perceived a decrease in flutter stimulation intensity with the addition of concurrent noxious heat, on average, the TMD group reported a 10.7% increase in perceived flutter intensity in the presence of heat producing pain.

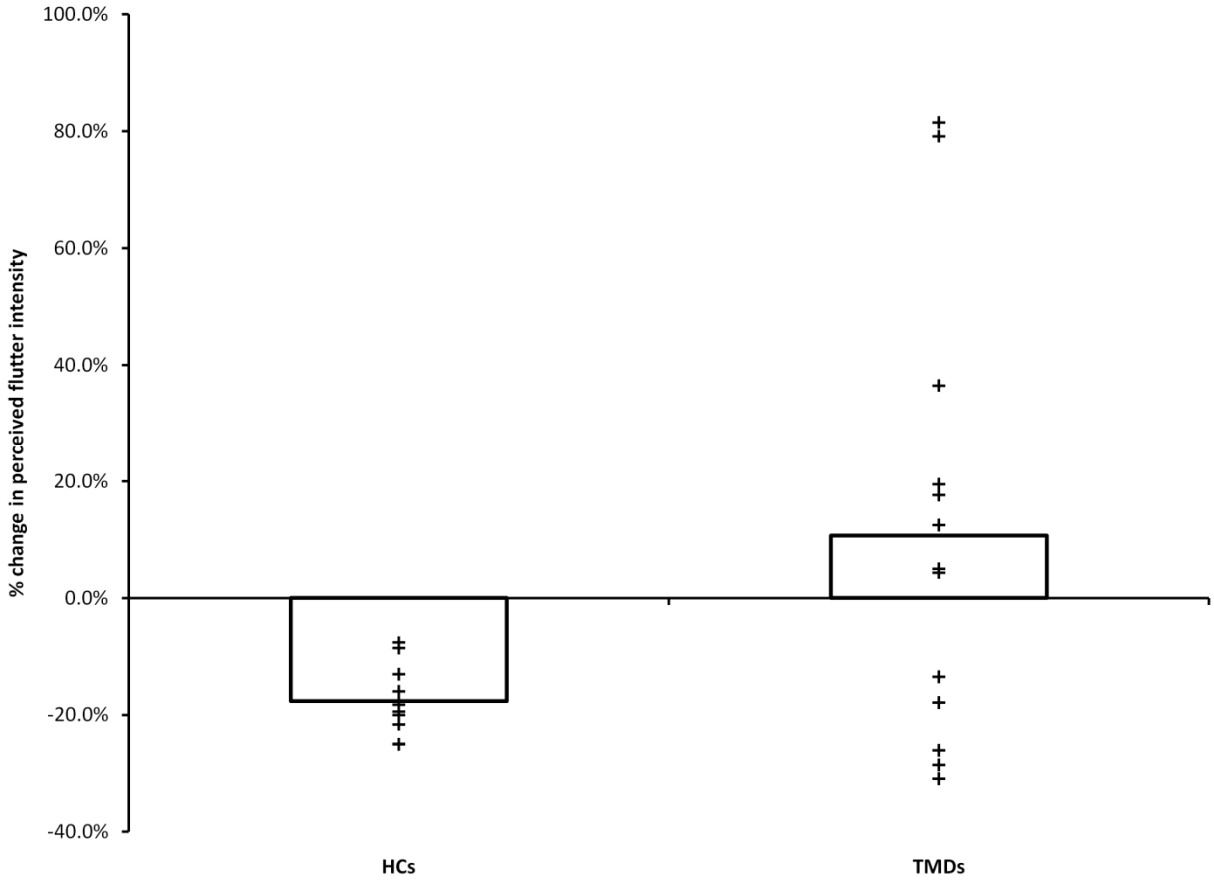

Figure 11. Group dissociation in innocuous and noxious interactions. (A) HCs only showed areas (in orange) in which the observed FH response was significantly less than the response predicted by responses to F and H separately (subadditive responses). **(B)** TMDs only showed areas (in blue) in which the observed FH response was significantly greater than the predicted FH response (superadditive responses). **(C)** A subset of voxels labeled subadditive in HCs demonstrated a reduction in the magnitude of response to F in the presence of noxious heat while **(D)** the remaining subadditive voxels showed no significant difference in the magnitude of response to F with or without noxious heat. **(E)** All SI voxels labeled superadditive in TMDs demonstrated reciprocal responses to F and H alone, but during concurrent FH stimulation, their responses were augmented. A cluster mean threshold of $z > 2.3$ and a cluster corrected significance of $p < 0.05$ were used. Activation masks are overlayed on average anatomical images for all 26 subjects.

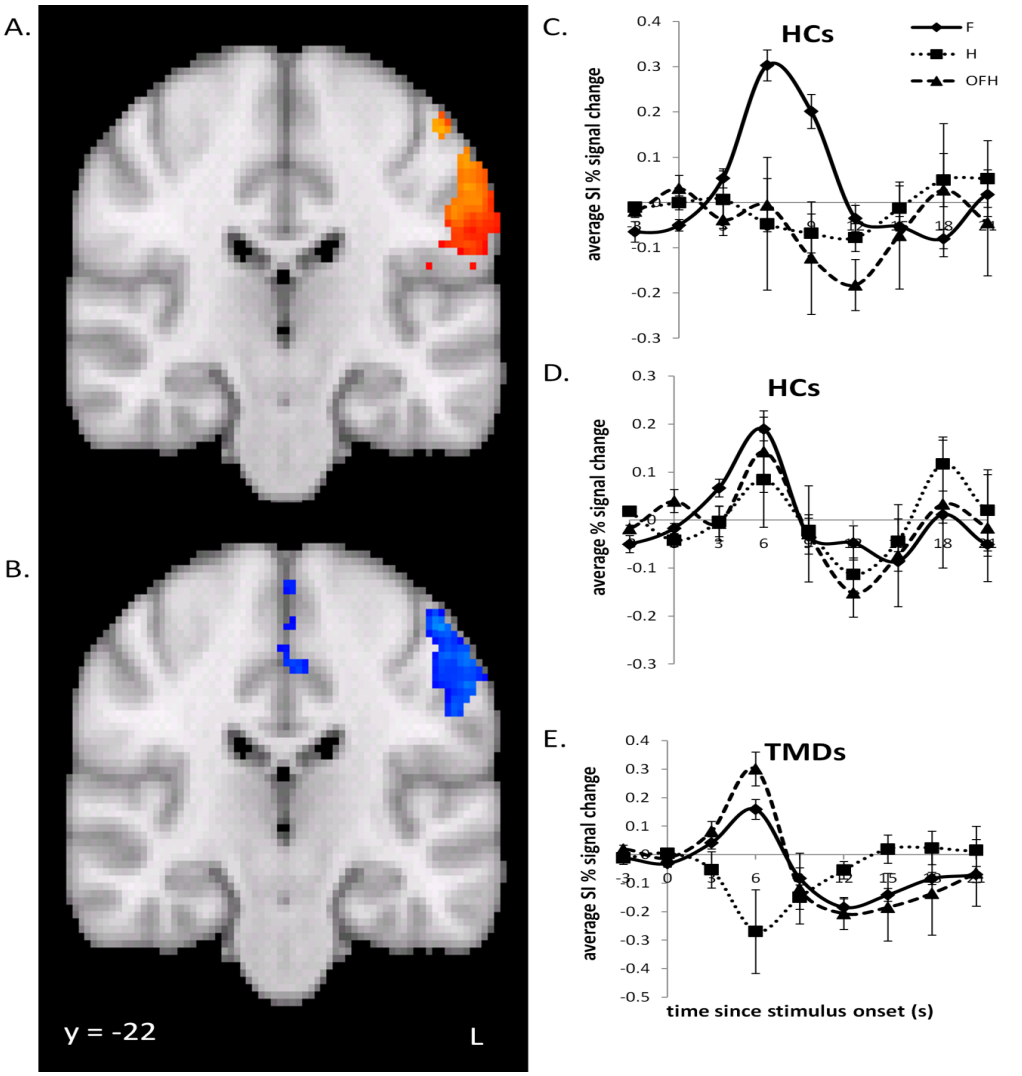

Figure 12. Relationship between effects of noxious heat on flutter perception and cortical processing. In controls, with the addition of noxious heat, the perceived intensity of flutter stimulation decreased as the difference between the predicted and observed SI FH responses increased. In TMDs, no significant correlation was observed between the magnitude of nociception-induced changes in flutter perception and SI processing.

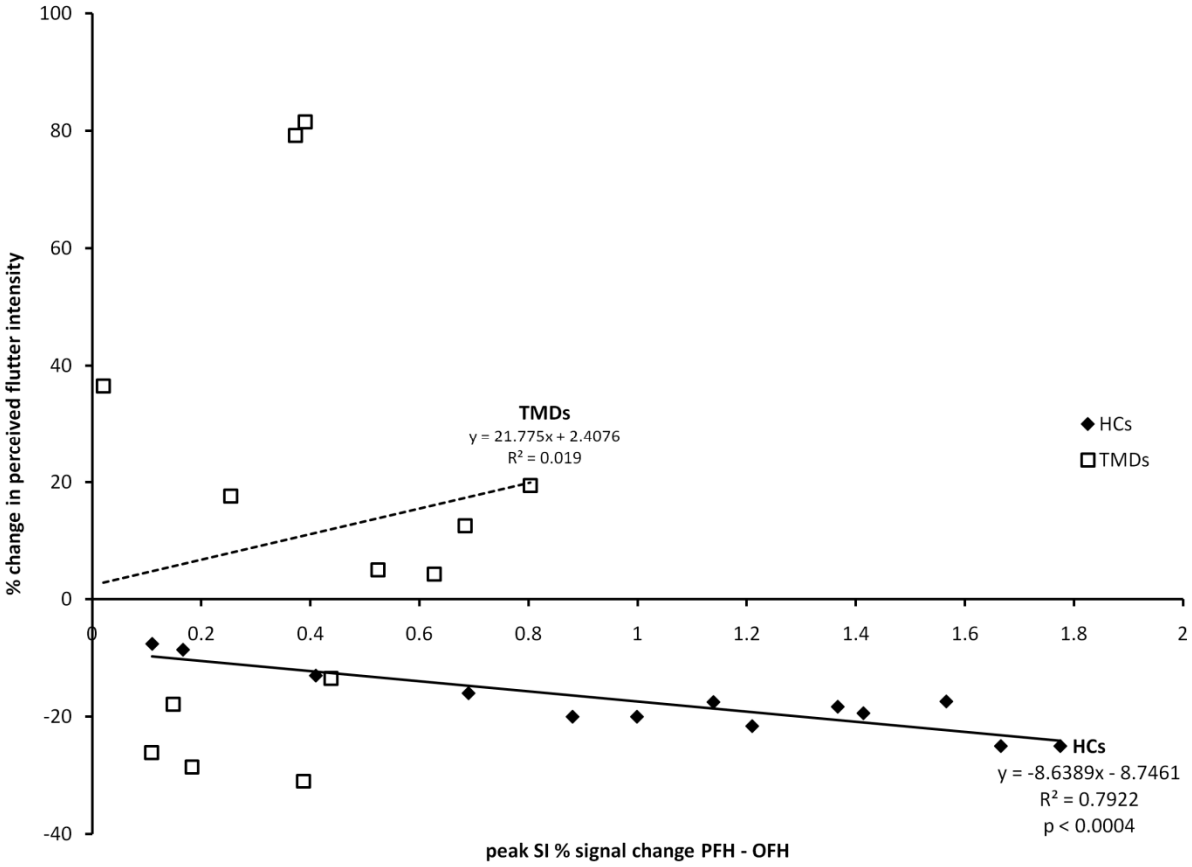

Figure 13. Relationship between present clinical pain and nociception-induced modulation of SI processing. (A) TMD subjects who experienced greater pain on the day of testing also demonstrated greater interaction between flutter and noxious heat input within SI; however, **(B)** pain on the day of testing was not significantly correlated with peak SI signal change responses to flutter (F) or noxious heat (H) stimulation alone.

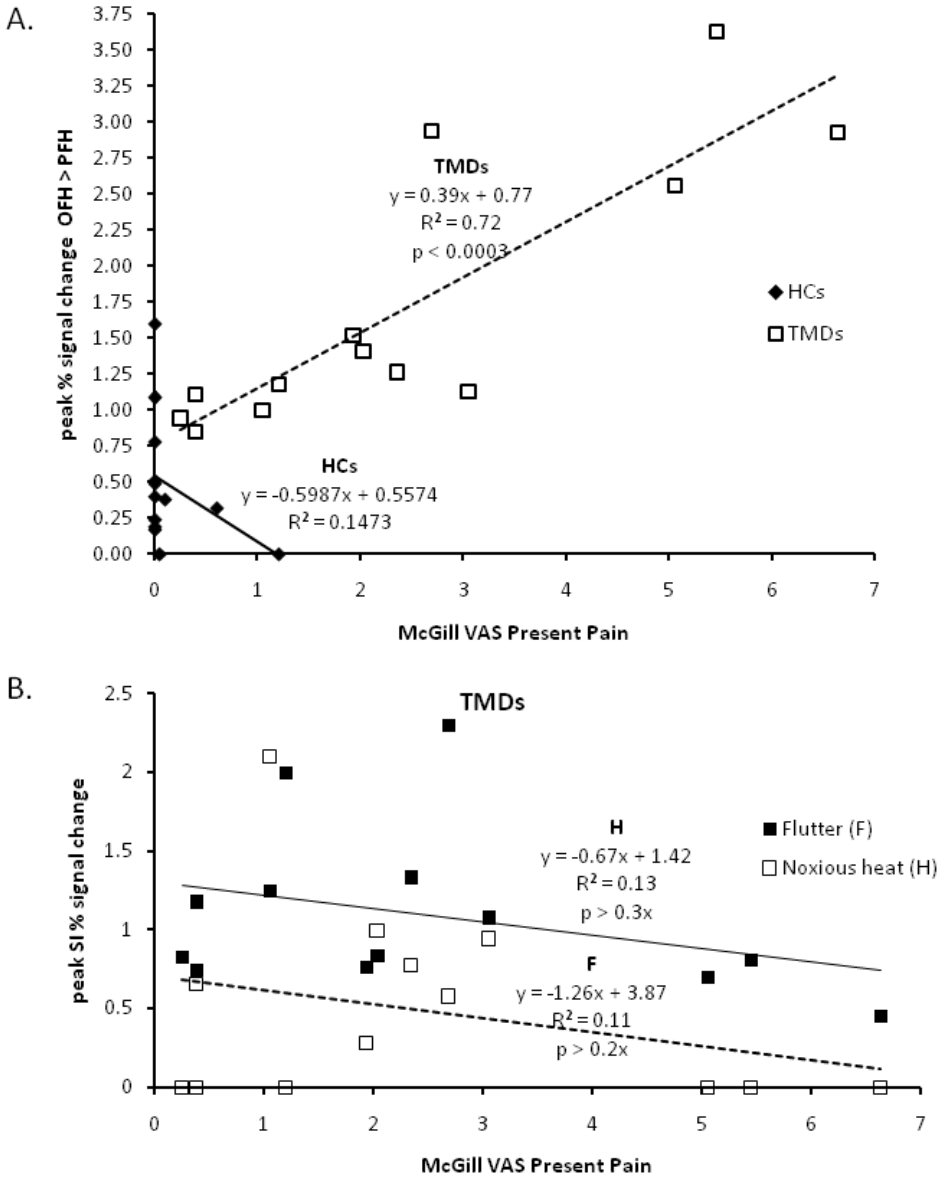

Figure 14. Peak SI percent signal change evoked by flutter in TMD subgroups. TMD subjects whose flutter intensity ratings decreased in the presence of noxious heat demonstrated a smaller peak SI percent signal change response to flutter alone than did TMD subjects whose flutter intensity ratings increased in the presence of noxious heat. This difference between TMD subgroups was significant ($p < 0.04$).

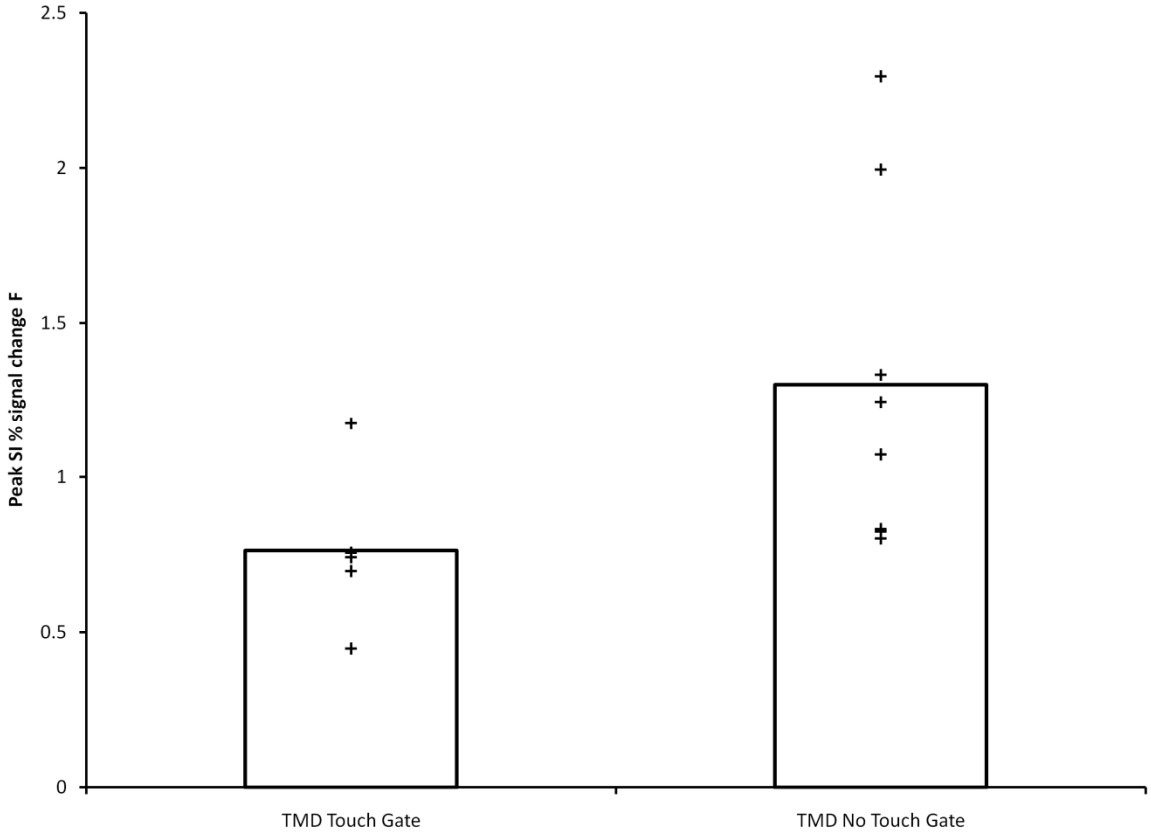

CHAPTER 4

TOUCH PAIN INTERACTIONS IN TMD: THE EFFECT OF INNOCUOUS VIBRATION ON CORTICAL RESPONSES TO NOXIOUS HEAT

A large portion of the work presented in this chapter was completed as a collaborative effort with the following researchers: Folger S, Tommerdahl M, Coghill R, and Essick G.

4.1 Abstract

To further our understanding of the extent of somatosensory disruption in temporomandibular disorders (TMD), we investigated the impact of high frequency vibration on cortical responses to painful skin heating using functional magnetic resonance imaging (fMRI). Innocuous high frequency vibration and noxious skin heating were delivered separately and concurrently to the hand of subjects with TMD and to healthy controls (HCs). Cortical somatosensory submodality convergence was differentially localized in HCs and TMDs. In HCs, SI responses evoked by concurrent submodality stimulation were smaller than predicted by SI responses to unimodal stimulation as has been demonstrated in previous studies reported in the literature. However, in TMDs, ACC responses evoked by concurrent submodality stimulation were larger than predicted by ACC responses to unimodal stimulation. Furthermore, these superadditive responses in the ACC were correlated with McGill present pain intensity scores in TMD subjects. This contrasts with the lack of a significant correlation between peak ACC responses evoked by either vibration or noxious skin heating alone and present pain intensity scores in TMD subjects, suggesting that processing interactions between innocuous vibration

and noxious heat input more closely reflect individual experiences of persistent clinical pain than the processing of innocuous vibrotactile or noxious heat input alone.

Perspective: This article presents evidence that cortical mechanisms underlying the modulation of painful heat processing by innocuous, high frequency vibration are abnormal in TMD. A potential neuromechanistic explanation for this abnormal processing may involve connections between the medial thalamus and the ACC that may be affected by ongoing clinical pain.

4.2. Introduction

The analgesic effect of vibratory stimulation of the skin has been observed in both clinical [129-131] and experimental settings [9, 132, 133]. The ability of vibration to attenuate pain perception has most often been explained in terms of the Gate Control Theory described by Melzack and Wall [9], which postulates that activity conducted through large, myelinated afferent fibers can block activity conducted through small, mostly unmyelinated afferent fibers. Although still accepted in principle, the details of the gating mechanism remain in question. The idea that touch in general inhibits pain fails to account for the fact that pain suppression has been shown to be limited to dynamic tactile stimulation [134], and the rapid onset of vibration-induced gating in the dorsal horn does not explain the gradual enhancement of the effect of vibration observed with the passage of time following its onset [132, 135].

The effect of vibration on pain perception and on central nervous system (CNS) processing of noxious input are not explicable solely in terms of vibration-induced central inhibition even in pain-free individuals. As an example, Watanabe et al observed no significant change in either perceived pain intensity or peak-to-peak amplitude of evoked potentials in response to noxious electrical stimulation in the presence of innocuous vibration [136]. In

addition, while many persistent pain patients demonstrate vibratory analgesia, some exhibit the opposite effect; vibration increases their spontaneous pain [135, 137].

One chronic pain condition in which substantial individual differences in the effect of vibration on pain have been observed is temporomandibular disorder (TMD), a non-specific diagnosis representing a constellation of conditions characterized by persistent facial pain and impaired oral function [17]. Continuous visual analog scale recordings of perceived pain intensity demonstrate that some subjects experience a decrease in pain following vibration onset while others experience an increase, and in some cases, an initial decrease in pain intensity is followed by a gradual increase, suggesting that both inhibitory and excitatory processes are at work [131]. However, the factors that determine the predominant response (i.e., vibratory analgesia or vibratory hyperalgesia) have not been identified.

Supra-spinal mechanisms could contribute to the individual variability observed in the effect of vibration on pain. Nearly ten times as many fibers project from primary somatosensory cortex (SI) to the thalamus as project from thalamus to cortex [138]. The presence of these corticoefferent fibers presents SI with a path through which to shape the nature of its own input dynamically [139], and descending inhibitory processes have been recognized to play a role in vibration-induced changes in pain perception [140]. Wang et al observed opposing modulatory effects of SI activity on nociception in animal models of acute and chronic pain states and suggested that a functional switch may exist for SI at different stages of pain disease [141]. In addition, we recently detected a disturbance in the cortical convergence of innocuous and noxious input in TMD that manifested itself as a reversal in the effect of noxious heat on SI responsivity to innocuous low frequency vibration compared to healthy controls (HCs), and the extent of the SI processing disruption was closely coupled with the severity of ongoing clinical pain [142]. Given this difference in the cortical convergence of innocuous and noxious input in

TMD, the purpose of the present study was to characterize the modulation of nociception by innocuous high frequency vibration of the skin.

4.3. Materials and Methods

4.3.1. Subjects

Twenty-three women consented to a protocol approved by the Institutional Review Board at University of North Carolina at Chapel Hill. Twelve participants fulfilled Research Diagnostic Criteria (RDC) for TMD [17]; average age (SD) was 28.3 (7.8) years. The remaining 11 participants were neurologically healthy controls whose average age (SD) was 28.3 (8.8) years. Immediately prior to imaging, each participant completed the Short-form McGill Pain Questionnaire (SF-MPQ) to assess her current level of pain [34].

4.3.2 Stimulation

To characterize the effect of vibrotactile stimulation on the brain's response to painful input, three types of stimuli were presented: 1) noxious skin heating (H), 2) innocuous, high frequency skin vibration (V), and 3) concurrent skin heating and vibration (HV). All stimuli were applied to the same dermatome of the hand. Skin heating stimuli were delivered to the right thenar eminence using an MR-compatible peltier device with a contact area of 2.6cm^2 (TSA-II, Medoc Advanced Medical Systems, Ramat Yishai, Israel). A Velcro strap was used to secure the thermal probe to the hand throughout the imaging session. During skin heating events, the thermal probe ramped from a level approximating skin temperature (32˚C) to a moderately noxious level (49˚C) at a rate of 6˚C/s. The probe remained at the noxious temperature for 4s before ramping down to the baseline level at a rate of -6˚C/s. Noxious skin heating events occurred every 62s to allow adequate observation of the hemodynamic response to each event during the interstimulus interval, and seven events comprised an imaging series. A piezoelectric tactile stimulator (PTS) was used to apply a 200Hz (200μ peak-to-peak amplitude) sinusoidal

stimulus to the distal pad of the right index finger; a static surround limited the stimulation to a region under the 8-mm diameter Teflon contactor. High frequency vibrotactile stimulation was chosen because animal studies have shown that 200Hz vibration preferentially evokes activity in secondary somatosensory cortex while reducing the spatial extent of activity in primary somatosensory cortex in the same hemisphere [143]. Vibration events were 4 seconds in duration and occurred every 32 seconds; 14 events comprised a single imaging series. The timing of HV events was similar to that of noxious skin heating with vibration being presented for 4s while the thermal probe was at 49˚C.

4.3.3. Experimental Protocol

All 23 subjects completed 10 fMRI scans divided over two imaging sessions to minimize subject fatigue. Session A consisted of four scans of noxious skin heating; session B consisted of two scans of skin vibration and four scans of concurrent heat and vibration. The order of imaging sessions for each subject and the order of scan types within each session were randomized. Subjects were instructed to keep their eyes closed and to concentrate on the presence of the stimulus. At the end of both H and HV scans, subjects were asked to rate the average intensity of heat pain experienced using a labeled magnitude scale with the following anchor points: felt nothing (0), barely detectable (1.5), weak pain (5), moderate pain (16), strong pain (33), very strong (50), and most intense pain imaginable (100). At the end of V scans, subjects rated the average intensity of vibration experienced using a similar scale. Subjects were instructed to choose the most appropriate label range to describe the intensity of the stimulus and then to convert that label range into a number. Subjects were familiarized with the scale and presented with two test stimuli to rate before entering the scanner room.

4.3.4. Imaging Parameters

Scanning was performed on a Siemens Magnetom Allegra, head-dedicated 3.0T scanner system with 40 -mT/m gradients and a 30 cm radio frequency (RF) volume coil. Foam cushions were used to restrict subject head motion, and earplugs and earphones were worn by subjects to reduce scanner noise. A total of 160 contiguous, high-resolution images covering the entire brain were acquired using a magnetization prepared rapid gradient echo (MPRAGE) T1-weighted sequence (TR: 1700ms, Echo Time (TE): 4.38 ms, Flip angle: 8, 1mm isotropic sampling). These structural images were aligned near-axially, parallel to the plane underlying the rostrum and splenium of the corpus callosum and were used for coregistration with the functional data. Whole brain functional images consisted of 50 slices collected using a gradient echo pulse sequence sensitive to blood oxygenation level dependent (BOLD) contrast with echo planar k-space sampling at a repetition rate (TR) of 3000ms (TE: 30ms, Flip angle: 90, Image matrix: 64 X 64, isotropic voxel size: $3mm^3$). The functional images were aligned similarly to the structural images. A semi-automated, high-order shimming program ensured global field homogeneity. Imaging series began with two discarded RF excitations to allow the change in net magnetization of the sample following excitation to reach steady state equilibrium.

4.3.5. Image Data Analysis

The image analysis package FMRIB Software Library (FSL) version 4.1.2 [37, 38] was used for image processing and statistical analysis. Functional data were temporally realigned to adjust for interleaved slice acquisition order, corrected for subject motion using MCFLIRT [40], and spatially smoothed using a Gaussian filter with a FWHM 5mm kernel. A high-pass temporal filter with a cutoff period of 100 seconds was applied to remove low frequency artifacts from functional data, and each 4D dataset was scaled by its mean global intensity. Functional and structural images were stripped of non-brain matter [39] to improve registration. Functional

images of each subject were then co-registered to structural images in native space, and structural images were warped into Montreal Neurological Institute (MNI) stereotaxic space and resampled to 2 X 2 X 2 mm voxels to allow for intersession and intersubject comparison. The same transformation matrices used for structural-to-standard transformations were then applied to the co-registered functional images, and all registrations were carried out using an intermodal registration tool (affine, 12 degrees of freedom). Voxel-wise temporal autocorrelation was estimated and corrected using FMRIB's Improved Linear Model [41].

The three event types (H, V, and HV) were modeled as separate explanatory variables; onset times of stimulation events were convolved with a double γ function to model the hemodynamic response (HDR). Data for each participant were pooled over sessions using fixed-effects general linear modeling, and within each subject, contrast images were created for each event type versus rest and for differences between the HV response observed (OHV) and the HV response predicted by the sum of the responses evoked by H and V alone (PHV), either superadditive (OHV > PHV) or subadditive (PHV > OHV).

Conventional voxel-by-voxel mixed-effects analyses were used to assess each of the contrasts across individuals and groups. Group-wise z statistic images were thresholded using clusters determined by $z > 2.3$ and a cluster corrected significance of $p < 0.05$ [42]. Following statistical thresholding, mixed-effects group contrast images were restricted to voxels in which a significant, cluster corrected HDR was evoked by the condition of interest in either group composing the contrast. The Harvard-Oxford cortical and subcortical structural atlases (Harvard Center for Morphometric Analysis, Charlestown, MA) and the Jülich histologic atlas were used to localize activation clusters [43, 44]. Average BOLD time courses were extracted from functional regions of interest (ROIs) identified to differentiate groups based on whole-brain analyses described above to help visualize the interaction between the responses to innocuous and

noxious stimuli in these areas. Peak parameter estimates were then extracted from these regions and converted to percent change values using the featquery utility within FSL. Finally, to investigate individual differences regarding the influence of clinical pain and the presence of innocuous vibration on the brain's response to experimental pain input, multiple regression analyses between fMRI data and reported pain intensity ratings were performed within these ROIs.

4.4. Results

In the two previous papers of this series, we described between-group differences in intensity ratings and central nervous system (CNS) BOLD responses to innocuous vibrotactile flutter stimuli [100] and noxious skin heating[144]. In this report, we focus on group responses to innocuous high frequency vibration and differences in the group interaction between noxious heat and vibration.

4.4.1. Self-reported Present Pain

On average, TMD subjects reported their present pain intensity on the day of imaging session A to be 2.56 on a 10 cm visual analog scale with end labels of no pain (0) and worst possible pain (10). TMD subjects reported an average present pain intensity of 2.13 out of 10 on the day of imaging session B. Control subjects reported an average present pain intensity of 0.16 out of 10 on the day of session A and 0.01 out of 10 on the day of session B. A paired t-test indicated that the difference in present pain intensity during the two sessions was not significant for either the TMD or control group (Figure 15); however, the TMD group reported significantly more pain on the day of testing than the HC group ($p < 0.001$).

4.4.2. Response to high frequency skin vibration

4.4.2.1. Perceptual Ratings

On average, the HC group rated the intensity of the high frequency vibration as 23.7 (SD = 10.9), corresponding to a level of "moderately intense" on the labeled magnitude scale while the TMD group rated the intensity of the same stimuli as 42.8, on average (SD = 24.0), corresponding to a level between "strong" and "very strong." This difference in mean perceived intensity was statistically significant (p=0.02). Average ratings of vibration intensity were not affected by the present pain intensity ratings of the TMD subjects (Figure 16A).

4.4.2.2. Imaging Data

Individual Group Analysis

Analysis of fMRI data revealed a common network of vibration evoked activity in controls and TMDs. For both groups, high frequency vibration elicited statistically significant, positive hemodynamic responses in somatosensory processing areas, namely bilateral SII and insular cortex. Both groups also demonstrated robust responses bilaterally in posterior mid-cingulate cortex (pmCC) and inferior parietal lobule (IPL). In addition, the HC group demonstrated bilateral BOLD responses in SI. Table 8 indicates the MNI coordinates of all significant activation clusters by group, and Figure 17A illustrates the pattern of activation for each group in these regions.

Between Group Analyses

Evaluation of (HC – TMD) and (TMD – HC) contrasts revealed several regions in which innocuous vibration evoked a larger BOLD response in the TMD group than in the HC group, including the thalamus and IPL. Table 9 lists MNI coordinates for all vibration-responsive clusters in which the TMD response exceeded the HC response. No regions were identified in which innocuous vibration elicited a greater BOLD response in HCs than in TMDs.

4.4.3. Effect of high frequency vibration on noxious skin heating

4.4.3.1 Perceptual Ratings

Healthy controls rated the intensity of heat pain in the presence of high frequency skin vibration as 24.0, on average (SD=10.4), which corresponded to a level between "moderately intense" and "strong." Compared to heat pain intensity ratings reported by HCs in the absence of innocuous skin vibration [144], these ratings were 25.0% lower, on average (SD=16.7%). TMD subjects rated the intensity of heat pain in the presence of high frequency skin vibration as 39.9 (20.3), on average, a rating that corresponded to a level between "strong" and "very strong." Although five of 12 TMD subjects, similar to the HCs, perceived a decrease in the intensity of heat pain with the addition of concurrent vibration; the TMD group on average reported a 17. 9% (SD=42.7%) increase in perceived heat pain intensity in the presence of vibration (Figure 18). The difference between groups in the vibration-evoked change in heat pain ratings was statistically significant ($p<0.01$). Although a trend is suggested, the present clinical pain intensity ratings of the TMD subjects were not significantly correlated with the magnitude of changes in the perceived intensity of heat pain upon application of vibration (Figure 16B).

4.4.3.2. Imaging Data

Individual Group Analysis

Brain areas that responded to concurrent noxious skin heating and innocuous vibration of the hand were similar to areas engaged by vibration and noxious heat stimulation delivered separately. In both groups, positive BOLD responses were evoked bilaterally in SII and insular cortex. In addition, HCs and TMDs demonstrated robust responses bilaterally in ACC, pmCC, and the inferior parietal lobule, which are sensory association areas. Table 10 lists the MNI coordinates of all significant activation clusters by group, and Figure 17B illustrates the pattern of activation for each group in these regions.

A number of the regions activated by either concurrent HV stimulation or by one of the unimodal stimulus conditions exhibited statistically significant differences between the HV response observed and the HV response predicted by the sum of the responses evoked by H and V alone, suggesting that processing of noxious heat and vibration inputs to these areas interacted. For the control group, subadditive responses (PHV > OHV) were identified in bilateral SI, SII, and insula, and no statistically significant superadditive responses were observed. For the TMD group, superadditive responses were found bilaterally in caudal ACC, and no statistically significant subadditive responses were identified. None of the areas in which TMDs demonstrated a greater response than HCs to vibration alone demonstrated superadditive responses to concurrent HV stimulation, suggesting that the superadditive responses were not due simply to a greater response to the vibration. Table 11 lists the coordinates of all clusters showing significant differences between predicted and observed BOLD responses evoked by concurrent noxious heat and vibration stimulation.

Between Group Analyses

Evaluation of (HC – TMD) and (TMD – HC) contrasts revealed several regions in which one group demonstrated a greater difference between the predicted and observed response evoked by concurrent stimulation. Consistent with the individual group analyses, HCs exhibited greater subadditive responses than TMDs in ipsilateral SI and SII (red areas, Figure 19A) and TMDs showed greater superadditive responses in caudal ACC (Figure 20A).

Imaging data from the TMD group was then subdivided into two groups: (1) TMD subjects who, like the HCs, demonstrated a pain-attenuating ("pain-gate") effect, i.e., reported a decrease in heat pain intensity ratings with the addition of high frequency vibration and (2) TMD subjects who demonstrated a pain-enhancing effect, i.e., reported an increase in heat pain intensity ratings with the addition of high frequency vibration. Additional differences were

found between HCs and TMDs who reported a pain-enhancing effect that were not observed between HCs and the entire TMD group. Table 12 lists MNI coordinates for all differences in convergence patterns observed between subgroups of TMD subjects. In addition to differences in subadditive responses observed on the ipislateral side in HCs as compared to the entire group of TMD subjects, differences in subadditive responses in contralateral SI and SII emerged between HCs and the TMDs who reported a pain-enhancing effect (blue areas, Figure 19A), suggesting that the cortical responses in TMD subjects who reported a pain-enhancing effect differed more greatly from those of HCs than did the entire group of TMD subjects. Extracting HDRs from contralateral SI voxels labeled subadditive in HCs, we observed that noxious heat and high frequency vibration delivered separately evoked weak, positive BOLD responses in HCs, but when delivered concurrently, they evoked negative responses (Figure 19B). This is in contrast with the SII voxels labeled subadditive, which, on average, responded similarly for all three stimulation conditions (Figure 19C), suggesting that noxious heat and vibration input converged in SII without interacting. In TMD participants who reported a pain-enhancing effect of the vibration, noxious heat and vibration elicited either no response or a negative response in SI delivered separately, but when delivered concurrently, they evoked a positive BOLD response (Figure 19D). The effect of SI submodality convergence in TMDs who reported a pain-attenuating effect of vibration fell in between HCs and TMDs who exhibited pain-enhancement: the SI response to concurrent HV stimulation closely matched the sum of the SI responses to noxious heat and vibration delivered separately (Figure 19E). Moreover, no cortical areas were found in which the HC group differed more greatly from these TMD subjects than from the TMDs who reported enhancement of experimental pain with the application of concurrent vibration.

In caudal ACC (Figure 20A), average superadditive responses for the entire TMD group (Figure 20B) appeared to be driven by the TMD subgroup that reported a pain-enhancing effect of vibration. In these subjects, noxious heat and high frequency vibration both elicited small positive responses when delivered separately, but when delivered concurrently, the evoked response was larger than predicted by the sum of the unimodal responses (Figure 20C). In contrast, in both HCs and TMDs who reported a pain-attenuating effect of vibration (Figure 20D and 20E, respectively), there was no significant difference among the peaks of the responses evoked by noxious heat, vibration and concurrent stimulation in the ACC.

4.4.3.3. Relationship between changes in pain perception and cortical processing

A negative correlation was observed in HCs between peak percent change values for subadditive responses in SI and changes in the perceived intensity of heat pain in the presence of high frequency vibration ($R^2 = 0.55$, $p < 0.01$; Figure 21A, solid line). In other words, upon application of high frequency vibration, the perceived intensity of heat pain decreased systematically as the difference between the predicted and observed SI HV responses increased among HCs. In TMDs who reported a pain-enhancing effect of the vibration, a trend suggested that subjects within this subgroup who demonstrated smaller subadditive responses in SI reported greater pain enhancement; however, this trend did not reach a level that was statistically significant ($R^2 = 0.23$, $p < 0.06$; Figure 21A, dashed line).

No correlation was found between ACC superadditive responses in TMDs and changes in the perceived intensity of heat pain in the presence of high frequency vibration (Figure 21B). However, ACC superadditive responses were found to be positively correlated with McGill present pain intensity scores for TMD subjects who experienced an enhancement of pain with the addition of vibration ($R^2=0.63$, $p < 0.03$) but not for TMD subjects who experienced an attenuation of pain (Figure 22, solid line). TMDs who experienced greater levels of clinical pain

on the day of imaging and who rated their experimentally-induced pain as more intense in the presence of vibration demonstrated greater augmentation of observed ACC HV responses with respect to predicted ACC HV responses (Figure 22, dashed line).

4.5. Discussion

To the best of our knowledge, the present report is the first examination of brain activity associated with the influence of high frequency vibration on noxious skin heating in individuals with TMD. The results highlight several main findings: (1) in healthy controls, interactions between noxious heat and vibration were consistent with the pain-gate effect, and the suppression of noxious processing occurred, at least in part, in the cortex. (2) In contrast, two subgroups emerged within the TMD group; TMDs who experienced vibration-induced pain attenuation similar to HCs and TMDs who experienced vibration-induced pain enhancement.

Vibration-induced attenuation of pain perception and processing

Consistent with published psychophysical evidence of vibration-induced analgesia in healthy individuals [9, 132, 133], all 11 HCs reported a reduction in the intensity of heat pain in the presence of high frequency vibration. Although activity in dorsal horn nociresponsive neurons has been shown to be modulated under various experimental conditions including segmental sensory stimulation [145], thalamic stimulation [146], and dorsal column stimulation [147], our results indicate that vibration-induced modulation of noxious input also occurs in the cortex. We observed a vibration-induced suppression of SI responsiveness to noxious heat stimulation. Inui et al also reported MEG evidence that SI is critical in the gating of nociceptive information processing [148]. Utilizing the superior temporal resolution of MEG, Inui et al observed that nociceptive processing in SI was equally inhibited by innocuous, tactile stimulation when the innocuous stimulation was delivered concurrently (as in our experiment)

or when the contribution of peripheral and spinal mechanisms were minimized by delaying the innocuous tactile stimulation with respect to the noxious stimulation.

We also observed a moderate correlation in HCs between the magnitude of vibration-induced changes in the perception of heat pain intensity and vibration-induced changes in SI responsivity, Similar to the role we observed SI to play in the interaction between low frequency flutter and noxious heat in the same HCs [144], SI was again identified as a region in which the interaction of innocuous and noxious processing produced responses that were smaller than predicted by the sum of the responses to unimodal stimulation. However, the subregion of SI in which the response to noxious heat was reduced in the presence of concurrent high frequency vibration was slightly anterior and medial to the subregion of SI in which the response to low frequency flutter was reduced in the presence of concurrent noxious heat. This finding is complimentary to animal neuroimaging data suggesting that noxious and innocuous stimuli drive different neuronal populations within SI [59, 60, 149]; the subregion of SI that responds to noxious stimulation of the hand, and thus the subregion in which we would expect to observe a pain-gating effect, was anterior and medial to the core hand tactile locus within SI in which we would expect to observe a touch-gating effect.

Cortical somatosensory information processing takes place in spatially distributed and reciprocally interconnected regions. Given that inhibitory corticocortical projections linking subdivisions of SI [59, 60, 93] may underlie the suppression of SI responsiveness to flutter in the presence of noxious heat, it seems possible that similar reciprocal connections among subdivisions of SI could be responsible for the suppression of SI responsiveness to noxious heat in the presence of vibration. However, high frequency vibration preferentially evokes activity in SII while reducing the spatial extent of activity in SI in the same hemisphere [143], which makes

reciprocal connections between SI and SII a more likely neuromechanistic candidate for the suppression of SI responsiveness to noxious heat.

Vibration-induced enhancement of pain perception and processing

In contrast to HCs, only 5 of 12 TMD participants reported a reduction in heat pain intensity in the presence of high frequency vibration. The remaining 7 TMD participants demonstrated a pain-enhancing effect and reported an increase in heat pain intensity with the addition of vibration. Roy et al also observed the effect of vibration on perceived pain intensity visual analog scale ratings to vary among individuals with TMD [131].

Although we observed SI contributions to pain-attenuation in HCs, we did not observe a statistically significant SI contribution to pain-attenuation or pain-enhancement in TMDs. The only brain region that demonstrated statistically significant, somatosensory submodality processing convergence in TMDs was a caudal region of the ACC. In TMDs, vibration enhanced the response of caudal ACC to noxious stimulation. Buffington et al also reported an enhanced response to pain in the ACC that was specific to individuals with osteoarthritis, another persistent musculoskeletal pain condition [150]. Moreover, the differences we observed in processing within the ACC were more pronounced when the TMD group was subdivided based on the effect of vibration on perceived heat pain. In TMD subjects who reported vibration-induced pain enhancement, noxious heat and high frequency vibration both elicited small positive responses when delivered separately, but when delivered concurrently, the evoked response was larger than predicted by the sum of the unimodal responses. In contrast, ACC responses evoked in TMDs who reported a pain-attenuating effect of vibration more closely resembled those of the HC group; whether presented separately or concurrently, noxious heat and vibration elicited small, positive responses in the ACC.

Because caudal ACC activity has been shown to respond preferentially to the processing of pain affect in humans more than to the processing of sensory discriminative information regarding pain [151, 152], it is not surprising that the magnitude of superadditive responses elicited in caudal ACC were not correlated with the magnitude of vibration-induced changes in heat pain intensity perception. However, the magnitude of caudal ACC superadditive responses correlated with the intensity of ongoing clinical pain. TMD subjects who experienced greater pain on the day of testing also demonstrated greater augmentation of the ACC response to noxious heat with the addition of concurrent vibration of the skin.

The cortical areas in which we observed superadditive responses in TMDs (caudal ACC) did not include any of the brain areas in which we observed a heightened response to innocuous vibration compared to controls. We did, however, observe augmented thalamic responses to vibration in the TMD group, and accumulating evidence suggests a functional link between the medial thalamus and the ACC in the modulation of pain affect [153-155]. High frequency stimulation of the medial thalamus results in reports of intense pain and unpleasantness in humans [156] while medial thalamic lesions have been shown to block evoked activity in the ACC [157]. In addition, the fact that the level of clinical pain on the day of testing was correlated with the magnitude of enhanced nociceptive processing and not with changes in the perception of vibration intensity suggests that the ability to control somatosensory input through gating mechanisms may be more critical to the persistence of clinical pain than the primary representation of somatosensory input in the brain. Whether an intervention designed to reduce clinical pain would also reduce the superadditive ACC responses observed in the present study is a question that remains for future investigation.

It should be mentioned that the ACC is activated by other experimental conditions such as during the performance of the Stroop task [158],and pain-associated activations may

represent non-pain specific effects (i.e., attention). However, there is evidence suggesting that pain- and attention-related activations in the ACC are not co-localized in individual participants even when group results indicate that they overlap [159], which suggests that group-level ACC activation reflects both pain specific and non-pain specific effects. Because we did not have a control task to localize attention-related activations, we cannot rule out the possibility that TMDs were more distracted from the heat pain by vibration than were HCs. Such attentional differences could have contributed to the vibration-induced, superadditive responses we observed in TMDs; however, it is unlikely that they were the result of attention effects exclusively.

One limitation of the present report is our sample size; although the number of subjects included in this study is comparable to many functional neuroimaging investigations, it may be small considering the heterogeneity in the clinical presentation of TMD. Indeed, two subgroups emerged within our TMD sample. Despite this heterogeneity, we detected a disruption in the modulation of noxious heat by innocuous vibration. The cortical convergence of noxious heat and innocuous vibration was not co-localized with the cortical convergence of innocuous flutter and noxious heat previously reported in these same HCs and TMDs [144]. The cortical dynamics evoked by concurrent noxious heat and innocuous vibration appear to be more closely coupled with individual clinical pain experience than the responses evoked by noxious skin heating alone. Normal interaction with the environment requires that relevant sensory information is identified and extracted from a vast array of concurrent inputs. Inability to combine inputs could influence sensorimotor or perceptual ability even in the presence of an intact primary sensory representation.

Acknowledgments

The authors would like to thank Angera Ma and MRI technologists Kathy Wilber, Amber Abernethy, James Barnwell, and Emilie Kearns for assistance with data acquisition as well as Ollie Monbureau and Mike Young for technical assistance. This work was supported by NIH grant P01 NS045685.

Table 8. Regions activated by high frequency vibration in control and TMD groups. Only significant clusters of activation corrected for multiple comparisons ($p<0.05$) are listed. Up to three significant peak activations in each cluster are listed. C = side contralateral to the site of skin stimulation, I = side ipsilateral to the site of skin stimulation.

Region	Side	Cluster Size	Peak Voxel Z	MNI Coordinates x,y,z (mm)
Controls				
SII, posterior insula, inferior parietal lobule, SI	C	4190	5.34	-58, -20, 16
			5.33	-38, -24, -4
			5.19	-60, -26, 16
Posterior insula, anterior insula, putamen	I	1406	4.62	40, -12, -8
			4.6	32, 22, 6
			4.36	20, 8, -6
Cerebellum	I	526	5.22	22, -64, -52
Inferior parietal lobule, SII, SI	I	496	4.62	66, -30, 34
			3.83	58, -16, 22
Posterior mid-cingulate gyrus	C, I	392	4.0	-4, -20, 28
			3.94	6, -36, 22
TMDs				
Putamen, Thalamus	C, I	7406	5.12	-16, 2, -12
			4.97	-2, -12, 6
			4.92	16, 6, -12
			4.82	18, -16, 10
Cerebellum	I	2650	5.42	26, -66, -52
Cerebellum	C	2133	4.99	-34, -64, -32
SII, Inferior parietal lobule	C	1902	4.92	-56, -22, 16
			4.57	-54, -42, 46
Inferior parietal lobule,	I	818	5.1	58, -36, 54
SII	I	667	4.52	48, -28, 22
Planum polare, insula	C	655	4.94	-42, -4, -20
			4.18	-42, -14, -2
Frontal pole	I	436	4.13	48, 40, 10

Table 9. Vibration responsive regions demonstrating a significant group effect. Only significant clusters of activation corrected for multiple comparisons ($p<0.05$) are listed. Up to three significant peak activations in each cluster are listed. C = side contralateral to the site of skin stimulation, I = side ipsilateral to the site of skin stimulation.

Region	Side	Cluster Size	Peak Voxel Z	MNI Coordinates x,y,z (mm)
TMDs > Controls				
Thalamus	I, C	1199	3.98	18, -22, 10
			3.50	-6, -10, 0
Cerebellum	C	1128	3.96	-10, -70, -46
Cerebellum	I	1066	3.88	26, -48, -28
Superior parietal lobule 7A/Inferior parietal lobule	I	970	4.66	38, -60, 58
Anterior intra-parietal sulcus/Inferior parietal lobule	C	876	3.9	-40, -48, 34
Inferior frontal gyrus	I	585	3.99	52, 6, 16
Cerebellum	I	512	3.91	0, -72, -22
Frontal Pole	I	487	4.81	48, 38, 10

Table 10. Regions activated by concurrent noxious skin heating and innocuous vibration in controls and TMDs. Only significant clusters of activation corrected for multiple comparisons ($p<0.05$) are listed. Up to three significant peak activations in each cluster are listed. C = side contralateral to the site of skin stimulation, I = side ipsilateral to the site of skin stimulation.

Region	Side	Cluster Size	Peak Voxel Z	MNI Coordinates x,y,z (mm)
Controls				
SII, Insula, Thalamus, Putamen	C	7076	5.18	-58, -26, 18
			4.84	-40, 12, -6
			4.83	-36, 0, 12
			4.71	-18, -20, 12
Insula, Putamen, Caudate,	I	5618	5.49	36, 16, 4
			4.84	18, 8, -2
			4.72	12, 10, 6
Paracingulate gyrus, ACC	I, C	1441	4.67	4, 28, 46
			4.43	4, 32, 24
			4.09	-6, 32, 30
Cerebellum	C	966	3.87	-34, -56, -40
Inferior parietal lobule, SII	I	822	4.47	58, -38, 48
			3.30	60, -28, 28
Frontal pole, middle frontal gyrus	I	554	4.80	38, 46, 22
			4.37	38, 36, 26
Frontal pole	C	527	4.37	-46, 42, 18
Posterior mid-cingulate	C, I	393	4.96	-4, -22, 30
			4.89	4, -20, 32
Cerebellum	I	236	4.34	2, -36, -52
TMDs				
Insula, Planum polare, SII	C	2990	4.70	-36, 8, 0
			4.70	-40, -4, -14
			4.29	-64, -24, 16
Cerebellum	C	2318	4.38	-38, -60, -48
Thalamus, Pallidum, Amygdala	C	2216	4.51	-18, -18, 10
			4.06	-12, 6, -2
			3.75	-14, -6, -10
Frontal pole, middle frontal gyrus	I	1920	5.12	44, 38, 22
			4.21	36, 36, 24
Inferior parietal lobule	I	1809	5.48	50, -48, 54
Insula, Planum polare	I	1797	4.53	36, 2, 8
			4.39	42, -10, -8
Paracingulate gyrus, ACC	I, C	1622	5.09	4, 14, 48
			4.81	8, 16, 36
			3.9	-10, 14, 32
Inferior parietal lobule	C	1551	4.7	-54, -44, 42
Cerebellum	I	1503	4.37	46, -60, -30
Middle frontal gyrus	C	714	4.81	-42, 34, 14

Table 11. Regions in which the processing of noxious heat is modulated by vibration in HCs and TMDs. Only significant clusters of activation corrected for multiple comparisons ($p<0.05$) are listed. Up to three significant peak activations in each cluster are listed. C = side contralateral to the site of skin stimulation, I = side ipsilateral to the site of skin stimulation.

Region	Side	Cluster Size	Peak Voxel Z	MNI Coordinates x,y,z (mm)
HC PHV > OHV				
A1, SII, Insula, SI	C	3082	3.96	-52, -20, 10
			3.94	-50, -32, 18
			3.93	-42, -6, -4
			3.77	-48, -24, 62
Inferior frontal gyrus, insula	I	1565	3.87	56, 12, 0
			3.83	40, -2, 4
SII, SI	I	985	4.72	56, -16, 14
			3.57	58, -16, 46
TMD OHV > PHV				
ACC	C, I	284	3.55	-2, 20, 32

Table 12. Regions in which HCs dissociated from TMDs in vibration-induced modulation of nociception. Up to three significant peak activations in each cluster are listed. C = side contralateral to the site of skin stimulation, I = side ipsilateral to the site of skin stimulation. TMD1 = pain-enhancing TMDs, TMD2 = pain-attenuating TMDs.

Region	Side	Cluster Size	Peak Voxel Z	MNI Coordinates x,y,z (mm)
HC – (TMD1 & TMD2) PHV > OHV				
SI, SII	I	266	3.65	54, -18, 40
			3.1	54, -14, 12
HC – TMD1 PHV > OHV				
A1, SII, Insula	C	710	3.55	-56, -16, 6
			3.36	-44, -2, -8
SI	C	66	2.73	-50, -24, 44
TMD1 – (HC & TMD2) OHV > PHV				
ACC	I, C	263	3.80	4, 20, 32

Figure 15. Average clinical pain on the day of testing. Clinical pain experienced on the day of testing did not differ significantly between session A and B within groups but did differ significantly between the healthy control (HC) group and the TMD group.

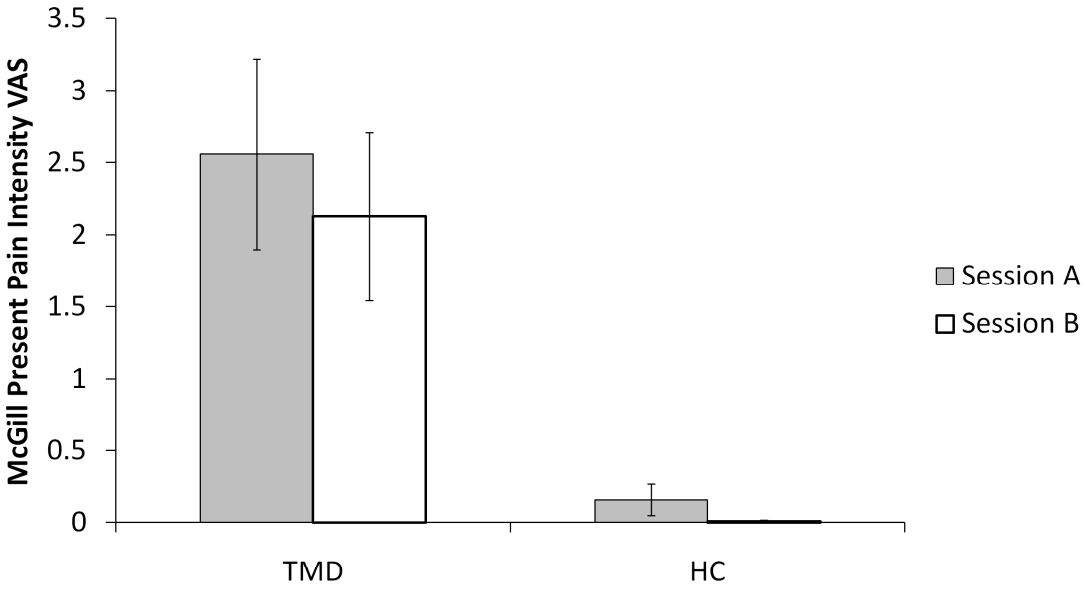

Figure 16. Effect of ongoing clinical pain on the perception of experimental stimuli. (A) Average vibration intensity ratings reported by TMD subjects were not significantly correlated with present clinical pain intensity ratings. **(B)** Although a trend was suggested, the magnitude of vibration induced changes in heat pain ratings were also not significantly correlated with clinical pain experienced on the day of testing.

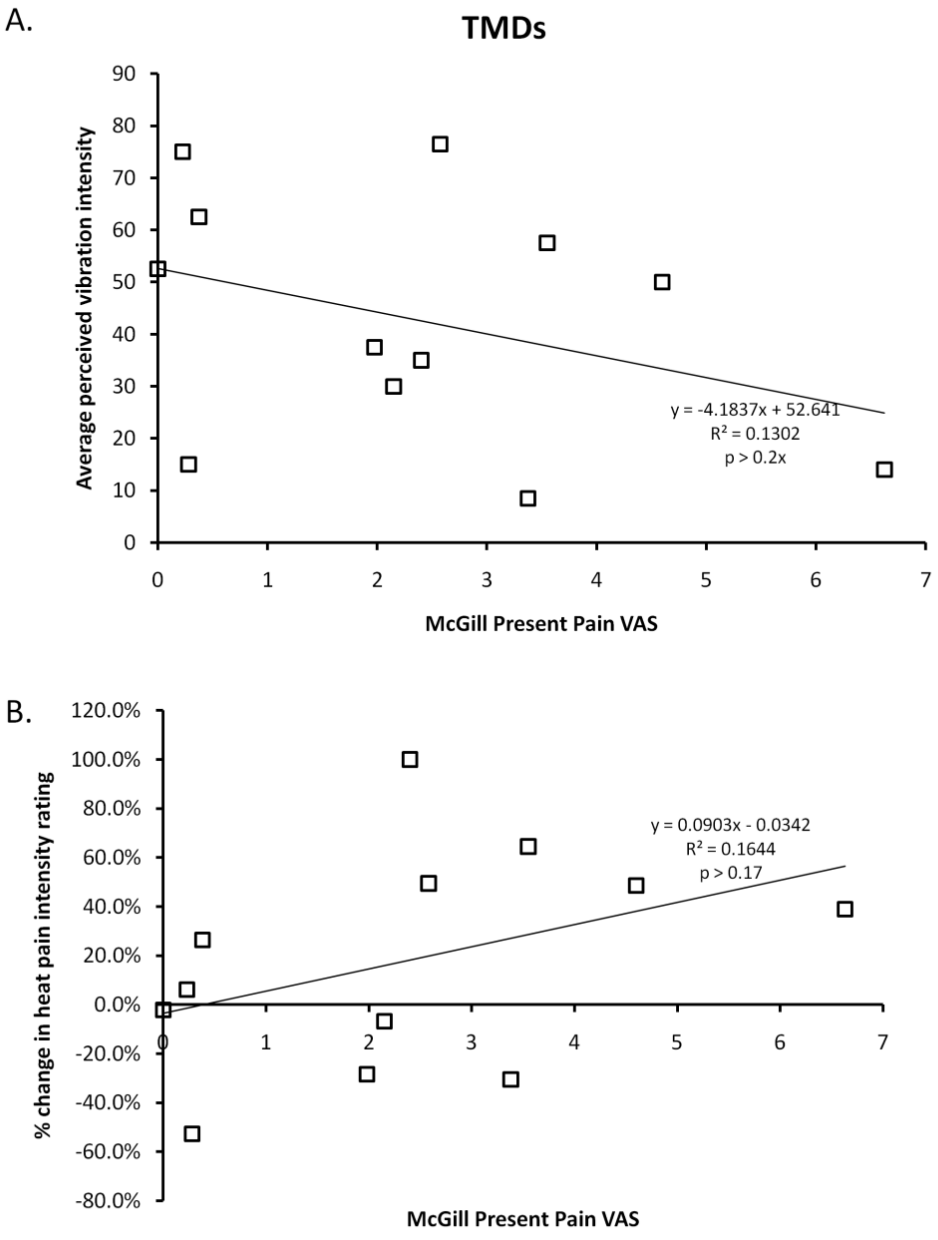

Figure 17. Regions responding to vibration alone and to concurrent noxious heat and vibration. Masks of significant clusters of activation evoked by **(A)** high frequency vibration and **(B)** concurrent noxious heat and vibration for the control group only in yellow, the TMD group only in blue, and for both groups in green. A cluster mean threshold of $z > 2.3$ and a cluster corrected significance of $p < 0.05$ were used. Insula activation is outlined. ACC = Anterior Cingulate Cortex, Ins = Insula, MFG = Middle Frontal Gyrus, PC = posterior Mid-Cingulate Cortex, IPL = Inferior parietal lobule, SII = Secondary Somatosensory Cortex, SI = Primary Somatosensory Cortex,Thal = Thalamus

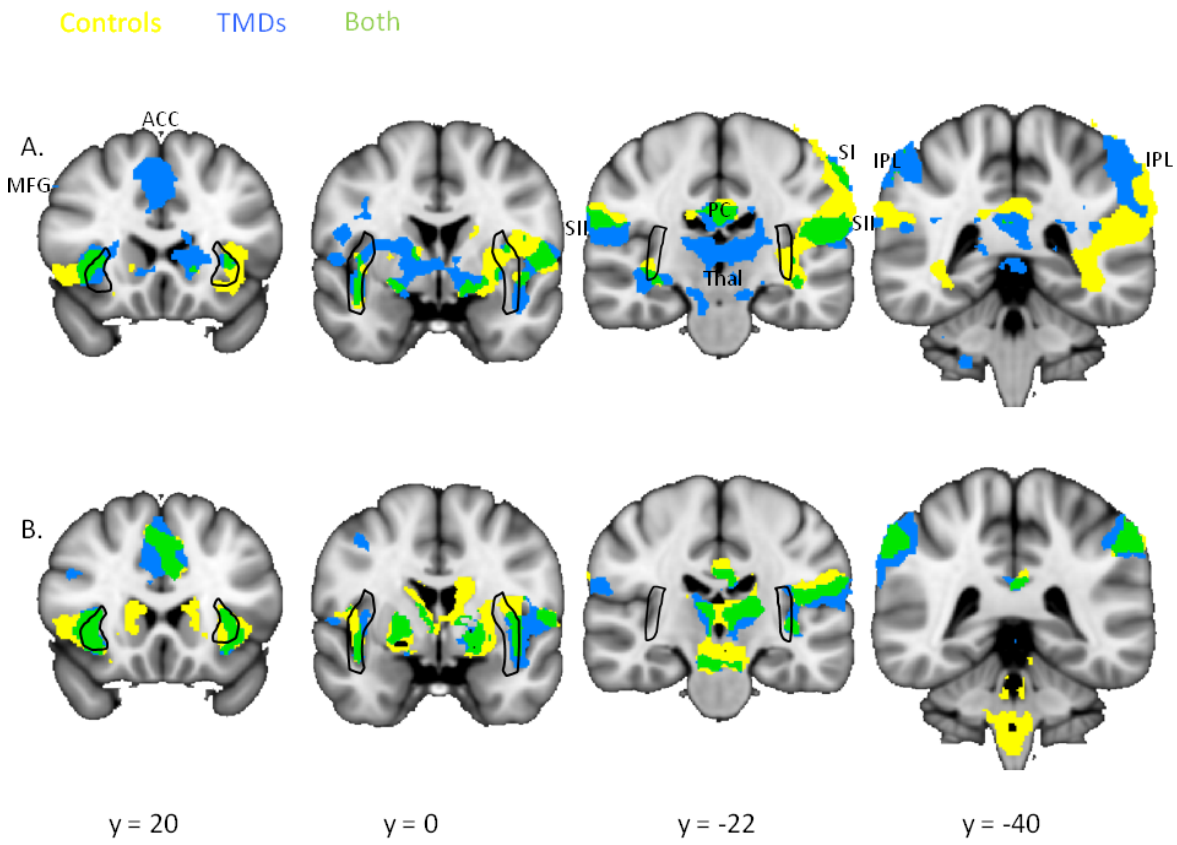

Figure 18. Effect of vibration on perceived heat pain intensity. On average, healthy control (HC) ratings of heat pain intensity decreased 25.0% in the presence of vibration. Although five of 11 TMD subjects perceived a decrease in heat pain intensity with the addition of concurrent vibration, on average, the TMD group reported a 24.4% increase in perceived heat pain intensity in the presence of vibration.

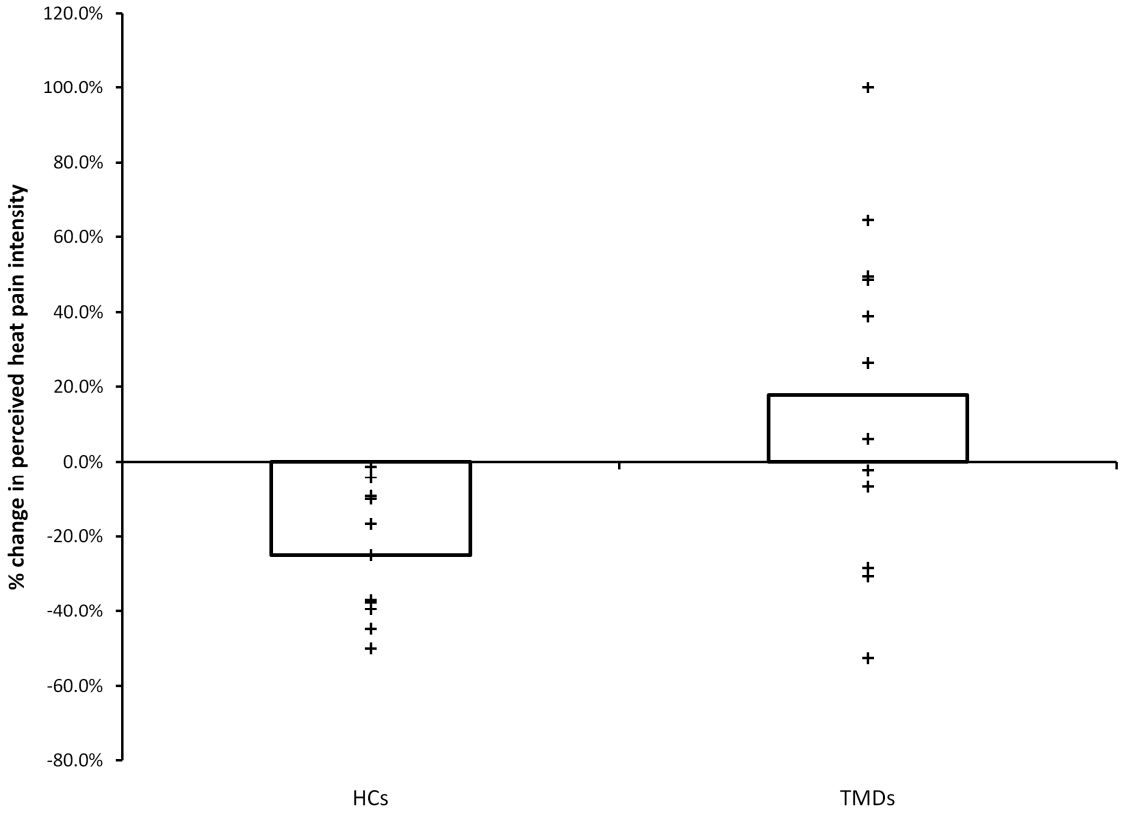

Figure 19. Group dissociation in subadditive responses. (A) HCs only showed areas in which the observed response to HV was significantly less than the response predicted by responses to H and V delivered separately. Significant subadditive responses compared to the entire TMD group are in red while significant subadditive responses compared only to the subset of TMD subjects who demonstrated a pain-amplifying effect in their heat pain intensity ratings are shown in blue. Average hemodynamic responses were extracted from SI voxels labeled blue for all three stimulation conditions and are illustrated for **(B)** HCs, **(D)** for TMDs who showed a pain-enhancing effect, and **(E)** for TMDs who demonstrated a pain attenuating effect of vibration. A cluster mean threshold of $z > 2.3$ and a cluster corrected significance of $p < 0.05$ were used. **(C)** Average hemodynamic responses extracted from blue SII voxels in HCs are shown for comparison with SI responses.

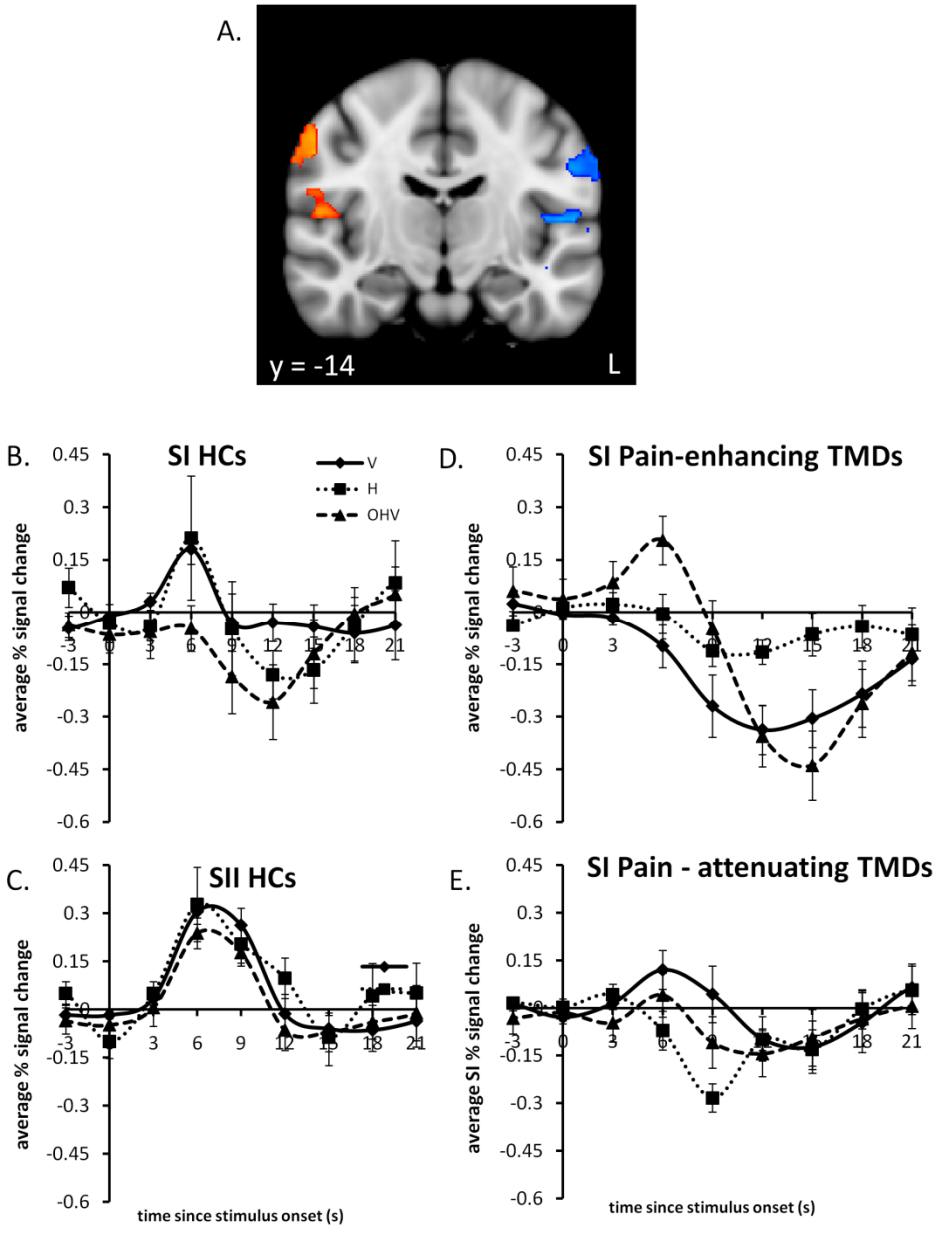

Figure 20. Group dissociation in superadditive responses. (A) TMDs only showed areas in which the observed HV response was significantly greater than the predicted HV response outside of traditional somatosensory areas (green region). Average hemodynamic responses evoked by all three conditions were extracted from the green voxels and are illustrated for **(B)** all TMDs, **(C)** TMDs who demonstrated a pain-enhancing effect of vibration, **(D)** TMDs who demonstrated a pain gate, and **(E)** HCs. A cluster mean threshold of $z > 2.3$ and a cluster corrected significance of $p < 0.05$ were used.

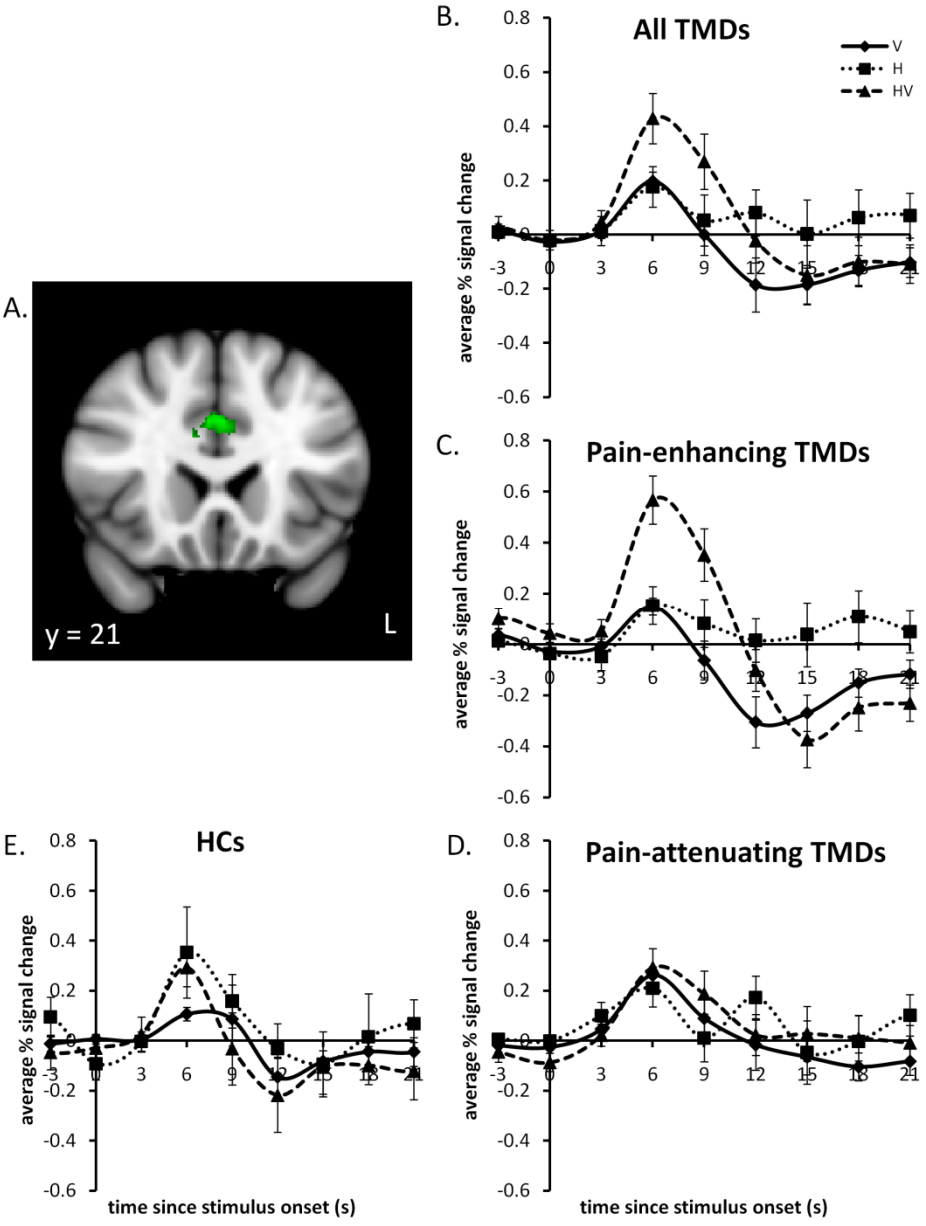

Figure 21. Relationship between effects of vibration on experimental pain perception and cortical processing. (A) In healthy controls (HCs, solid line), the perceived intensity of heat pain decreased with the addition of vibration as the difference between the predicted and observed SI HV responses increased. A trend between the effects of vibration on experimental pain and SI processing was also observed in the TMD subgroup that reported pain enhancement with the addition of vibration (dashed line). Within this TMD subgroup, subjects who demonstrated greater subadditive responses in SI reported less pain enhancement. **(B)** No correlation was found between superadditive ACC responses observed in TMDs and the effect of vibration on heat pain perception.

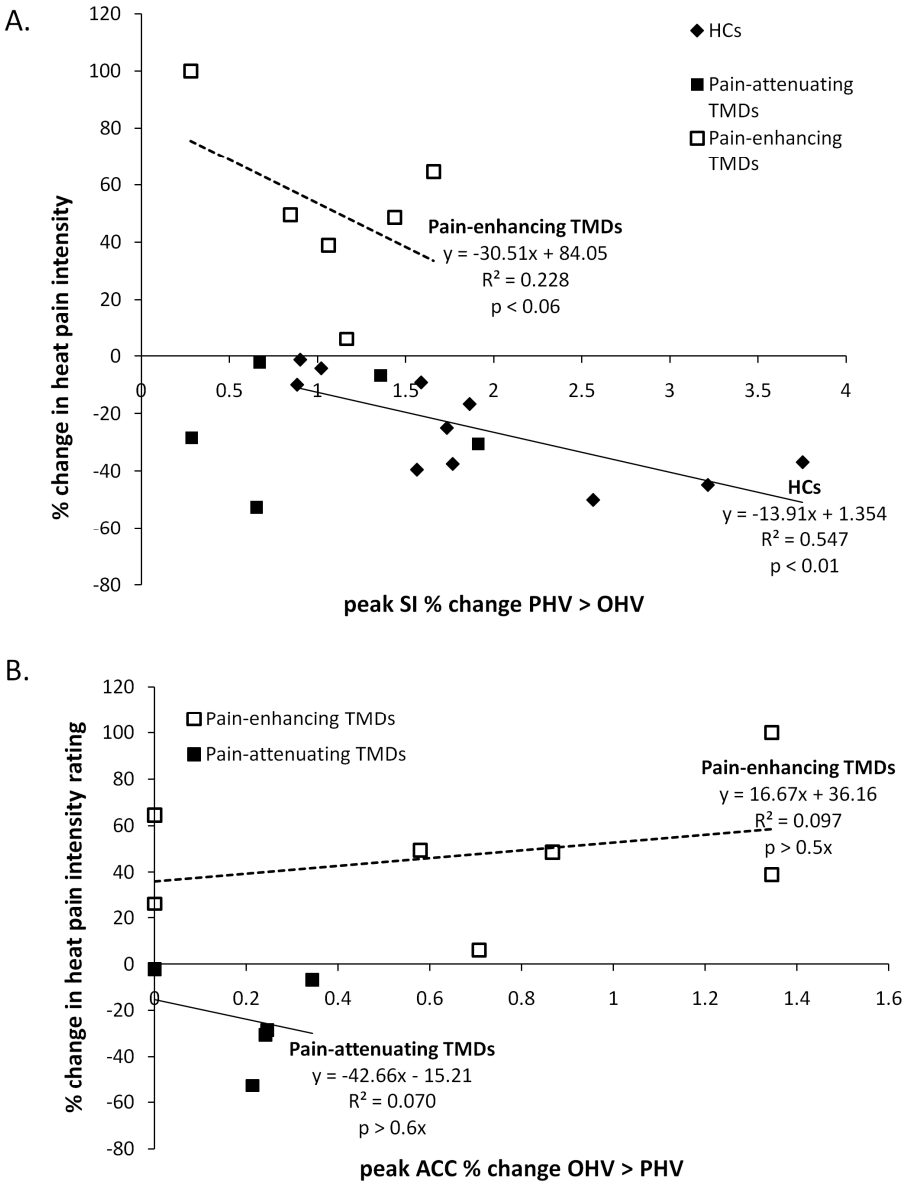

Figure 22. Relationship between present clinical pain and vibration-induced modulation of ACC responsiveness to noxious heat. TMD subjects who experienced greater pain on the day of testing also demonstrated greater interaction between vibration and noxious heat input within the ACC.

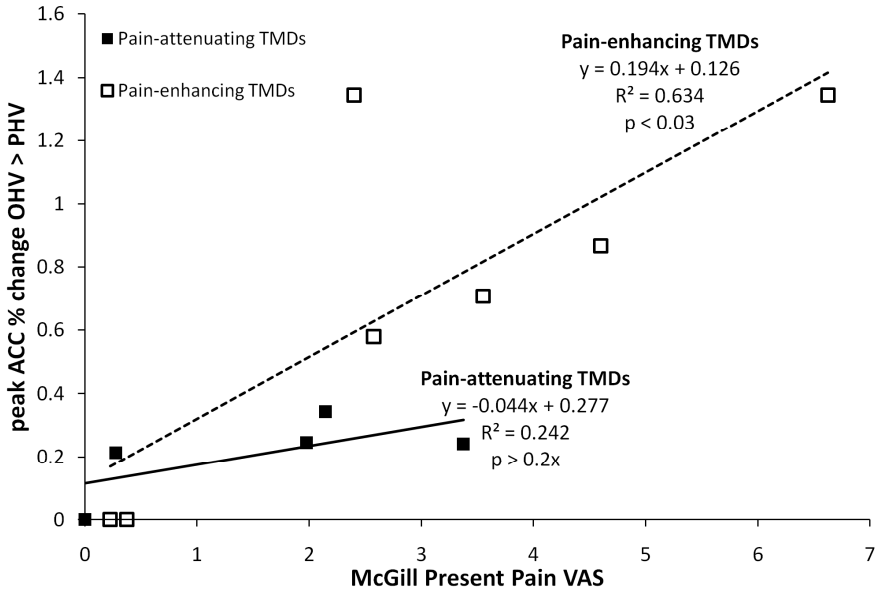

Chapter 5

GENERAL DISCUSSION

It has long been established that robust interactions occur between the somatosensory submodalities of pain and touch. Two complimentary expressions of the normal, competitive interactions that take place between pain and touch in the CNS are the gate control theory of touch [11, 12] and the gate control theory of pain [9]. The convergence of pain and tactile processing in the CNS suggests that the experience of pain might not only be reflected in the processing of painful input, but might also be associated with modulation of somatosensory processing more generally, and examination of the processing interactions that occur between pain and touch can reveal processes that would not be apparent when considering each submodality in isolation. In the experiments reported in this dissertation, we investigated how cortical processing interactions that occur between innocuous and noxious somatosensory stimulation contribute to persistent TMD pain.

In the first experiment, we investigated whether the abnormalities in vibrotactile perception reported in the literature it be associated with TMD reflect an abnormal topography of cortical somatosensory processing in the absence of experimentally evoked pain. We observed that responses in distinct subregions of contralateral SI, secondary somatosensory cortex (SII) and insular cortex differentiated TMD from HCs [100], and the differences between groups in these subregions paralleled previously reported differences in responses evoked in healthy individuals by noxious and innocuous stimulation, respectively. We suggested that

these subtle, yet significant, differences may reflect cortical plasticity in TMD, manifesting itself as increased readiness for non-orofacial cortical areas to respond to innocuous vibrotactile input that normally would not.

Having established that cortical responsivity to non-painful tactile stimulation is abnormal in TMD, we then investigated whether the endogenous modulation of tactile processing by experimentally induced heat pain was also disrupted in TMD. Within the processing network common to unimodal and bimodal somatosensory stimulation, differences emerged in the cortical patterns characterizing interactions between submodalities in subjects with and without TMD. While noxious heat interfered with innocuous vibrotactile processing within SI in HCs, noxious heat appeared to facilitate innocuous vibrotactile processing within SI in TMDs. A potential neuromechanistic explanation for this abnormal processing may involve activity dependent interneurons connecting subregions of SI that are affected by persistent clinical pain. Furthermore, we found that the enhancement of vibrotactile processing by nociception was related to the severity of the TMD patients' clinical pain and emerged despite the fact that pain ratings and cortical responses to noxious heat alone did not differ significantly between TMD patients and control subjects.

In the third experiment, we investigated whether the endogenous modulation of noxious heat processing by innocuous tactile processing was also disrupted in TMD. In contrast to the first two experiments, we utilized high frequency vibrotactile stimulation because it has been shown to be more effective at alleviating pain than low frequency flutter [131]. In healthy controls, interactions between noxious heat and vibration were consistent with the pain-gate effect, and the suppression of noxious processing occurred, at least in part, in the cortex. Similar to the role we observed SI to play in the second experiment, SI was again identified as a

region in which the interaction of innocuous and noxious processing produced responses that were smaller than predicted by the sum of the responses to unimodal stimulation. However, vibration-induced suppression of the SI response to noxious heat was not co-localized with the nociceptive-induced suppression of the SI response to flutter, which is consistent with evidence from other human and animal neuroimaging experiments suggesting that noxious and innocuous stimuli drive different neuronal populations within SI [59, 60, 149]. In contrast to HCs, two subgroups emerged within the TMD group; TMDs who experienced vibration-induced pain attenuation similar to HCs and TMDs who experienced vibration-induced pain enhancement. The cortical areas in which we observed superadditive responses in TMDs (caudal ACC) did not include any of the brain areas in which we observed a heightened response to innocuous vibration compared to controls. We did, however, observe augmented thalamic responses to vibration in the TMD group, and accumulating evidence suggests a functional link between the medial thalamus and the ACC in the modulation of pain affect [153-155]. A potential neuromechanistic explanation for this abnormal processing may involve connections between the medial thalamus and the ACC that may be affected by ongoing clincal pain.

TMDs and HCs responded differently to both low and high frequency innocuous vibrotactile stimulation. By comparing the observed response to concurrent stimulation to the response predicted by the sum of the responses to unimodal stimulation, we were able to establish that the group differences we observed in processing interactions between innocuous and noxious input were not solely due to the group differences in cortical responsivity to vibrotactile stimulation alone. Some of these differences in the interaction of innocuous and noxious somatosensory inputs were correlated with the severity of the TMD patients' clinical pain despite the fact that no significant correlations were observed between TMD pain and responses to vibrotactile or noxious heat stimulation alone. This suggests that cortical

processing interactions between somatosensory submodalities more closely reflect individual experiences of persistent clinical pain than does the unimodal processing of innocuous vibrotactile or noxious heat input alone. Whether the enhancement of cortical responsivity we observed in the second and third experiments would be reduced with the reduction of clinical pain is a question that remains for future investigation.

References

1. Mantyselka, P.T., et al., *Chronic pain and poor self-rated health.* Jama, 2003. **290**(18): p. 2435-42.

2. Stewart, W.F., et al., *Lost productive time and cost due to common pain conditions in the US workforce.* Jama, 2003. **290**(18): p. 2443-54.

3. Meldrum, M.L., *A capsule history of pain management.* Jama, 2003. **290**(18): p. 2470-5.

4. Bonica, J.J., *History of pain concepts and pain therapy.* Mt Sinai J Med, 1991. **58**(3): p. 191-202.

5. Sabatowski, R., et al., *Pain treatment: a historical overview.* Curr Pharm Des, 2004. **10**(7): p. 701-16.

6. Perl, E.R., *Ideas about pain, a historical view.* Nat Rev Neurosci, 2007. **8**(1): p. 71-80.

7. Finger, S., *Origins of Neuroscience: A History of Explorations into Brain Function*. 1994, New York: Oxford University Press.

8. Sherrington, C.S., *The Integrative Action of the Nervous System*. 1906, Cambridge, UK: Cambridge University Press.

9. Melzack, R. and P.D. Wall, *Pain mechanisms: a new theory.* Science, 1965. **150**(699): p. 971-9.

10. Melzack, R., *Pain: past, present and future.* Can J Exp Psychol, 1993. **47**(4): p. 615-29.

11. Apkarian, A.V., R.A. Stea, and S.J. Bolanowski, *Heat-induced pain diminishes vibrotactile perception: a touch gate.* Somatosens Mot Res, 1994. **11**(3): p. 259-67.

12. Bolanowski, S.J., et al., *The effects of stimulus location on the gating of touch by heat- and cold-induced pain.* Somatosens Mot Res, 2000. **17**(2): p. 195-204.

13. Nathan, P.W., *Improvement in cutaneous sensibility associated with relief of pain.* J Neurol Neurosurg Psychiatry, 1960. **23**: p. 202-6.

14. Leffler, A.S., E. Kosek, and P. Hansson, *The influence of pain intensity on somatosensory perception in patients suffering from subacute/chronic lateral epicondylalgia.* Eur J Pain, 2000. **4**(1): p. 57-71.

15. Voerman, V.F., J. van Egmond, and B.J. Crul, *Elevated detection thresholds for mechanical stimuli in chronic pain patients: support for a central mechanism.* Arch Phys Med Rehabil, 2000. **81**(4): p. 430-5.

16. Jensen, R., et al., *Quantitative sensory testing of patients with long lasting Patellofemoral pain syndrome.* Eur J Pain, 2007. **11**(6): p. 665-76.

17. Dworkin, S.F. and L. LeResche, *Research diagnostic criteria for temporomandibular disorders: review, criteria, examinations and specifications, critique.* J Craniomandib Disord, 1992. **6**(4): p. 301-55.

18. Dworkin, S.F., et al., *Epidemiology of signs and symptoms in temporomandibular disorders: clinical signs in cases and controls.* J Am Dent Assoc, 1990. **120**(3): p. 273-81.

19. Yap, A.U., et al., *Multiple pains and psychosocial functioning/psychologic distress in TMD patients.* Int J Prosthodont, 2002. **15**(5): p. 461-6.

20. Hagberg, C., *General musculoskeletal complaints in a group of patients with craniomandibular disorders (CMD). A case control study.* Swed Dent J, 1991. **15**(4): p. 179-85.

21. Plesh, O., F. Wolfe, and N. Lane, *The relationship between fibromyalgia and temporomandibular disorders: prevalence and symptom severity.* J Rheumatol, 1996. **23**(11): p. 1948-52.

22. Zolnoun, D.A., et al., *Overlap between orofacial pain and vulvar vestibulitis syndrome.* Clin J Pain, 2008. **24**(3): p. 187-91.

23. Aaron, L.A., M.M. Burke, and D. Buchwald, *Overlapping conditions among patients with chronic fatigue syndrome, fibromyalgia, and temporomandibular disorder.* Arch Intern Med, 2000. **160**(2): p. 221-7.

24. Hollins, M., et al., *Vibrotactile threshold is elevated in temporomandibular disorders.* Pain, 1996. **67**(1): p. 89-96.

25. Hollins, M. and A. Sigurdsson, *Vibrotactile amplitude and frequency discrimination in temporomandibular disorders.* Pain, 1998. **75**(1): p. 59-67.

26. LaMotte, R.H. and V.B. Mountcastle, *Disorders in somesthesis following lesions of parietal lobe.* J Neurophysiol, 1979. **42**(2): p. 400-19.

27. Hollins, M., et al., *Perceived intensity and unpleasantness of cutaneous and auditory stimuli: an evaluation of the generalized hypervigilance hypothesis.* Pain, 2009. **141**(3): p. 215-21.

28. Tommerdahl, M., et al., *Effects of spinal dorsal column transection on the response of monkey anterior parietal cortex to repetitive skin stimulation.* Cereb Cortex, 1996. **6**(2): p. 131-55.

29. Lamour, Y., G. Guilbaud, and J.C. Willer, *Altered properties and laminar distribution of neuronal responses to peripheral stimulation in the SmI cortex of the arthritic rat.* Brain Res, 1983. **273**(1): p. 183-7.

30. Guilbaud, G., et al., *The organization of spinal pathways to ventrobasal thalamus in an experimental model of pain (the arthritic rat). An electrophysiological study.* Pain, 1986. **26**(3): p. 301-12.

31. Flor, H., et al., *Phantom-limb pain as a perceptual correlate of cortical reorganization following arm amputation.* Nature, 1995. **375**(6531): p. 482-4.

32. Birbaumer, N., et al., *Effects of regional anesthesia on phantom limb pain are mirrored in changes in cortical reorganization.* J Neurosci, 1997. **17**(14): p. 5503-8.

33. Bush, F.M., et al., *Analysis of gender effects on pain perception and symptom presentation in temporomandibular pain.* Pain, 1993. **53**(1): p. 73-80.

34. Melzack, R., *The short-form McGill Pain Questionnaire.* Pain, 1987. **30**(2): p. 191-7.

35. Francis, S.T., et al., *fMRI of the responses to vibratory stimulation of digit tips.* Neuroimage, 2000. **11**(3): p. 188-202.

36. Simons, S.B., et al., *Amplitude-dependency of response of SI cortex to flutter stimulation.* BMC Neurosci, 2005. **6**(1): p. 43.

37. Smith, S.M., et al., *Advances in functional and structural MR image analysis and implementation as FSL.* Neuroimage, 2004. **23 Suppl 1**: p. S208-19.

38. Woolrich, M.W., et al., *Bayesian analysis of neuroimaging data in FSL.* Neuroimage, 2009. **45**: p. S173-186.

39. Smith, S.M., *Fast robust automated brain extraction.* Hum Brain Mapp, 2002. **17**(3): p. 143-55.

40. Jenkinson, M., et al., *Improved optimization for the robust and accurate linear registration and motion correction of brain images.* Neuroimage, 2002. **17**(2): p. 825-41.

41. Jenkinson, M. and S. Smith, *A global optimisation method for robust affine registration of brain images.* Medical Image Analysis, 2001. **5**(2): p. 143-56.

42. Beckmann, C.F., M. Jenkinson, and S.M. Smith, *General multilevel linear modeling for group analysis in FMRI.* Neuroimage, 2003. **20**(2): p. 1052-63.

43. Eickhoff, S.B., et al., *Assignment of functional activations to probabilistic cytoarchitectonic areas revisited.* Neuroimage, 2007. **36**(3): p. 511-21.

44. Eickhoff, S.B., et al., *A new SPM toolbox for combining probabilistic cytoarchitectonic maps and functional imaging data.* Neuroimage, 2005. **25**(4): p. 1325-35.

45. Eickhoff, S.B., et al., *The human parietal operculum. II. Stereotaxic maps and correlation with functional imaging results.* Cereb Cortex, 2006. **16**(2): p. 268-79.

46. Eickhoff, S.B., et al., *The human parietal operculum. I. Cytoarchitectonic mapping of subdivisions.* Cereb Cortex, 2006. **16**(2): p. 254-67.

47. Morosan, P., et al., *Human primary auditory cortex: cytoarchitectonic subdivisions and mapping into a spatial reference system.* Neuroimage, 2001. **13**(4): p. 684-701.

48. Ozcan, M., et al., *Spatial resolution of fMRI in the human parasylvian cortex: comparison of somatosensory and auditory activation.* Neuroimage, 2005. **25**(3): p. 877-87.

49. Kurth, R., et al., *fMRI assessment of somatotopy in human Brodmann area 3b by electrical finger stimulation.* Neuroreport, 1998. **9**(2): p. 207-12.

50. Maldjian, J.A., et al., *The sensory somatotopic map of the human hand demonstrated at 4 Tesla.* Neuroimage, 1999. **10**(1): p. 55-62.

51. McGlone, F., et al., *Functional neuroimaging studies of human somatosensory cortex.* Behav Brain Res, 2002. **135**(1-2): p. 147-58.

52. Blatow, M., et al., *Altered somatosensory processing in trigeminal neuralgia.* Hum Brain Mapp, 2009. **30**(11): p. 3495-508.

53. Geyer, S., A. Schleicher, and K. Zilles, *Areas 3a, 3b, and 1 of human primary somatosensory cortex.* Neuroimage, 1999. **10**(1): p. 63-83.

54. Geyer, S., et al., *Areas 3a, 3b, and 1 of human primary somatosensory cortex. Part 2. Spatial normalization to standard anatomical space.* Neuroimage, 2000. **11**(6 Pt 1): p. 684-96.

55. Zhang, N., et al., *Dependence of BOLD signal change on tactile stimulus intensity in SI of primates.* Magn Reson Imaging, 2007. **25**(6): p. 784-94.

56. Ohara, S., et al., *Cutaneous painful laser stimuli evoke responses recorded directly from primary somatosensory cortex in awake humans.* J Neurophysiol, 2004. **91**(6): p. 2734-46.

57. Moulton, E.A., et al., *Regional intensive and temporal patterns of functional MRI activation distinguishing noxious and innocuous contact heat.* J Neurophysiol, 2005. **93**(4): p. 2183-93.

58. Stammler, T., et al., *Functional imaging of sensory decline and gain induced by differential noxious stimulation.* Neuroimage, 2008. **42**(3): p. 1151-63.

59. Tommerdahl, M., et al., *Anterior parietal cortical response to tactile and skin-heating stimuli applied to the same skin site.* J Neurophysiol, 1996. **75**(6): p. 2662-70.

60. Tommerdahl, M., et al., *Response of anterior parietal cortex to different modes of same-site skin stimulation.* J Neurophysiol, 1998. **80**(6): p. 3272-83.

61. Whitsel, B.L., et al., *Area 3a neuron response to skin nociceptor afferent drive.* Cereb Cortex, 2009. **19**(2): p. 349-66.

62. Pleger, B., et al., *Patterns of cortical reorganization parallel impaired tactile discrimination and pain intensity in complex regional pain syndrome.* Neuroimage, 2006. **32**(2): p. 503-10.

63. Vartiainen, N.V., E. Kirveskari, and N. Forss, *Central processing of tactile and nociceptive stimuli in complex regional pain syndrome.* Clin Neurophysiol, 2008. **119**(10): p. 2380-8.

64. Whitsel, B.L., L.M. Petrucelli, and G. Werner, *Symmetry and connectivity in the map of the body surface in somatosensory area II of primates.* J Neurophysiol, 1969. **32**(2): p. 170-83.

65. Ferretti, A., et al., *Functional topography of the secondary somatosensory cortex for nonpainful and painful stimuli: an fMRI study.* Neuroimage, 2003. **20**(3): p. 1625-38.

66. Coghill, R.C., et al., *Distributed processing of pain and vibration by the human brain.* J Neurosci, 1994. **14**(7): p. 4095-108.

67. Coghill, R.C., et al., *Pain intensity processing within the human brain: a bilateral, distributed mechanism.* J Neurophysiol, 1999. **82**(4): p. 1934-43.

68. Mao, J., D.J. Mayer, and D.D. Price, *Patterns of increased brain activity indicative of pain in a rat model of peripheral mononeuropathy.* J Neurosci, 1993. **13**(6): p. 2689-702.

69. Fu, K.M., et al., *Auditory cortical neurons respond to somatosensory stimulation.* J Neurosci, 2003. **23**(20): p. 7510-5.

70. Schurmann, M., et al., *Touch activates human auditory cortex.* Neuroimage, 2006. **30**(4): p. 1325-31.

71. Caetano, G. and V. Jousmaki, *Evidence of vibrotactile input to human auditory cortex.* Neuroimage, 2006. **29**(1): p. 15-28.

72. Foxe, J.J., et al., *Auditory-somatosensory multisensory processing in auditory association cortex: an fMRI study.* J Neurophysiol, 2002. **88**(1): p. 540-3.

73. Frostig, R.D., et al., *Large-scale organization of rat sensorimotor cortex based on a motif of large activation spreads.* J Neurosci, 2008. **28**(49): p. 13274-84.

74. Budinger, E. and H. Scheich, *Anatomical connections suitable for the direct processing of neuronal information of different modalities via the rodent primary auditory cortex.* Hear Res, 2009.

75. Cappe, C. and P. Barone, *Heteromodal connections supporting multisensory integration at low levels of cortical processing in the monkey.* Eur J Neurosci, 2005. **22**(11): p. 2886-902.

76. Jousmaki, V. and R. Hari, *Parchment-skin illusion: sound-biased touch.* Curr Biol, 1998. **8**(6): p. R190.

77. Guest, S., et al., *Audiotactile interactions in roughness perception.* Exp Brain Res, 2002. **146**(2): p. 161-71.

78. Yau, J.M., et al., *Temporal frequency channels are linked across audition and touch.* Curr Biol, 2009. **19**(7): p. 561-6.

79. Pinchoff, R.J., et al., *Modulation of tinnitus by voluntary jaw movements.* Am J Otol, 1998. **19**(6): p. 785-9.

80. Gelb, H., M.L. Gelb, and M.L. Wagner, *The relationship of tinnitus to craniocervical mandibular disorders.* Cranio, 1997. **15**(2): p. 136-43.

81. Neugebauer, V. and W. Li, *Differential sensitization of amygdala neurons to afferent inputs in a model of arthritic pain.* J Neurophysiol, 2003. **89**(2): p. 716-27.

82. Han, J.S. and V. Neugebauer, *mGluR1 and mGluR5 antagonists in the amygdala inhibit different components of audible and ultrasonic vocalizations in a model of arthritic pain.* Pain, 2005. **113**(1-2): p. 211-22.

83. Jasmin, L., et al., *Analgesia and hyperalgesia from GABA-mediated modulation of the cerebral cortex.* Nature, 2003. **424**(6946): p. 316-20.

84. Senapati, A.K., et al., *Electrical stimulation of the anterior cingulate cortex reduces responses of rat dorsal horn neurons to mechanical stimuli.* J Neurophysiol, 2005. **94**(1): p. 845-51.

85. LaBar, K.S., et al., *Human amygdala activation during conditioned fear acquisition and extinction: a mixed-trial fMRI study.* Neuron, 1998. **20**(5): p. 937-45.

86. Apkarian, A.V., *Pain perception in relation to emotional learning.* Curr Opin Neurobiol, 2008. **18**(4): p. 464-8.

87. Rollman, G.B. and J.M. Gillespie, *Disturbances of pain perception in temporomandibular pain syndrome*, in *Pathophysiology of pain perception*, S. Lautenbacher and R.B. Fillingim, Editors. 2004, Plenum: New York. p. 107-18.

88. Albanese, M.C., et al., *Differential effects of cognitive demand on human cortical activation associated with vibrotactile stimulation.* J Neurophysiol, 2009. **102**(3): p. 1623-31.

89. Weissman, D.H., et al., *The neural bases of momentary lapses in attention.* Nat Neurosci, 2006. **9**(7): p. 971-8.

90. Sawamoto, N., et al., *Expectation of pain enhances responses to nonpainful somatosensory stimulation in the anterior cingulate cortex and parietal operculum/posterior insula: an event-related functional magnetic resonance imaging study.* J Neurosci, 2000. **20**(19): p. 7438-45.

91. Bolanowski, S.J., et al., *The effects of heat-induced pain on the detectability, discriminability, and sensation magnitude of vibrotactile stimuli.* Somatosens Mot Res, 2001. **18**(1): p. 5-9.

92. Magerl, W. and R.D. Treede, *Secondary tactile hypoesthesia: a novel type of pain-induced somatosensory plasticity in human subjects.* Neurosci Lett, 2004. **361**(1-3): p. 136-9.

93. Whitsel, B.L., et al., *Nociceptive Afferent Activity Alters the SI RA Neuron Response to Mechanical Skin Stimulation.* Cereb Cortex.

94. Tran, T.D., et al., *Electrical-induced pain diminishes somatosensory evoked magnetic cortical fields.* Clin Neurophysiol, 2003. **114**(9): p. 1704-14.

95. Apkarian, A.V., et al., *Persistent pain inhibits contralateral somatosensory cortical activity in humans.* Neurosci Lett, 1992. **140**(2): p. 141-7.

96. Rosso, T., et al., *Functional plasticity in the human primary somatosensory cortex following acute lesion of the anterior lateral spinal cord: neurophysiological evidence of short-term cross-modal plasticity.* Pain, 2003. **101**(1-2): p. 117-27.

97. Hollins, M., A. Sigurdsson, and K.A. Morris, *Local vibrotactile and pain sensitivities are negatively related in temporomandibular disorders.* J Pain, 2001. **2**(1): p. 46-56.

98. Ayesh, E.E., T.S. Jensen, and P. Svensson, *Hypersensitivity to mechanical and intra-articular electrical stimuli in persons with painful temporomandibular joints.* J Dent Res, 2007. **86**(12): p. 1187-92.

99. Apkarian, A.V., et al., *Cortical responses to thermal pain depend on stimulus size: a functional MRI study.* J Neurophysiol, 2000. **83**(5): p. 3113-22.

100. Nebel, M.B., et al., *Temporomandibular Disorder Modifies Cortical Response to Tactile Stimulation.* J Pain.

101. Peyron, R., et al., *Role of operculoinsular cortices in human pain processing: converging evidence from PET, fMRI, dipole modeling, and intracerebral recordings of evoked potentials.* Neuroimage, 2002. **17**(3): p. 1336-46.

102. Peyron, R., et al., *Haemodynamic brain responses to acute pain in humans: sensory and attentional networks.* Brain, 1999. **122 (Pt 9)**: p. 1765-80.

103. Maihofner, C., B. Herzner, and H. Otto Handwerker, *Secondary somatosensory cortex is important for the sensory-discriminative dimension of pain: a functional MRI study.* Eur J Neurosci, 2006. **23**(5): p. 1377-83.

104. Davis, K.D., et al., *Functional MRI study of thalamic and cortical activations evoked by cutaneous heat, cold, and tactile stimuli.* J Neurophysiol, 1998. **80**(3): p. 1533-46.

105. Fulbright, R.K., et al., *Functional MR imaging of regional brain activation associated with the affective experience of pain.* AJR Am J Roentgenol, 2001. **177**(5): p. 1205-10.

106. Ploghaus, A., et al., *Neural circuitry underlying pain modulation: expectation, hypnosis, placebo.* Trends Cogn Sci, 2003. **7**(5): p. 197-200.

107. Apkarian, A.V., et al., *Human brain mechanisms of pain perception and regulation in health and disease.* Eur J Pain, 2005. **9**(4): p. 463-84.

108. Strigo, I.A., et al., *Association of major depressive disorder with altered functional brain response during anticipation and processing of heat pain.* Arch Gen Psychiatry, 2008. **65**(11): p. 1275-84.

109. Seminowicz, D.A. and K.D. Davis, *Cortical responses to pain in healthy individuals depends on pain catastrophizing.* Pain, 2006. **120**(3): p. 297-306.

110. Jones, S.R., et al., *Neural correlates of tactile detection: a combined magnetoencephalography and biophysically based computational modeling study.* J Neurosci, 2007. **27**(40): p. 10751-64.

111. Stefanovic, B., J.M. Warnking, and G.B. Pike, *Hemodynamic and metabolic responses to neuronal inhibition.* Neuroimage, 2004. **22**(2): p. 771-8.

112. Tran, T.D., et al., *Temporal summation of heat pain in humans: Evidence supporting thalamocortical modulation.* Pain.

113. Gracely, R.H., et al., *Functional magnetic resonance imaging evidence of augmented pain processing in fibromyalgia.* Arthritis Rheum, 2002. **46**(5): p. 1333-43.

114. Giesecke, T., et al., *Evidence of augmented central pain processing in idiopathic chronic low back pain.* Arthritis Rheum, 2004. **50**(2): p. 613-23.

115. Gustin, S.M., et al., *NMDA-receptor antagonist and morphine decrease CRPS-pain and cerebral pain representation.* Pain.

116. Maixner, W., et al., *Sensitivity of patients with painful temporomandibular disorders to experimentally evoked pain.* Pain, 1995. **63**(3): p. 341-51.

117. Malow, R.M., L. Grimm, and R.E. Olson, *Differences in pain perception between myofascial pain dysfunction patients and normal subjects: a signal detection analysis.* J Psychosom Res, 1980. **24**(6): p. 303-9.

118. Kashima, K., et al., *Increased pain sensitivity of the upper extremities of TMD patients with myalgia to experimentally-evoked noxious stimulation: possibility of worsened endogenous opioid systems.* Cranio, 1999. **17**(4): p. 241-6.

119. King, C.D., et al., *Deficiency in endogenous modulation of prolonged heat pain in patients with Irritable Bowel Syndrome and Temporomandibular Disorder.* Pain, 2009. **143**(3): p. 172-8.

120. Bragdon, E.E., et al., *Group differences in pain modulation: pain-free women compared to pain-free men and to women with TMD.* Pain, 2002. **96**(3): p. 227-37.

121. Carlson, C.R., et al., *Psychological and physiological parameters of masticatory muscle pain.* Pain, 1998. **76**(3): p. 297-307.

122. Cook, D.B., et al., *Functional imaging of pain in patients with primary fibromyalgia.* J Rheumatol, 2004. **31**(2): p. 364-78.

123. Coghill, R.C., J.G. McHaffie, and Y.F. Yen, *Neural correlates of interindividual differences in the subjective experience of pain.* Proc Natl Acad Sci U S A, 2003. **100**(14): p. 8538-42.

124. Peyron, R., B. Laurent, and L. Garcia-Larrea, *Functional imaging of brain responses to pain. A review and meta-analysis (2000).* Neurophysiol Clin, 2000. **30**(5): p. 263-88.

125. Davis, K.D., et al., *Event-related fMRI of pain: entering a new era in imaging pain.* Neuroreport, 1998. **9**(13): p. 3019-23.

126. Kenshalo, D.R., Jr., et al., *SI nociceptive neurons participate in the encoding process by which monkeys perceive the intensity of noxious thermal stimulation.* Brain Res, 1988. **454**(1-2): p. 378-82.

127. Kenshalo, D.R., et al., *Response properties and organization of nociceptive neurons in area 1 of monkey primary somatosensory cortex.* J Neurophysiol, 2000. **84**(2): p. 719-29.

128. Stanford, T.R., S. Quessy, and B.E. Stein, *Evaluating the operations underlying multisensory integration in the cat superior colliculus.* J Neurosci, 2005. **25**(28): p. 6499-508.

129. Lundeberg, T., *Long-term results of vibratory stimulation as a pain relieving measure for chronic pain.* Pain, 1984. **20**(1): p. 13-23.

130. Lundeberg, T., R. Nordemar, and D. Ottoson, *Pain alleviation by vibratory stimulation.* Pain, 1984. **20**(1): p. 25-44.

131. Roy, E.A., M. Hollins, and W. Maixner, *Reduction of TMD pain by high-frequency vibration: a spatial and temporal analysis.* Pain, 2003. **101**(3): p. 267-74.

132. Bini, G., et al., *Analgesic effect of vibration and cooling on pain induced by intraneural electrical stimulation.* Pain, 1984. **18**(3): p. 239-48.

133. Yarnitsky, D., et al., *Vibration reduces thermal pain in adjacent dermatomes.* Pain, 1997. **69**(1-2): p. 75-7.

134. Green, B.G., *Temperature perception on the hand during static versus dynamic contact with a surface.* Atten Percept Psychophys, 2009. **71**(5): p. 1185-96.

135. Ottoson, D., A. Ekblom, and P. Hansson, *Vibratory stimulation for the relief of pain of dental origin.* Pain, 1981. **10**(1): p. 37-45.

136. Watanabe, I., P. Svensson, and L. Arendt-Nielsen, *Influence of segmental and extra-segmental conditioning, stimuli on cortical potentials evoked by painful electrical stimulation.* Somatosens Mot Res, 1999. **16**(3): p. 243-50.

137. Lundeberg, T., *The pain suppressive effect of vibratory stimulation and transcutaneous electrical nerve stimulation (TENS) as compared to aspirin.* Brain Res, 1984. **294**(2): p. 201-9.

138. Deschenes, M., P. Veinante, and Z.W. Zhang, *The organization of corticothalamic projections: reciprocity versus parity.* Brain Res Brain Res Rev, 1998. **28**(3): p. 286-308.

139. Monconduit, L., et al., *Corticofugal output from the primary somatosensory cortex selectively modulates innocuous and noxious inputs in the rat spinothalamic system.* J Neurosci, 2006. **26**(33): p. 8441-50.

140. Wall, P.D., *The gate control theory of pain mechanisms. A re-examination and re-statement.* Brain, 1978. **101**(1): p. 1-18.

141. Wang, N., J.Y. Wang, and F. Luo, *Corticofugal outputs facilitate acute, but inhibit chronic pain in rats.* Pain, 2009. **142**(1-2): p. 108-15.

142. Nebel, M.B., et al., *Touch-pain interactions in TMD: Noxious heat induced changes in vibrotactile processing.* (in preparation).

143. Tommerdahl, M., et al., *Responses of contralateral SI and SII in cat to same-site cutaneous flutter versus vibration.* J Neurophysiol, 1999. **82**(4): p. 1982-92.

144. Nebel, M.B., et al., *Touch-pain interactions in TMD: Noxious heat induced changes in vibrotactile processing.* (submitted).

145. Handwerker, H.O., A. Iggo, and M. Zimmermann, *Segmental and supraspinal actions on dorsal horn neurons responding to noxious and non-noxious skin stimuli.* Pain, 1975. **1**(2): p. 147-65.

146. Gerhart, K.D., et al., *Inhibition of primate spinothalamic tract neurons by stimulation in ventral posterior lateral (VPLc) thalamic nucleus: possible mechanisms.* J Neurophysiol, 1983. **49**(2): p. 406-23.

147. Foreman, R.D., et al., *Effects of dorsal column stimulation on primate spinothalamic tract neurons.* J Neurophysiol, 1976. **39**(3): p. 534-46.

148. Inui, K., T. Tsuji, and R. Kakigi, *Temporal analysis of cortical mechanisms for pain relief by tactile stimuli in humans.* Cereb Cortex, 2006. **16**(3): p. 355-65.

149. Chen, L.M., R.M. Friedman, and A.W. Roe, *Area-specific representation of mechanical nociceptive stimuli within SI cortex of squirrel monkeys.* Pain, 2009. **141**(3): p. 258-68.

150. Buffington, A.L., C.A. Hanlon, and M.J. McKeown, *Acute and persistent pain modulation of attention-related anterior cingulate fMRI activations.* Pain, 2005. **113**(1-2): p. 172-84.

151. Porro, C.A., et al., *Independent time courses of supraspinal nociceptive activity and spinally mediated behavior during tonic pain.* Pain, 2003. **104**(1-2): p. 291-301.

152. Bentley, D.E., et al., *Caudal cingulate cortex involvement in pain processing: an inter-individual laser evoked potential source localisation study using realistic head models.* Pain, 2003. **102**(3): p. 265-71.

153. Harte, S.E., C.A. Spuz, and G.S. Borszcz, *Functional interaction between medial thalamus and rostral anterior cingulate cortex in the suppression of pain affect.* Neuroscience.

154. Zubieta, J.K., et al., *Placebo effects mediated by endogenous opioid activity on mu-opioid receptors.* J Neurosci, 2005. **25**(34): p. 7754-62.

155. Cho, Z.H., et al., *Pain dynamics observed by functional magnetic resonance imaging: differential regression analysis technique.* J Magn Reson Imaging, 2003. **18**(3): p. 273-83.

156. Velasco, M., et al., *Effect of fentanyl and naloxone on a thalamic induced painful response in intractable epileptic patients.* Stereotact Funct Neurosurg, 1998. **71**(2): p. 90-102.

157. Yang, J.W., H.C. Shih, and B.C. Shyu, *Intracortical circuits in rat anterior cingulate cortex are activated by nociceptive inputs mediated by medial thalamus.* J Neurophysiol, 2006. **96**(6): p. 3409-22.

158. Pardo, J.V., et al., *The anterior cingulate cortex mediates processing selection in the Stroop attentional conflict paradigm.* Proc Natl Acad Sci U S A, 1990. **87**(1): p. 256-9.

159. Derbyshire, S.W., B.A. Vogt, and A.K. Jones, *Pain and Stroop interference tasks activate separate processing modules in anterior cingulate cortex.* Exp Brain Res, 1998. **118**(1): p. 52-60.